KERATOSE HYDROGELS PROMOTE VASCULAR SMOOTH MUSCLE DIFFERENTIATION FROM C-KIT$^+$ HUMAN CARDIAC STEM CELLS: UNDERLYING MECHANISM AND THERAPEUTIC POTENTIAL

Benjamin Tyler Ledford

Dissertation submitted to the faculty of the Virginia Polytechnic Institute and State University in Partial Fulfillment of the Requirements for the Degree of

Doctor of Philosophy
In
Biomedical and Veterinary Sciences

Jia-Qiang He, Chair
Mark Van-Dyke
Robert Gourdie
William Huckle
Gangjian Qin

January 30, 2018
Blacksburg, VA

Keywords: Keratin/Keratose, Biomaterials, Human c-kit$^+$ cardiac stem cells, Differentiation, Vascular smooth muscle cells, Hind limb ischemic mouse model, Laser Doppler Imaging, Blood flow, Cardiovascular diseases

Keratose Hydrogels Promote Vascular Smooth Muscle Differentiation from c-kit$^+$ Human Cardiac Stem Cells: Underlying Mechanism and Therapeutic Potential

Benjamin Tyler Ledford

ABSTRACT

Cardiovascular disease is the leading cause of death in the United States, and coronary artery disease (CAD) kills over 370,000 people annually. There are available therapies that offer a temporary solution; however, only a heart transplant can fully resolve heart failure, and donor organ shortages severely limit this therapy. C-kit$^+$ human cardiac stem cells (hCSCs) offers a viable alternative therapy to treat cardiovascular disease by replacing damaged cardiac tissue; however, low cell viability, low retention/engraftment, and uncontrollable *in vivo* differentiation after transplantation has limited the efficacy of stem cell therapy. Tissue engineering solutions offer potential tools to overcome current limitations of stem cell therapy. Materials derived from natural sources such as keratin from human hair offers innate cellular compatibility, bioactivity, and low immunogenicity. Keratin proteins extracted using oxidative chemistry known as keratose (KOS) have shown therapeutic potential in a wide range of applications including cardiac regeneration. My studies utilize KOS hydrogels to modulate c-kit$^+$ hCSC differentiation, and explore the capability of differentiated cells to regenerate vascular tissue.

In the first Chapter, we reviewed literature relevant to keratin-based biomaterials and their biomedical applications, the use of stem cells in cardiovascular research, and the differentiation of vascular smooth muscle cells (VSMCs). The section on biomedical applications of keratin biomaterials focuses on the oxidized form of keratin known as keratose (KOS), because this was the material used for our research. Since we planned to use this material in conjunction with c-kit$^+$ hCSCs, we also briefly explored the use of stem cells in cardiovascular research. Additionally, we

examined some key signaling pathways, developmental origins, and the cell phenotype of VSMCs for reasons that will become clear after observing results from chapters 2 and 3. Based upon our review of the literature, KOS biomaterials and c-kit$^+$ hCSCs were determined to be promising as a combined therapeutic for the regeneration of cardiac tissue.

Research in Chapter 2 focused on characterizing the effects of KOS hydrogel on c-kit$^+$ hCSC cell viability, proliferation, morphology, and differentiation. Results demonstrated that KOS hydrogels could maintain hCSC viability without any observable toxic effects, but it modulated cell size, proliferation, and differentiation compared to standard tissue culture polystyrene cell culture (TCPS). KOS hydrogel produced gene and protein expression consistent with a VSMC phenotype. Further, we also observed novel "endothelial cell tube-like" microstructures formed by differentiated VSMCs only on KOS hydrogel, suggesting a potential capability of the hCSC-derived VSMCs for *in vitro* angiogenesis. Results from this study lead us to question what signaling pathways might be responsible for the apparent VSMC differentiation pattern we observed on KOS hydrogels.

Research in Chapter 3 explored the time course of VSMC differentiation, cell contractility, inhibition of VSMC differentiation, and measured protein expression of transforming growth factor beta 1 (TGF-. $_1$) and its associated peptides for hCSCs cultured on KOS hydrogels, tissue culture polystyrene, and collagen hydrogels. A review of VSMC differentiation signaling pathways informed our decision to investigate the role of TGF-β_1 in VSMC differentiation. Results demonstrated that KOS hydrogel differentiated hCSCs significantly increased expression for all three vascular smooth muscle (VSM) markers compared to TCPS differentiated cells. Additionally, KOS differentiated hCSCs were significantly more contractile than cells differentiated on TCPS. Recombinant human (rh) TGF-β_1 was able to induce VSM differentiation on TCPS. VSM differentiation was successfully inhibited using TGF-β NABs and A83-01. Enzyme-Linked Immunosorbent Assay (ELISA) analysis revealed that both TCPS and KOS hydrogel differentiated cells produced TGF-β_1, with higher levels being measured at early time points on TCPS and later time points on KOS hydrogels. Results from supplementing rhTGF-β_1 to TCPS and KOS hydrogels revealed that KOS

seems to interact with TGF-β to a greater extent than TCPS. Western blot results revealed that latency TGFβ binding protein (LTBP-1) and latency associated peptide (LAP) had elevated levels early during differentiation. Further, the levels of LTBP-1 and LAP were higher on KOS differentiated hCSCs than TCPS hCSCs. This study reaffirms previous results of a VSM phenotype observed on KOS hydrogels, and provides convincing evidence for TGF-β_1 inducing VSM differentiation on KOS hydrogels. Additionally, results from ELISA and western blot provide evidence that KOS plays a direct role in this pathway via interactions with TGF-β_1 and its associated proteins LTBP-1 and LAP. Results from chapter 2 and 3 offered significant evidence that our cells exhibited a VSMC phenotype, and that TGF-β_1 signaling was a key contributor for the observed phenotype, but we still needed an animal model to explore the therapeutic potential of our putative VSMCs.

Research in Chapter 4 investigated a disease model to test the ability of KOS hydrogel differentiated cells to regenerate vascular tissue. To measure vascular regenerative capability, we selected a murine model of critical limb ischemia (CLI). CLI was induced in 3 groups (n=15/group) of adult mixed gender NSG mice by excising the femoral artery and vein, and then treated the mice with either PBS (termed as PBS-treated), Cells differentiated on TCPS (termed as Cells from TCPS), or KOS hydrogel-derived VSMCs (termed as Cells from KOS). Blood perfusion of the hind limbs was measured immediately before and after surgery, then 14, and 28 days after surgery using Laser Doppler analysis. Tissue vascularization, cell engraftment, and skeletal muscle regeneration were measured using immunohistochemistry, 1,1'-Dioctadecyl3,3,3',3'-Tetramethylindocarbocyanine Perchlorate (DiL) vessel painting, and hematoxylin and eosin (H&E) pathohistological staining. During the 4-week period, both cell treatment groups showed significant increases in blood perfusion compared to the PBS-treated control, and at day 28 the Cells from KOS group had significantly better blood flow than the Cells from TCPS group. Additionally, the Cells from KOS group demonstrated a significant increase in the ratio of DiL positive vessels, capillary density, and a greater density of small diameter arterioles compared to the PBS-treated group. Further, both cell-treated groups had similar levels of engraftment into the host tissue. We conclude that Cells from KOS therapy increases

blood perfusion in an NSG model of CLI, but does not lead to increased cell engraftment compared to other cell based therapies.

Overall, the results from this dissertation demonstrated that KOS hydrogels produce VSMC differentiation from c-kit$^+$ hCSCs mediated by TGF-β_1 signaling, and that the differentiated cells are able to increase blood perfusion in a CLI model by increasing capillary density, suggesting enhanced angiogenesis. Future studies should explore potential protein-protein interactions between KOS, TGF-β_1 and its associated proteins. Additionally, we should plan animal studies that examine the efficacy of our cells to regenerate cardiac tissue following an acute myocardial infarction (AMI).

Keratose Hydrogels Promote Vascular Smooth Muscle Differentiation from c-kit$^+$ Human Cardiac Stem Cells: Underlying Mechanism and Therapeutic Potential

Benjamin Tyler Ledford

GENERAL AUDIENCE ABSTRACT

Cardiovascular disease is the leading cause of mortality in the United States, responsible for 1 out of every 4 deaths, and accounting for over 200 billion dollars in health care related cost. There are several available therapies that offer a temporary solution; however, only a heart transplant can fully resolve heart failure, and donor organ shortages severely limit this therapy. Cardiac stem cells are a promising alternative therapy to treat cardiovascular disease by replacing damaged cardiac tissue; however, low cell viability, low retention/engraftment, and uncontrollable *in vivo* differentiation after transplantation has limited the efficacy of stem cell therapy. Tissue engineering solutions offer potential tools to overcome current limitations of stem cell therapy. Keratin proteins extracted from human hair have shown therapeutic potential in a wide range of applications including cardiac regeneration. My studies utilize human hair-derived keratin biomaterials to modulate c-kit$^+$ human cardiac stem cell (hCSC) differentiation and explored the capability of differentiated cells to regenerate vascular tissue. My dissertation demonstrated that keratin biomaterials modified c-kit$^+$ hCSC differentiation and produced VSMCs (a major component of vascular tissue), and that TGF-β_1 signaling was key in producing this differentiation pattern. Additionally, our keratin differentiated hCSCs were able to recover vascular tissue and blood perfusion in a critical limb ischemia (CLI) mouse model. Results demonstrated that our cells increased both blood flow and the density of vascular tissue. Future studies should explore potential protein-protein interactions between KOS, TGF-β_1 and its associated proteins. Additionally, we should

plan animal studies that examine the efficacy of our cells to regenerate cardiac tissue in a myocardial infarction disease model.

DEDICATION

I dedicate this work to my wife Sara; you are loving, kind, and my most loyal friend. I am incredibly fortunate to have such a wonderful partner, and I could not have done this without your unwavering support.

AKNOWLEDGEMENTS

First, I would like to thank my advisor Dr. Jia-Qiang He. In addition to financial support and research expertise, you have treated me like family. You have provided help when needed, while allowing me to grow and learn own my own. I appreciate your honesty, gritted determinedness, and literally being available all hours of the day.

To my committee members, Dr. Mark Van-Dyke, Dr. Robert Gourdie, and Dr. William Huckle. You have all helped by kindly pointing out any deficiencies in my experimental designs and provided sage time saving advice. I also appreciate your generosity of time and resources during my time as a graduate student.

To my external examiner Dr. Gangjian Qin, thank you very much for your time and traveling to Virginia Tech to be a part of my final examination.

I would like to thank He lab members past and present. Dr. Lijuan Kan, you were patient and always very helpful with demonstrating various experimental techniques, and your sense of humor enriched the lab environment. Miao Chen, and Catherine Baron you have been excellent collaborators on many projects, and wonderful friends.

ICTAS, and the VMCVM Office of Research and Graduate Studies thank you for your financial support.

Dr. Ansar Ahmed and Dr. Roger Avery, thank you for being supportive and available to me and many other students in the BMVS program. I would also like to thank Susan Rosebrough and Becky Jones for answering questions and always being there for the students in the BMVS program.

Throughout my entire life, my family has been a constant source of support. I cannot begin to thank my parents, who have always been an inexhaustible source of love and encouragement.

A special thank you to Cindy Shaw for her love, support, and willingness to help with any request.

TABLE OF CONTENTS

LIST OF FIGURES

LIST OF ABBREVIATIONS

5-Aza	5-Azacytidine
AMI	Acute Myocardial Infarction
AĀOVA	Analysis of Variance (one way or two-way)
B2M	Beta-2-Microglobulin
BAM	Bladder Acellular Matrix
b-FGF	Basic Fibroblast Growth Factor
BMMĀCs	Bone Marrow Mononuclear Cells
BMMSCs	Bone Marrow Mesenchymal Stem Cells
BSA	Bovine Serum Albumin
CAD	Coronary Artery Disease
CArG	Carg Elements (CC(A/T)6GG)
CLI	Critical Limb Ischemia
CMs	Cardiomyocytes
DiL	1,1'-Dioctadecyl 3,3,3',3'-Tetramethylindocarbocyanine Perchlorate
DM	Differentiation Medium
ECs	Endothelial Cells
ECM	Extracellular Matrix
EdU	5-Ethynyl-2´-Deoxyuridine
ELISA	Enzyme-Linked Immunosorbent Assay
EMT	Endothelial Mesenchymal Transition
EPCs	Endothelial Progenitor Cells
EPDCs	Epicardial Derived Cells
EPO	Erythropoietin
ESCs	Embryonic Stem Cells
FA	Femoral Artery
FBS	Fetal Bovine Serum
FS	Fractional Shortening
FV	Femoral Vein
H&E	Hematoxylin And Eosin

hCSCs	Human Cardiac Stem Cells
HDAC7	Histone deacetylase 7
hSMMs	Human Skeletal Muscle Myoblasts
ICC	Immunocytochemistry
IF	Immunofluorescence
IHC	Immunohistochemistry
iPSCs	Induced Pluripotent Stem Cells
IRB	Institutional Review Board
KOS	Keratose
KTN	Kerateine
LAP	Latency Associated Peptide
LD	Latissimus Dorsi
LLC	Large Latent Complex
LTBP-1	Latent TGF-B1 Binding Protein-1
LVEF	Left Ventricular Ejection Fraction
MI	Myocardial Infarction
MPCs	Muscle Progenitor Cells
MRTF	Myocardin Related Transcription Factor
Myh11	Myosin Heavy Chain 11
MYOCD	Myocardin
ĀAB	Āeutralizing Antibodies
ĀRCMs	Āeonatal Rat Cardiomyocytes
ns	Āot Significant
ĀSG	Āon-obese diabetic SCID Gamma
OCT	Optimal Cutting Temperature Compound
P/S	Penicillin/Streptomycin
PAD	Peripheral Artery Disease
PBS	Phosphate Buffered Saline
PDGF-BB	Platelet-Derived Growth Factor-BB
PDGRF-β	Platelet-Derived Growth Factor Receptor-β

PFA	Paraformaldehyde
Pre-Diff	Pre-Differentiation
qRT-PCR	Quantitative Real Time Polymerase Chain Reaction
rhBMP-2	Recombinant Human Bone Morphogenic Protein-2
rhIGF	Recombinant Human Insulin-Like Growth Factor
RIPA	Radio Immunoprecipitation Assay
ROI	Region of Interest
RT	Room Temperature
SCs	Schwan Cells
SDS	Sodium Dodecyl Sulfate
SE	Standard Error
SEM	Standard Error of Mean
SKMs	Skeletal Muscle Myoblasts
SLC	Small Latent Complex
SMMHC	Smooth Muscle Myosin Heavy Chain (or Myh-11)
SPR	Surface Plasmon Resonance
SR	(Knockout) Serum Replacement
SRF	Serum Response Factor
TBST	Tris-Buffered Saline And Tween-20
TCPS	Tissue Culture Polystyrene
TGFβR1/TGFβR2	Transforming Growth Factor-β Receptor 1 and 2
TGF-β	Transforming Growth Factor-β
VSM/VSMCs	Vascular Smooth Muscle/Vascular Smooth Muscle Cells
vWF	von Willebrand Factor
α-SMA	Alpha-Smooth Muscle Actin
β-A	Beta-Actin
β-ME	Beta-Mercaptoethanol

CHAPTER 1: LITERATURE REVIEW

1.1 Abstract

Keratin, a structural protein present in a wide range of tissues, comes in two varieties: “soft” cytosolic keratins, found primarily in epithelial tissues; and “hard” keratins, found in protective tissues such as hair, horns, and hooves. The keratin used in biomedical research is isolated predominately from “hard” keratins. Āumerous methods to isolate keratin proteins have been developed. These methods generally take advantage of the high sulfur and disulfide bond content of hard keratins. Extraction of the protein involves chemically denaturing the protein, mediated through either oxidative or reductive conditions. Oxidatively extracted keratins are typically denoted as keratose (KOS). KOS can then be processed into various physical formats such as films, gels, fibers, and coatings. These materials have shown great cell and tissue compatibility. KOS alone or in conjunction with cells, drugs and/or various growth factors has been tested in a variety of biomedical applications ranging from drug release, wound regeneration, skeletal muscle regeneration, cardiac regeneration, and nerve regeneration. Āone of these applications has shown KOS to illicit an adverse immune response. Additionally, KOS has shown salubrious effects in a number of animal studies that merit further investigation in large animal studies, and has demonstrated great potential to progress towards human trials. The goal of this chapter is to outline the current status of KOS biomaterials in biomedical research and its applications in animal models which have demonstrated the greatest potential of entering into human clinical trials.

Stem cells have been widely used in cardiovascular research, and these cells fall in one of two categories, non-resident cardiac stem cells, and cardiac stem cells. Generally, therapies target replacing beating CMs, pace making cells, or vasculature. Among the cell types used to treat ischemia, vascular smooth muscle cells (VSMCs) are under-represented. To design VSMC based therapies it is necessary to examine key signaling pathways, developmental origins, and the cell phenotype of VSMCs. Based upon our review of the literature, KOS biomaterials and c-kit^{+} hCSCs were determined to be beneficial as a combined therapeutic for the regeneration of cardiac tissue.

1.2 Introduction

Cardiovascular disease is the leading cause of mortality in the United States, responsible for 1 out of every 4 deaths, and accounting for over 200 billion dollars in health care related cost. Ischemic myocardial infarction (MI), mainly due to coronary artery disease (CAD), is the most common type of heart disease killing over 370,000 people each year (1). MI is a result of occlusion of coronary arteries due to atherosclerosis plaque buildup in the intima of arteries (2-4). Clinically available therapies include dietary intervention, angioplasty, coronary artery bypass, and in the most extreme cases heart transplantation (4). These therapies can be effective to various degrees, but once the end-stage heart failure occurs, heart transplantation becomes the last resource to rescue a patient's life. Unfortunately, a shortage of donor hearts is a limiting factor for this option. An alternative to heart transplantation is stem cell-based therapy.

An effective stem cell-based therapy for MI would either replace host cardiomyocytes, or promote host CMs to proliferate, and also create new vasculature to provide nutrients to the CMs (5). Stem cell therapy holds potential to achieve these goals, but to date no therapy has addressed all of the challenges (6-8). C-kit$^+$ human cardiac stem cells (hCSCs) are resident cardiac stem cells that exhibit basic stem cell properties (self-renewing, clonogenic, and multipotent) (8, 9). Although the functional ability of c-kit$^+$ hCSCs to become CMs *in vivo* is one of the centrally debated issues concerning their regenerative potential (7, 10), abundant preclinical and clinical studies have provided evidence to demonstrate their *in vitro* abilities of cardiac lineage differentiation (*i.e.,* cardiomyocytes-CMs, endothelial cells-ECs, and VSMCs) as well as *in vivo* capacity to improve cardiac function following transplantation (7, 8, 11-14). Regardless of differences between *in vitro* and *in vivo* studies of c-kit$^+$ hCSCs, the inability of stem cells to engraft into host tissue still remains unsolved (6, 11, 12, 14). Therefore, methods to improve cell based therapy are currently being explored. One strategy is to use biomaterials, alone or in conjunction with stem cell-based therapies.

Biomaterials possess several properties that are ideal for regenerative medicine applications, which include biocompatibility, biodegradability, low/non-immunogenicity, and low/non-cytotoxicity (15). Keratin is a natural structural protein that can be formulated into biomaterials that achieve all of the above properties. Keratin is evolutionarily well

conserved and therefore can be used from allogenic and even xenogeneic sources (16). Further, because keratin can be obtained from human hair it offers a readily available and cheap source of biomaterial that can be obtained from the patient's own tissue and formulated in a variety of ways (film, sponges, and hydrogels) to suit a diverse set of tissue engineering applications (17).

A key molecular feature of keratin is its high thiol content, which extensively forms disulfide bonds that provides the macromolecule with mechanical strength (18, 19). When formulating keratin based biomaterials the disulfide bonds are typically targeted for modification primarily using two approaches, reductive chemistry to produce kerateine (KTN), or oxidative chemistry to produce KOS. Cell culture studies have shown that KTN and KOS can control and modulate stem cell behavior in a variety of ways, including cell adhesion, proliferation, colony-forming efficiency, and differentiation (20-24). Both materials have been successfully used in various applications, including controlled drug release (25, 26) and treatments of various diseases in animal models, such as dermal wound regeneration healing (27), skeletal muscle regeneration (28-30) peripheral nerve regeneration (31-35) and cardiac regeneration (36). Findings of these aforementioned studies demonstrate that KOS hydrogels possess an innate biocompatibility non-immunogenicity, thus meriting further exploration of KOS hydrogels in cardiovascular therapies. However, prior to the above, a better understanding of the *in vitro* interaction between c-kit$^+$ hCSCs and KOS hydrogels will provide a more natural cell culture condition, and offer novel information of how the resident cardiac stem cells may interact with KOS hydrogels *in vivo*. Knowledge of how both cells and material interact should provide novel pathways to investigate how each are able to improve cardiac function and in due course design improved therapies.

1.3 Keratin Biomaterials

1.3.1 Sources, Basic Properties, and Extraction

Biomaterials come in myriad forms ranging from full synthetic materials to biologically derived materials and play an integral role in regenerative medicine and are often used in biomedical applications (37). For applications that require mechanical strength, polysaccharides or proteins are typically used (38, 39); while protein based

material like collagen, silk fibroin, and keratin are well-suited for tissue engineering applications that necessitate interactions with tissues and cells (40-42). Protein materials integrate many of the properties of the extracellular matrix (ECM), mimicking the innate ability of the ECM to facilitate cell-cell and cell-matrix interactions. This in turn creates a unique microenvironment with a defined three-dimensional structure that can facilitate cellular guided proliferation and tissue formation, which is a crucial aspect of a biomaterial scaffold. The diverse physiochemical and biological activities present in proteinaceous biomaterials offer a complex interaction between scaffold and tissue matrix integration that is not easily obtained in synthetically derived medical devices. Keratin based biomaterials offer a unique set of properties that make them attractive for tissue engineering. For instance, they are not susceptible to collagenase present in tissue (43, 44), they offer mechanical resilience beyond other protein based biomaterials (collagen, elastin, fibrin) (42), and they are abundantly available and easily procurable in the form of hair, horn, and feathers (35, 45, 46).

While still nascent in biomedical research, keratin biomaterials have shown that they are well-suited for a wide range of biomedical applications. In addition, as a result of the strong bioactivities and diverse physiochemical properties of keratin biomaterials, there are several attractive features that are unique to keratin. For example, keratin is a self-renewing source of autologous biomaterial that can be obtained without any invasive procedures in the form of human hair. These properties make keratin very attractive for other biomedical applications that require biocompatibility such as medical devices, bioactive surfaces, hygiene products, *etc.*

KOS biomaterials are composed of protein from hard keratin sources, typically hair or wool (18, 19). Various methods to break down disulfide bonds for protein extraction have been described (47, 48). KOS is a chemically modified formulation of native keratin fibers that have greatly diminished disulfide bond content. Preparation of KOS involves fission and conversion of disulfide linkages to sulfonic acid groups (18). KOS is commonly extracted using oxidative chemistry; one common method is peracetic acid extraction (32, 34, 48-51).

Oxidative extraction reduces the cysteine/thiol content of the source keratin, which cleaves disulfide bonds and converts the resulting sulfhydryl groups into sulfonic acid (18). KOS loses its ability to spontaneously self-assemble through formation of disulfide bonds.

However, the resulting material easily wets and can form an elastic solid-like hydrogel, and upon wetting the lyophilized material reverts to a hydrogel (18). It has been demonstrated that increasing oxidation increases the rate at which KOS is degraded (46). The process of

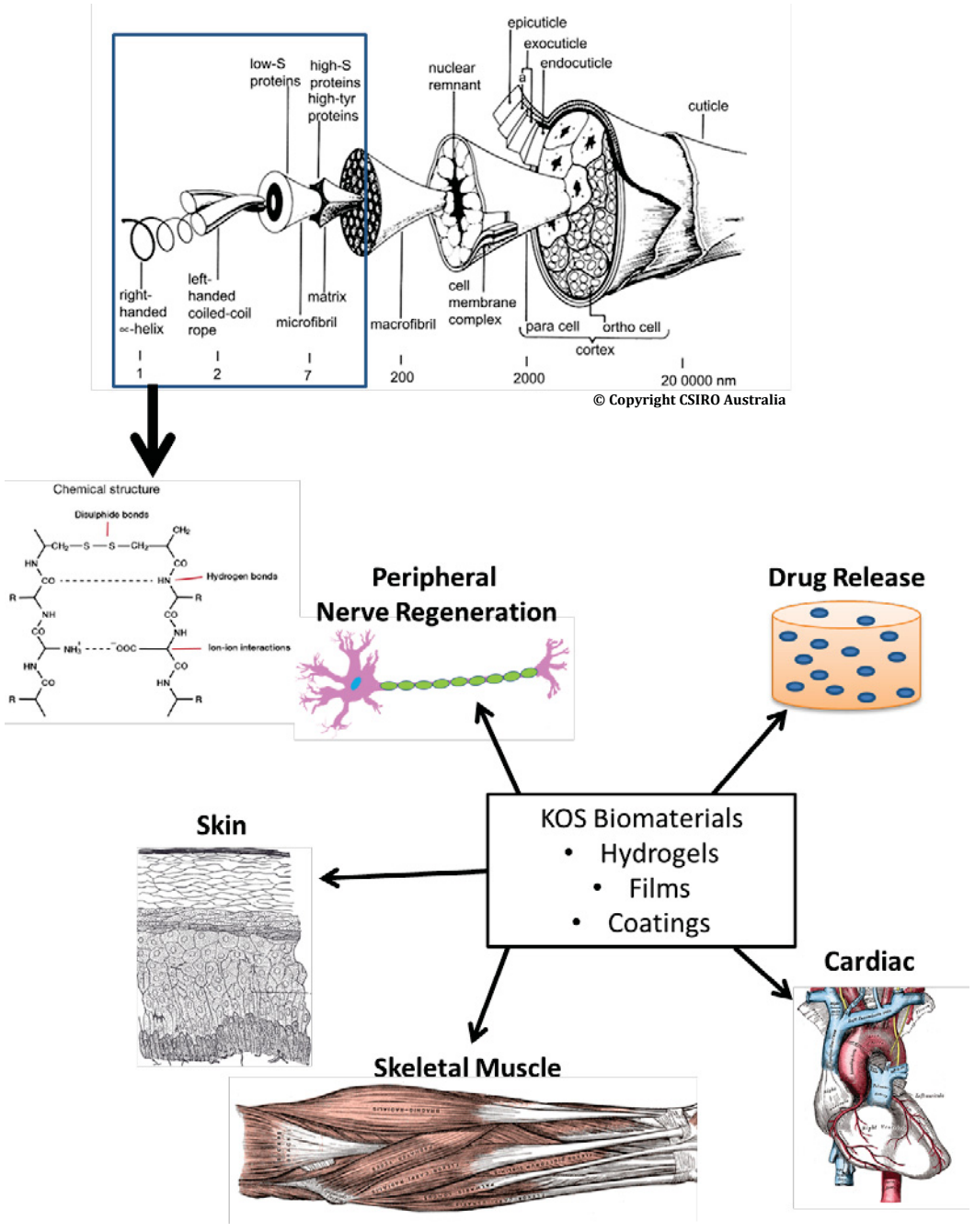

Figure 1.1 Structure of human hair and potential biomedical applications of keratin (Images are used with permission from CSIRO Publishing or under fair use of Gray's Anatomy 2018)

oxidative extraction leads KOS to erode more quickly than KTĀ, which is extracted using reductive chemistry preserving thiol groups allowing reformation of disulfide bonds (25, 51). Using a combination of KOS and KTĀ degradation can be fine-tuned by varying ratio of KTN to KOS (51). The capability to control erosion is useful for applications such as drug delivery (25, 26). The reason KOS degrades more rapidly than KTN is typically explained by the diminished capacity to form disulfide bonds. Han *et al.* have shown that that altering thiol content through alkylation of human hair keratin (25) directly alters the degradation rate of keratin biomaterials. Capacity to form disulfide bonds is likely the key contributor to material degradation. Observations with scanning electron microscopy have shown that upon drying the KOS hydrogels from wool, they form interconnected pores which are conducive to cell infiltration and tissue regeneration (32, 36, 51). Pore size ranges from 20-100 μm and fiber diameter between 2-20μm (51). In solution or in a hydrogel, KTN is more elastic and less viscous than KOS due to the presence of disulfide bonding (28). In the absence of a chemical cross-linker, KOS at 12% (wt/vol) has elastic moduli around 100Pa, which is more suitable for cell cultivation (28). Under compressive stress KOS has less mechanical strength than KTN (51). These differences in rheology make KOS more suitable for certain applications compared to KTN and vice versa. Mixing different amounts of KOS and KTN can be used to control the extent of disulfide crosslinking, thus altering the material's rheological properties and tailoring it to a specific application such as drug delivery (51).

1.3.2 Biomedical Applications

1.3.2.1 Tissue Compatibility

A number of studies examined the tissue compatibility of KOS with a variety of cell types: THP-1 monocytes, fibroblast, HUVECs, human skeletal muscle myoblast (hSMM), schwannoma cells, neonatal rat cardiomyocytes, and hCSCs (18, 24, 26, 28, 32, 36, 46, 51). No cell line reported cytotoxicity from being cultured in the presence of KOS biomaterials in the various formulations examined.

A key consideration for a biomaterial is how the material will interact with blood. The way that a biomaterial reacts to blood will determine its suitability for distinct types of medical applications. The hemocompatibility of oxidized and native horn keratin were

analyzed based upon hemolysis ratio, platelet adhesion, and platelet activation (46). A biomaterial is considered hemocompatible if it meets the following criteria: no platelet adhesion, not thrombogenic, and not pro-inflammatory. Additionally, the material or device should be technically functional and promote healing (52). Oxidized horn keratin showed good hemocompatibility with hemolysis values below 2% (46). Values below 5% are considered good hemocompatibility for novel biomaterials (53). Platelet adhesion and activation are typically used as the main intuitive factors for hemocompatibility of biomaterials (54). Platelet activation studies using rabbit blood demonstrated that platelets adhered to oxidized horn keratin but did not spread or aggregate at an elevated level (46), suggesting that the material is passivated with a thin layer of platelets. Additionally low levels of fibrin, a lack of platelet activation and no elevated levels of aggregation suggest that KOS is unlikely to cause a thrombus (46). These results were in agreement with cell culture results, which indicated that KOS decreased rate of M1 pro-inflammatory macrophages and increased level of anti-inflammatory M2 macrophages, indicating that KOS would likely be a good candidate for further investigation *in vivo* (55, 56).

Nakata *et al.* demonstrated that L929 fibroblasts could be cultured on KOS biomaterials (26). Guzman and Zhang both demonstrated that KOS is not cytotoxic (18, 46). Oxidized horn keratin showed no significant effect on viability or proliferation of 3T3 or HUVECs (46). Work in our lab also showed elevated levels of viability for c-kit$^+$ hCSCs on KOS, and viability was maintained over three passages on the biomaterial (24). Other groups have also shown that KOS can maintain extended cell culture; Ham *et al.* observed no loss in viability over a time course of 7 days (51). These results all indicate that there is no adverse or cytotoxic response of any cell types in response to KOS.

Studies performed in mice, rats, rabbits, and non-human primates did not show a negative or acute immune response to KOS biomaterials (18, 34-36, 57). In addition, KOS showed no negative response across a number of tissues and organ systems: skin, subcutaneous implantation, cardiac tissue, and nerve tissue (18, 35, 36, 58). Subcutaneous tissue implantations studies found that KOS integrated with host tissue (18). Histological analysis found that KOS was infiltrated by leukocytes and fibroblasts (18) and demonstrated bulk material angiogenesis and minimal fibrous encapsulation (18). The degradation profile of KOS follows a rectangular hyperbolic regression pattern of resorption of the material (18)

and within 8 weeks, 92% of the material was degraded (18). Further, KOS was found to have superior tissue integration to 90:10 PLGA mesh (18). The source of the keratin material also did not seem to impact the tissue response; oxidized horn demonstrated comparable results to the human hair keratin. The material showed no obvious signs of inflammation or fibrosis at the later time points and no signs of being toxic such as cell lysis or tissue destruction (46). Both studies indicate excellent tissue compatibility for subcutaneous implantation of KOS biomaterials extracted from horn or human hair (46, 50). The biocompatibility of KOS certainly seems to be no barrier to further investigation, making it an excellent candidate for many biomedical applications.

1.3.2.2 Controlled Drug and Growth Factor Release

Controlling the delivery of a therapeutic agent is an attractive technique to supply engineered amounts of the treatment for a prolonged timeframe to a targeted site of injury or disease. This is a challenge for traditional drug delivery methods such as ingestion of pills or injection of the drug in an aqueous solution. Controlled release is particularly important when dealing with bioactive agents like growth factors or cytokines, which can be sensitive to processing treatments. KOS biomaterials have shown capability as a carrier system for drug release and controlled delivery.

A pair of studies by Han *et al.* and Āakata *et al.* showed that altering the thiol content of keratin biomaterials by mixing KOS and KTN modifies the release time of drugs (25, 26). Decreasing thiol content can be achieved by mixing KTN and KOS (51) or by chemical modifications such as iodoacetamide treatment. Both processes alter the amount of thiol groups available to form disulfide bonds, thus altering the release rate of the drug or growth factor of interest (25). KOS is an excellent material for drug release demonstrated by studies with recombinant human insulin-like growth factor-1 (rhIGF-1), recombinant human bone morphogenic protein-2 (rhBMP-2), and ciprofloxacin (28, 51). Drug release for ciprofloxacin shows a strong correlation with degradation of the hydrogel; and therefore, it is likely that the release of any number of small molecules with electron withdrawing groups would be regulated primarily by degradation of KOS hydrogel and unlikely due to the simple diffusion from the material (50, 59). These studies also demonstrated that KOS biomaterials were suitable for the release of both low molecular weight drugs (ciprofloxacin) and high

molecular weight growth factors (rhIGF+rhBMP-2).

A study conducted by Peyton *et al.* examining drug release properties of KOS hydrogels *in vivo* investigated delivery of the antibiotic halofuginone in a cecal abrasion model of female Sprague Dawley rats (59). KOS halofuginone hydrogel-treated rodents had fewer and less dense abdominal adhesions, compared to the halofuginone and negative controls (59). Low or undetectable levels of halofuginone throughout the body indicate that KOS has the ability to localize the drug to the delivery site (59). Additionally, the sustained release of the antibiotic is due to the degradation of the KOS hydrogel, which is consistent with the results from *in vitro* studies by Saul *et al.*, where KOS hydrogels released 60% of loaded ciprofloxacin over the first 10 days and continued release was detectable over the course of 3 weeks (50). Released ciprofloxacin was bioactive, inhibiting growth of Staphylococcus aureus for 23 days *in vitro* and for 2 weeks in a mouse subcutaneous model (50). These results suggest that KOS-halofuginone hydrogel would be a feasible therapeutic barrier as well as a controlled delivery system of antibiotic for preventing postoperative bacterial adhesions.

1.3.2.3 Dermal Wound Regeneration

As the outer layer of tissue, skin is composed primarily of collagen, elastin, and various other proteins, and it provides a physical barrier to protect underlying tissues and organs. Burns and other injuries to the skin require medical interventions in the form of a skin graft or other biomaterial. Park *et al.* investigated the ability of KOS to aid in regeneration of full dermal thickness wound healing (27). KOS was able to enhance vascularization, collagen deposition, and fibroblast infiltration compared to hydrocolloid wound dressing and a control that received no treatment. Evaluation of Masson's trichrome staining early in the healing process (Day7) demonstrated enhanced vascularization, collagen deposition, and fibroblast infiltration for the KOS-treated group (27). Lower number of fibroblasts at latter time points in the KOS-treated group compared to the negative and positive controls suggested less adverse wound healing (27, 58). Additionally, the injury size was smaller in the KOS group compared to the negative control (27). The results demonstrated that improved wound healing by KOS was achieved by earlier fibroblast infiltration, collagen production, and enhanced vascularization. In Figure 2 of

Park's study, the orientation of the treatments in images A, B, and C do not match (27). It seems that the groups were mislabeled or that the same mouse was not used for each time point. It should also be mentioned that a paper was published investigating the use of enzymatically digested mouse fur in a full skin thickness injury model of mice, but since this study did not specifically use KOS, the finding was not discussed in this review (60). KOS biomaterials have also been tested in more complex applications that necessitate 3-dimensional scaffolds and innervation of tissue.

1.3.2.4 Skeletal Muscle Regeneration

Skeletal muscle is a tissue composed of multinucleated contractile cells which are critical for locomotion. Some research has investigated the potential of KOS for skeletal muscle regeneration (28). *In vitro* data demonstrated that hSMM cell viability could be maintained after encapsulation in KOS hydrogels (28). Cell proliferation and adhesion showed that all KTĀ and KOS conditions was comparable to other cell culture conditions (TCPS/collagen/Matrigel) (28). Additionally, alpha KOS, gamma KOS, and alpha KTĀ were shown to promote the number of multinucleated cells when compared to biomaterial controls (Matrigel and collagen) (28). The presence of more multinucleated cells is indicative of a more mature skeletal muscle phenotype (61). Cells cultured on alpha KOS and alpha KTN led to more ordered structure consistent with skeletal muscle and no aberrant morphology (28).

The same study examined the effects of subcutaneous implantation of KOS and muscle progenitor cells (MPCs) in C57/BL6J mice (28). Histological assessment of KOS implants showed no significant immune response to the implants (28). Cells within the hydrogels had morphologies consistent with MPCs, and addition VEGF to the constructs promoted formation of vascular tissue (28).

Two studies examined the combined KOS and KTN hydrogels' regenerative capability in models of volumetric muscle loss. Both studies used a 70:30 blend of KOS and KTN hydrogel, with or without the combination of growth factors (IGF+bFGF) and MPCs (29, 30). The first study conducted by Baker *et al.* was a mouse model of volumetric muscle loss induced by surgery in the latissimus dorsi (LD) (30). Results showed greater force generation by the group treated with keratin IGF + bFGF (30). They also determined that

there was no significant benefit by supplementing the keratin hydrogels with MPCs (30). Histological analysis demonstrated that keratin hydrogels and keratin hydrogels + IGF + bFGF had a greater regenerative effect than the control and bladder acellular matrix (BAM) groups, indicated by higher levels of regenerative muscle fibers (measured with H&E) and less fibrotic tissue (Masson's trichrome) (30). IHC results determined that there were more myosin positive cells in the surgical defect region for the two keratin groups as well (30). The second study, headed by Passipieri, examined a rat model of volumetric muscle loss in the tibialis anterior muscle (29). They tested the same keratin experimental groups, and among the groups examined, keratin hydrogels with both bFGF and IGF showed the greatest improvement for all time points examined (29). Histological results demonstrated that all keratin hydrogel-treated groups had a significantly higher number of central nuclei positive cells indicating more robust skeletal muscle regeneration than BAM or no repair groups. Masson's trichrome stain further revealed that there was significantly less fibrotic tissue in the keratin-treated groups than the BAM and no repair groups (29).

The results of these *in vitro* and *in vivo* studies merit further investigation of KOS/KTN based hydrogels for regenerative applications involving volumetric muscle loss. Further research in large animal models of volumetric muscle loss is the logical next step for these studies before launching into clinical trials. Based upon current evidence, it seems that the most logical course would be to investigate the use of keratin hydrogels for sustained release of growth factors and for use as a scaffold material for cellular infiltration and regeneration of injured tissue. Additionally, more work should be done to determine if higher numbers of cells would improve the efficacy of co-delivery of combination therapies of keratin hydrogels and MPCs. Interestingly, neither animal study used magnetic or fluorescent cell sorting to purify for satellite muscle cells (29, 30). The use of a defined cell population that utilized enrichment for known satellite cell markers such as Pax3 or Pax7 (62) via MACS/FACS could potentially provide a greater therapeutic benefit than keratin or keratin and growth factors alone. A common injury that coincides with or causes volumetric muscle loss is peripheral neuropathy (63-66), and a number of studies have used KOS to treat this disorder.

1.3.2.5 Peripheral Nerve Regeneration

The functional unit of the nervous system is the neuron (31). Peripheral nervous

tissue is composed of two main divisions: motor and sensory. Motor nerves can be further broken down into somatic (voluntary) and autonomic (involuntary) motor neurons (31). Āerve regeneration is the most extensively studied biomedical application of KOS biomaterials. A study conducted by Sierpinski *et al.* examined *in vitro* cell culture of a schwannoma cell line (RT4-D6P2T) in the presence of KOS and measured proliferation, migration, adhesion, and gene expression (32). Results showed that KOS induced a statistically significant increase in proliferation for all but the highest concentration of KOS when compared to FBS containing basal medium (32). KOS also improved cell migration, attachment and up-regulated S100Ā (a binding protein responsible for homeostasis and normal glial cell function), and CD104 (important for Schwan cell axon interaction) (32). Given the improved viability, migration, and gene expression consistent with healthy nerve function, KOS was considered a promising biomaterial for nerve regeneration and warranted further investigation.

KOS peripheral nerve regeneration was evaluated in a number of animal models including mice, rats, rabbits, and non-human primates (32, 34, 35). In these studies, peripheral nerve damage was induced by surgically creating defects 4mm-3cm in either the sciatic nerve (rats), tibial nerve (mice and rabbits), or the wrist (macaques) (32-35).

In Sprague Dawley rats, KOS demonstrated the ability to enhance Schwan cell (SC) function (33). In nerve conduits containing KOS, migration of Schwan Cells (SCs) occurred earlier and the differentiation of SCs from the proximal nerve end was enhanced compared to saline and Matrigel filled conduits (33). KOS conduits also showed faster SC dedifferentiation, myelin debris clearance, and decreased macrophage infiltration during Wallerian degeneration of distal nerve tissue (33). The rat study shows that the interactions between KOS proteins and PNS cells enhance early peripheral nerve injury recovery. Data seems to indicate that KOS promotes debris clearance via SC activation at the distal stump of the injury site, and KOS is permissive for growth cone advancement (33). For mice treated with KOS, all animals showed visible nerve regrowth at 6 weeks compared to 50% of empty Silastic conduits (32). Additionally, there was a greater increase in nerve area and axon density in the KOS-treated group than the empty conduit or autograft group (32). In rabbit studies conducted by Hill *et al.*, KOS-treated rabbits had less muscle atrophy than autograft or empty conduit (not significant), a statistically significant increase in myelin thickness

compared to empty conduit, and larger nerve area and total axons per nerve than the empty conduit (not significant) (34). Āerve function studies showed that KOS-treated rabbits had a statistically significant increase in amplitude and less nerve conduction delay than both autograft and empty conduit (34). KOS also enhanced nerve regeneration in non-human primates (35). KOS hydrogel showed significant improvement in return of compound motor action potential, latency, and recovery of nerve conduction velocity compared to saline treatment (35). The KOS-treated non-human primates also showed significantly larger nerve area and myofibril density than the saline control (35). Human hair-derived KOS did not instigate an inflammatory response in any of the animal studies (32-35).

The success of KOS in several animal models of peripheral nerve regeneration, including non-human primates, indicates that KOS is a strong candidate for use in subcritical peripheral nerve injury. Further research in this area should use an animal model, such as pigs, to create a more appropriate size match before going forward with clinical trials (67). Further investigations should use KOS hydrogels in applications beyond a nerve conduit filler. KOS has shown potential in drug and cell deliver in other regenerative medicine applications, future studies should examine these applications in nerve regeneration. Additionally, detailed studies of what cell signaling pathways are involved in KOS hydrogel mediated nerve regeneration will be critical to understand and enhance the therapeutic capability of KOS hydrogel based therapies.

1.3.2.6 Cardiac Regeneration

The action of pumping blood is mediated by the contraction of cardiomyocytes; consistent and constant function is key to life (68). As a result of various pathologies such as MI, CMs are lost through apoptosis and replaced by fibrotic remodeling (36, 68-73). This process leads to cardiac dysfunction, morbidity and eventually death. Cardiomyocyte loss and pathological remodeling can be diminished by providing a scaffold in the form of injectable hydrogels or other biomaterials (68).

In a study conducted by Shen *et al.*, injectable KOS hydrogels are explored as a potential biomaterial to minimize loss of cardiomyocytes, negative remodeling, and promote regeneration. The study examined the characteristics of KOS hydrogels i*n vitro* and *in vivo* (36). To assess the feasibility of KOS for cardiac applications, they examined the effect of

culturing neonatal rat cardiomyocytes (NRCM) from Sprague Dawley rats in KOS hydrogels, and measuring cell behavior with various microscopy and molecular biology techniques (36). NRCMs are commonly used to evaluate biomaterial potential for cardiac applications (69, 73). NRCMs cultured in KOS hydrogels exhibited normal cell morphology, significantly superior migration, and superior viability compared to NRCMs in basal medium (36). KOS hydrogels also afforded NRCMs the ability to distribute three dimensionally (36). Gene expression analysis demonstrated statistically higher expression of cardiac specific genes (36). Additionally, KOS hydrogels were able to improve left ventricular ejection fraction (LVEF) and fractional shortening (FS), while these parameters declined for the saline treated rats (36). Further, KOS prevented left ventricular dilation, preserved more viable tissue, and reduced scar size (36). Perhaps most intriguing IHC analysis found that injected KOS hydrogels were infiltrated with CMs and promoted revascularization of damaged tissue without inducing an adverse immune response (36). KOS degraded steadily, and by day 28, 50% of the gel remained (36). Western blot analysis revealed increased secretion of TGF-β, NGF, and BMP4 (36). Results of this study demonstrate that KOS hydrogels significantly improved preservation of infarct cardiac tissue function and morphology compared to the saline control. Additionally, KOS hydrogels seemed to promote greater regeneration of the infarct region by allowing infiltration of vascular tissue and cardiomyocytes, all without inducing acute inflammation. This study indicates that KOS hydrogels are an excellent biomaterial candidate for cardiac regenerative therapies.

A reasonable course for future study would be to inspect the efficacy of KOS hydrogels in additional small animal models such as mice. Additionally, it would be interesting to examine co-administration of KOS hydrogels with growth factors and/or cells. Based upon KOS hydrogel studies in other tissues, using KOS for controlled delivery of growth factors or cells could increase the regenerative capability of this therapy (26, 29, 30, 59, 74).

1.4 Stem Cells in Cardiovascular Research

Extensive research has investigated for use in cardiomyopathies, much of which has focused on cell therapies for left ventricle dysfunction. A review by James Chong succinctly summarizes many approaches and their clinical benefits (5). Stem cell based therapies fall in

clinical practice fall in one of two categories, non-resident cardiac stem cells, and cardiac stem cells. Āon-resident cardiac stem cells investigated in either clinical trials or pre-clinical trials include: skeletal muscle myoblasts (SKM), bone marrow mononuclear cells (BMMNCs), bone marrow mesenchymal stem cells (BM-MSCs), endothelial progenitor cells (EPCs), adipose MSCs, embryonic stem cells (ESCs), and induced pluripotent stem cells (iPSCs). Cardiac stem cells include: side populations cells, c-kit$^+$ cells, cardiosphere derived cells, Sca1$^+$ cells, Isl1$^+$ cells, and epicardial derived cells (EPDCs). Each cell type comes with benefits and potential drawbacks.

1.4.1 Non-Resident Cardiac Stem Cells

Clinical trials examining non-resident cardiac stem cells have provided mixed results. Early studies examining SKM found that they induced arrhythmias, BMMNCs and MSCs were able to improve cardiac function at early time points, but this effect was lost in most trials after 12 months to 5 years, and neither cell type has offered convincing evidence that they significantly contribute CMs to the injured heart (5). ESCs and iPSCs are the only non-resident cardiac stem cells that definitively can differentiate into CMs and offer great potential in a variety of regenerative therapies (5, 75-78). Pluripotent cells are not without their own drawbacks, both cell types have been shown to generate tumors (79-81). ESCs and iPSCs have also shown issues with immune rejection (5). ESCs additionally have ethical issues since they are sourced from human embryos.

1.4.2 Resident c-kit$^+$ Human Cardiac Stem Cells

C-kit$^+$ hCSCs are resident cardiac stem cells that exhibit basic stem cell properties (self-renewing, clonogenic, and multipotent) as well as an ability to differentiate into all cardiovascular lineages (8, 12). These cells are variously postulated to arise at various time points and from different compartments during cardiac development (10), but adult hCSCs are primarily derived from the epicardial niche (82). Āumerous publications have previously demonstrated that c-kit$^+$ hCSCs can be differentiated into three cardiac lineage cell types (*i.e.,* CMs, ECs, and VSMCs) in both *in vitro* and *in vivo* settings (8, 14, 83-85); however, whether hCSCs are able to differentiate into CMs after transplantation is still under debate (10). Although the functional contribution of c-kit$^+$ hCSCs to *in vivo* cardiomyocyte turnover is one

of the centrally debated issues concerning their regenerative potential (7, 10), plentiful preclinical and clinical studies have provided enormous evidence to demonstrate their *in vitro* abilities of cardiac lineage differentiation (*i.e.,* cardiomyocytes-CMs, endothelial cells-ECs, and VSMCs) as well as *in vivo* capacity to improve cardiac function following transplantation (7, 8, 11-14). Regardless of differences between *in vitro* and *in vivo* studies of c-kit$^+$ hCSCs, the major challenges described above still remain to be solved for all stem cell-based therapies (6, 11, 12, 14).

1.5 Vascular Smooth Muscle Cells

1.5.1 Origin and Cell Phenotypes

VSMCs have several origins during embryo development (86). Research by Amali *et al.* found that in zebrafish vasculogeneisis is initiated invagination of epiblastic cells through primitive streak and formation of mesoderm during gastrulation (87). Upon formation of a functional vascular network angiogenesis recruits VSMCs via PDGF-BB and refines the existing vessels (88). Embryonic origin of VSMCs is largely dependent upon the stage of development and the location of vascular tissue at the time of development. For instance, proximity of epicardial progenitors to the coronary arteries during development produce VSMCs of the coronary arteries, and sclerotome somites produce dorsal aorta VSMCs (89-91). Literature reviews of the origins of VMSC have compiled research demonstrating similar developmental origins of VSMCs from the secondary heart field, neural crest, pleural mesothelium, splanchnic mesoderm, and nephrogenic stromal cells (86, 92).

While there has been a decent body of work investigating VSMCs origins there are still features of these cells that confound researchers. Many issues occur when observing adult VSMCs, due to the plasticity of the cell phenotype *in vivo*. Normal VSMCs in the vessel wall are characterized by their contractility, low motility and proliferation, but they are sensitive to external stimuli. Growth factors, low levels of oxygen, and/or inflammation can cause VSMCs to lose contractility, become proliferative and motile. This cell phenotype known as a synthetic VSMC. If unchecked this phenotypic switch leads to atherosclerosis and cardiovascular pathologies (93). Additional examples of VSMC plasticity include TGF-β_1 mediated endothelial to mesenchymal transition (EMT) (94, 95), and differentiation

induction of bone marrow stem cells (96, 97) both producing cells with phenotypic characteristics of VSMCs.

1.5.2 Signaling Pathways Regulating VSMC Differentiation

1.5.2.1 Integrin Signaling

Integrins are transmembrane heterodimers, and the primary receptor proteins that bind and respond to elements of the ECM (98). Integrin plays a key role in VSM differentiation by stretch activation of TGF-β_1 and co-factor crosstalk with downstream TGF-β_1 signaling (99-101) (Figure 1.2). Some of the key co-factors involved in both integrin and TGF-β_1 signaling include: myocardin related transcription factor (MRTF), serum response factor (SRF), and myocardin (Myocd). MRTF is a transcriptional cofactor activated by RhoA/ROCK signaling, which is involved in regulation of TGF-β_1 initiated EMT (102). SRF is a highly conserved regulator of cytoskeleton and contractile actin. In conjunction with TGF-β_1 signaling, SRF, MRTF, and Myocd play a crucial role in homeostasis of contractile actin for smooth muscle cells (103). SRF binds the upstream CArG elements ($CC(A/T)_6GG$) for VSM contractile protein genes such as α-smooth muscle actin (α-SMA) and smooth muscle myosin heavy chain (SMMHC) (103-106). Inhibiting SRF or Myocd can decrease contractile phenotypes in smooth MPCs (106, 107). Through these mechanisms, integrin plays a direct role in maintaining mature contractile VSMCs alongside TGF-β_1 signaling.

1.5.2.2 TGF-β Signaling

TGF-β_1 is a member of the TGF-β superfamily which includes three variants of TGF-β (TGF-$\beta_{1,2,3}$) and a number of other proteins (108). It is a potent regulator of several cellular functions, such as cell spreading and proliferation and is strongly related with VSM differentiation in a variety of stem cells (109-112). TGF-β_1 upon binding to its receptor complex, transforming growth factor-β receptor 1 and 2(TGFBR1/TGFBR2) canonical SMAD signaling is activated (113-118). This signaling pathway produces a mature VSMC phenotype associated with contractility, minimal ECM deposition, lower proliferation, and low cell motility (119). While many processes are crucially important to VSMC recruitment and maintenance of phenotype TGF-β_1 is the key player in producing mature VSMCs. Of the

various methods used to induce smooth muscle differentiation *in vitro* TGF-β_1 signaling is certainly among the most commonly reported (111, 114, 120-122). TGF-β_1 has been observed to produce VSMC differentiation in ESCs and adult stem cells (111, 119, 123, 124), by increasing expression of VSMC proteins involved in cell contractility (125-127).

Additionally, the manner in which TGF-β_1 is secreted from cells and its association with ECM is also critically important to VSMC, maintenance and differentiation. TGF-β_1 is translated as an inactive form known as Pro-TGF-β_1 (128) which consists of LAP +TGF-β_1. This pro-peptide is packaged and processed in the rough endoplasmic reticulum and Golgi apparatus (128) to form the small latent complex (SLC) composed of LAP + TGF-β_1 bound by noncovalent bonds. The complex is further bound to LTBP-1 to the LAP via a covalent bond to form the Large Latent Complex (LLC) (113). After formation LLC is then excreted from the

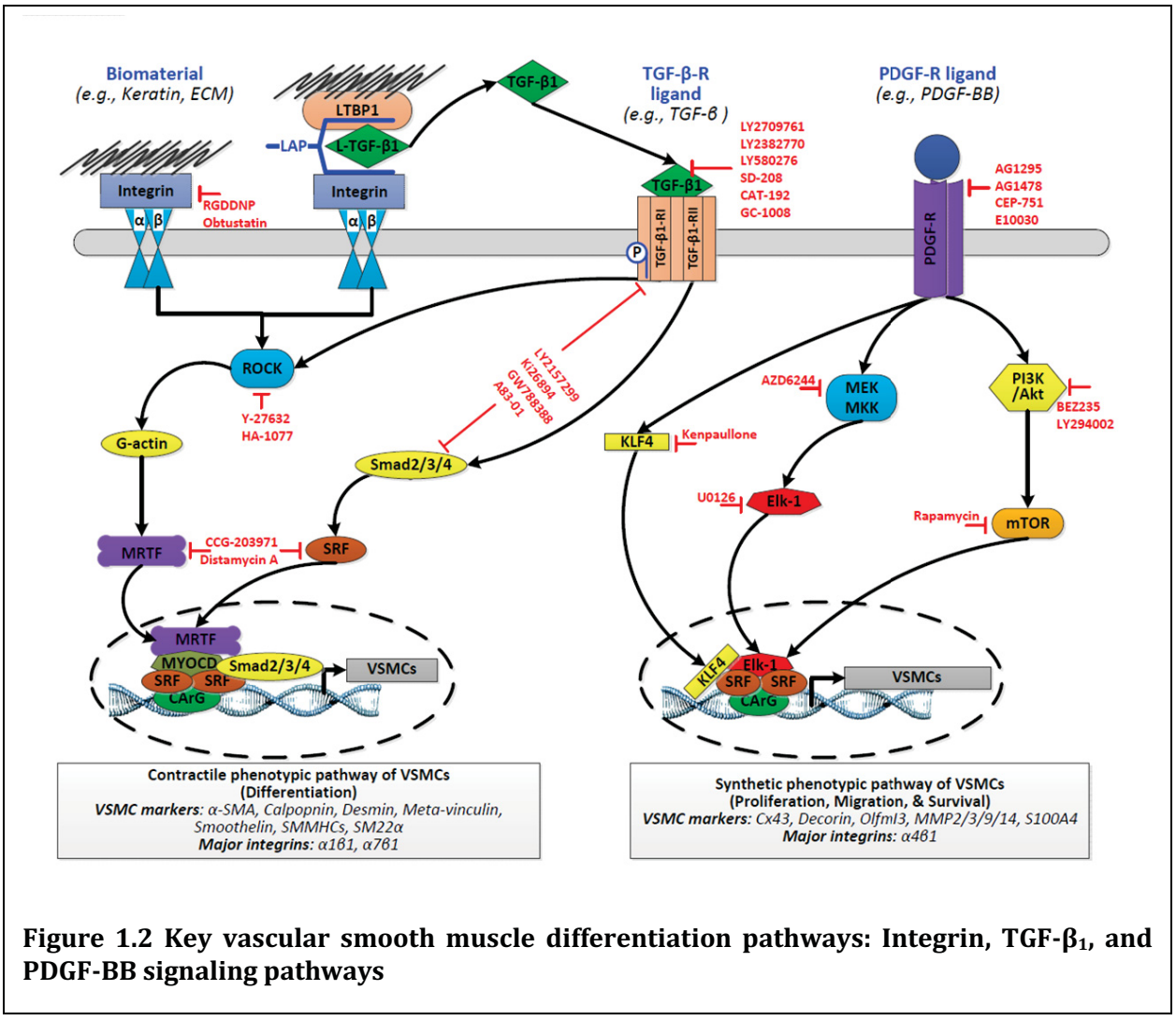

Figure 1.2 Key vascular smooth muscle differentiation pathways: Integrin, TGF-β_1, and PDGF-BB signaling pathways

cell and then is bound by fibrillin and fibronectin in the extra cellular matrix (ECM) (113). The LLC can be releases TGF-β_1 via various mechanisms including mechanical stretch via integrin's, or by proteolysis (99-101).

1.5.2.3 PDGF-BB Signaling

Platelet-derived growth factor-BB is the ligand (PDGF-BB) for Platelet-Derived Growth Factor Receptor-β (PDGRF-β) a tyrosine kinase receptor. PDGF-BB and its receptor PDGFR-β are crucial in cardiovascular development. PDGRF-β is expressed by mural cells (VSMCs and pericytes), PDGF-BB is concentrated to the developing endothelium and functions recruit mural cells to the developing vascular structure (129). PDGF-BB has been widely reported to play a critical role in VSMCs proliferation, recruitment and migration (88, 130-134). During development PDGF-BB plays an important role in producing contractile VSMCs, and this has been demonstrated both *in vivo* (135), and *in vitro* (136-139). During development PDGF-BB works alongside histone deacetylase 7 (HDAC7) to direct differentiation through histone modification (139, 140). Interestingly in mature VSMC and adult stem cells PDGF-BB promotes a synthetic phenotype and is commonly associated with atherosclerosis (132, 133). Features associated with PDGF-BB activated VSMCs include: hypertrophy, increased proliferation, low contractility, and increased ECM deposition (131, 141).

1.6 Summary and Overall Experimental Design

1.6.1 Summary

Keratin based biomaterials and KOS specifically represent a burgeoning material source in biomedical research. KOS based materials have not caused an acute immune response in any of the studies we found reported in the literature. These studies include a wide range of biomedical applications including drug release studies and several tissue engineering applications. Āovel formulations of KOS based biomaterials allow for better control of material degradation and strength, which have expanded the use of these materials for purposes such as drug and cell delivery. Such advances have made KOS suitable for complex tissue engineering applications.

Still, there are limitations of both the KOS material and the scope of research that has been conducted. KOS does not spontaneously self-assemble like KTN due to the oxidation of cysteine, which diminishes its ability to form disulfide bonds. Techniques to impart greater mechanical strength in KOS have been investigated by our lab using a natural chemical cross linker (genipin) (24), but more research is needed in this area. Other researchers have examined combinations of KOS and other biomaterials to increase its mechanical strength (45, 142). The use of KOS hydrogels combined with other material, chemical, and/or enzymatic cross linkers can enhance the mechanical strength and broaden the range of applications for KOS based biomaterials.

Further, exploration into the complex interactions of cells and tissues with KOS are needed to optimize and take advantage of the inherent biocompatibility of the KOS material. Detailed studies of the interactions of KOS with bioactive compounds such as growth factors like BMP-2 are necessary to understand the mechanisms behind these interactions. Selecting a few key growth factors and examining the biochemistry behind these interactions would be very useful to aid in the design of KOS based materials and select applications for which KOS would be particularly well suited. Detailed binding studies and examination of downstream signaling triggered by these interactions will allow researchers to engineer more materials that are precisely applicable to induce desired regenerative outcomes at the molecular level.

Another area that we found lacking was there were no studies in large animals, which would be useful in translation to human trials. Skeletal muscle and nerve regeneration are the two applications that could benefit tremendously from studies in large animals such as pigs. A larger animal would be a better size match and thus more anatomically comparable with humans. If KOS based regenerative approaches have success in larger animal models, then both skeletal muscle and peripheral nerve regeneration would become very strong candidates to move forward into human clinical trials.

Stem cell based therapies used in clinical practice fall in one of two categories, non-resident cardiac stem cells, and cardiac stem cells (5). Non-resident cardiac stem cells investigated in either clinical trials or pre-clinical trials include: SKM, BMMĀCs, BM-MSCs, EPCs, adipose MSCs, ESCs, and iPSCs. Cardiac stem cells include: side populations cells, c-kit$^+$ cells, cardiosphere derived cells, Sca1$^+$ cells, Isl1$^+$ cells, and EPDCs. Each cell type comes with

benefits and potential drawbacks. While many cell types have been extensively investigated to regenerate vasculature in ischemic tissue, VSMCs (a major component of vascular tissue) has only been sparsely used to treat these disorders.

In the present study, we hypothesize that KOS hydrogel are able to maintain c-kit$^+$ hCSC culture and to promote the preferred differentiation of VSMCs via interactions between KOS and TGF-Ā1 receptor, while increased blood flow in ischemic hind limb may be related with increased revascularization following transplantation of VSMCs. Three Aims were proposed below to examine the hypothesis.

1.6.2 Overall Experimental Design

1.6.2.1 Aim 1 (CHAPTER 2)

The goal of the first study was to determine the effects of KOS hydrogels on c-kit$^+$ hCSC, viability, proliferation, morphology, and differentiation compared against a standard tissue culture poly styrene (TCPS) dish. Cell viability was measured with live dead assays, at days 1, 3 and 5 of culture. The same conditions were used for c-kit$^+$ hCSC proliferation, and morphology. Cell viability was equally high on both TCPS and KOS hydrogels, but proliferation and morphology were altered. Differentiation was induced with and without 5-Azacytidine (5-Aza) and measured at days 28 after induction. Differentiation was analyzed, by measuring genes and protein expression markers specific to cardiomyocyte, endothelial and VSM cell phenotypes. On TCPS c-kit$^+$ hCSCs differentiated toward a cardiomyocyte lineage as expected with 5-Aza induction, but on KOS hydrogels they preferentially differentiated toward VSMCs. This study demonstrated that KOS hydrogels could culture c-kit$^+$ hCSCs, and alter their differentiation towards a VSMC phenotype.

1.6.2.2 Aim 2 (CHAPTER 3)

The goal of the second study was to determine potential mechanisms behind the differentiation pattern of c-kit$^+$ hCSCs on KOS hydrogels. To accomplish this, we developed a protocol to produce VSMC differentiation on TCPS using rhTGF-β_1. Results demonstrated that c-kit$^+$ hCSCs could produce a similar phenotype on TCPS when supplemented rhTGF-β_1. We then measured the differentiation time-course and contractility of c-kit$^+$ hCSCs on TCPS and KOS hydrogels during a 28 day period of time using three VSMC protein markers, and a

collagen lattice assay. These experiments showed dramatic increases for all markers on KOS hydrogels without supplementing TGF-β_1, and that the KOS differentiated cells were more contractile. Additionally, we measured TGF-β_1 and its associated proteins during the course of differentiation. TGF-β_1 and its associated proteins were seen both on TCPS and KOS hydrogels. To demonstrate that TGF-β_1 was responsible for VSMC differentiation on KOS hydrogels we used inhibitory small molecules and neutralizing antibodies (ĀABs) against TGF-β_1 signaling. Our experiments show that both methods of inhibiting TGF-β_1 drastically decreased VSMC phenotype on KOS hydrogels.

1.6.3.2 Aim 3 (CHAPTER 4)

The main goal of this study is to determine the therapeutic potential of KOS hydrogel-derived VSMCs (Cells from KOS). We induced hind limb ischemia in 3 groups (n=15/group) of adult mixed gender non-obese diabetic Severely combined immunodeficient Gamma mice (NOD SCID Gamma/ ĀSG) by excising the femoral artery and vein, and then treated the mice with PBS, Cells differentiated on TCPS (Cells from TCPS), or Cells from KOS. Blood perfusion of the hind limbs was measured immediately before and after surgery, then 14, and 28 days after surgery using Laser Doppler analysis. Tissue vascularization, cell engraftment, and skeletal muscle regeneration were measured using immunohistochemistry, DiL vessel painting, and hematoxylin and eosin (H&E) pathohistological staining. During the 4-week period, both cell treatment groups showed significant increases in blood perfusion compared to the PBS-treated control, and at day 28 the Cells from KOS group had significantly better blood flow than the Cells from TCPS group. Additionally, the Cells from KOS group demonstrated a significant increase in the ratio of DiL positive vessels, capillary density, and a greater number of small diameter arterioles compared to the PBS-treated group. Further, both cell-treated groups had similar levels of engraftment into the host tissue. We conclude that Cells from KOS therapy increases blood perfusion in an NSG model of CLI, but does not lead to increased cell engraftment compared to other cell based therapies.

The short-term goal of this study is to investigate both *in vitro* and *in vivo* effects of KOS hydrogel on c-kit$^+$ hCSC culture, proliferation, differentiation, therapeutic potentials to treat ischemic hind limb, as well as to explore the mechanisms underlying the preferred-

VSMC differentiation. The long-term goal is to develop KOS-based stem cell therapy to treat ischemic diseases, such as heart attack or peripheral artery diseases.

CHAPTER 2: KERATOSE HYDROGELS PROMOTE VASCULAR SMOOTH MUSCLE DIFFERENTIATION FROM C-KIT POSITIVE HUMAN CARDIAC STEM CELLS

2.1 Abstract

Stem cell-based therapies have demonstrated great potential for the treatment of cardiac diseases, *e.g.,* MI; however, low cell viability, low retention/engraftment, and uncontrollable *in vivo* differentiation after transplantation are still major limitations, which lead to low therapeutic efficiency. Biomaterials provide a promising solution to overcome these issues due to their biocompatibility, biodegradability, low/non-immunogenicity, and low/non-cytotoxicity. The present study aims to investigate the impacts of KOS hydrogel biomaterial on cellular viability, proliferation, and differentiation of c-kit$^+$ hCSCs. Briefly, hCSCs were cultured on both KOS hydrogel-coated dishes and regular tissue culture dishes (TCPS control). Cell viability, stemness, proliferation, cellular morphology, and cardiac lineage differentiation were compared between KOS hydrogel and the TCPS control at different time points. We found that KOS hydrogel is effective in maintaining hCSCs without any observable toxic effects, although cell size and proliferation rate appeared smaller on the KOS hydrogel compared to the TCPS control. To our surprise, KOS hydrogel significantly promoted VSMC differentiation (~72%), while on the TCPS control dishes, most of the hCSCs (~78%) became cardiomyocytes. Further, we also observed "endothelial cell tube-like" microstructures formed by differentiated VSMCs only on KOS hydrogel, suggesting a potential capability of the hCSC-derived VSMCs for *in vitro* angiogenesis. To the best of our knowledge, this is the first report to discover the preferred differentiation of hCSCs toward VSMCs on KOS hydrogel. The underlying mechanism remains unknown. This innovative methodology may offer a new approach to generate a robust number of VSMCs simply by culturing hCSCs on KOS hydrogel, and the resulting VSMCs may be used in animal studies and clinical trials in combination with an injectable KOS hydrogel to treat cardiovascular diseases.

2.2 Introduction

Cardiovascular disease is the leading cause of death in the United States, and acute MI alone accounts for over 18% of all deaths associated with heart disease (143). Stem cell therapy holds great promise for regenerative medicine, but the major challenges, such as cell death, uncontrollable *in vivo* differentiation, and inability of cells to successfully incorporate into the host tissue, limits the efficiency of stem cell-based therapy (6-8). C-kit$^+$ hCSCs are resident cardiac stem cells that exhibit basic stem cell properties (self-renewing, clonogenic, and multipotent) as well as an ability to differentiate into all cardiovascular lineages (8, 9). Although the functional contribution of c-kit$^+$ hCSCs to *in vivo* cardiomyocyte turnover is one of the centrally debated issues concerning their regenerative potential (7, 10), plentiful preclinical and clinical studies have provided enormous evidence to demonstrate their *in vitro* abilities of cardiac lineage differentiation (*i.e.,* CMs, endothelial cells-ECs, and VSMCs) as well as *in vivo* capacity to improve cardiac function following transplantation (7, 8, 11-14). Regardless of differences between *in vitro* and *in vivo* studies of c-kit$^+$ hCSCs, the major challenges described above still remain to be solved for all stem cell-based therapies (6, 11, 12, 14).

Biomaterials possess several beneficial attributes, such as biocompatibility, biodegradability, low/non-immunogenicity, and low/non-cytotoxicity, to overcome the above issues (15). Keratin is a natural biomaterial that has all of the above beneficial properties. More importantly, this structural protein can be readily isolated from various tissues such as the hair and skin of animals or humans and easily produced in various formats (film, sponges, and hydrogels) (17). Over the last few decades, knowledge of keratin and its derivatives has significantly increased, especially in regard to their ultrastructure, molecular and cell biology, physiological and pathological roles, as well as their practical applications in drug delivery and cellular/tissue engineering in regenerative medicine (144). Due to its low/non-immunological response, keratin does not induce immune response, even in allogeneic or xenogeneic transplantation (17, 35). *In vitro* studies have shown that keratin can significantly enhance the colony-forming efficiency of human mesenchymal stem cells (20), regulate differentiation and proliferation of blastemal cells (21), modulate adhesion, proliferation, and differentiation of adipose-derived stem cells (22); and it was

even suggested as a potential stem cell marker (23). However, to date, no studies have been reported regarding the utilization of KOS hydrogels to culture c-kit$^+$ hCSCs. The only *in vivo* study using a keratin-based hydrogel in repairing heart infarction is the rat model reported by Shen and colleagues (36), in which direct injection of keratin into infarct hearts was shown to significantly promote angiogenesis, preserve cardiac function, and attenuate ventricular remodeling compared to the vehicle control. Thus, it is important to understand the basic impacts of keratin on hCSC proliferation and differentiation.

In the present study, we aim to examine whether KOS hydrogel is capable of maintaining hCSC culture and proliferation and how KOS hydrogel affects cardiac lineage differentiation compared to regular TCPS. Various techniques, including Live/Dead cell viability assay, cell proliferation assay, Real-time PCR, Western blot, and ICC were used in the study. Our long-term goal is to investigate the feasibility of using c-kit$^+$ hCSCs in combination with KOS hydrogels as a new platform for stem cell differentiation and/or for biomaterial-based stem cell therapy to treat cardiovascular diseases.

2.3 Materials and Methods

2.3.1 Reagents

All chemicals used in the present study are listed below unless otherwise stated elsewhere: 30% Bis Acrylamide Clarity ECL Western Blotting Substrate, and Laemmli Buffer (all from Bio-Rad, Hercules, CA), 5-Aza, Beta-mercaptoethanol (Ā-ME), Bovine Serum Albumin (BSA), Bradford Reagent, Erythropoietin (EPO), L-glutathione, Paraformaldehyde (PFA), and Peracetic Acid (all from Sigma-Aldrich, St. Louis, MO), Click-iT Plus EdU Proliferation kit (EdU), Ham F12 Āutrient Mixture, High Capacity cDĀA Reverse Transcriptase kit, Hoechst 33342 (Hoechst), Optimal Cutting Temperature Compound (OCT), Power SYBR Green PCR Master Mix, PageRuler Prestained Protein Ladder, Penicillin/Streptomycin (P/S), Radio Immunoprecipitation Assay Buffer (RIPA), Sodium Dodecyl Sulfate (SDS), Sucrose S5-500, TRIzol, Tris base, Trypan Blue, Calcein-AM, and Tween-20 (all from Thermo Fisher, Waltham, MA), basic Fibroblast Growth Factor (b-FGF) (PeproTech, Rocky Hill, ĀJ), Ethanol (Decon Laboratories, King of Prussia, PA), Fetal Bovine Serum (FBS) (JR Scientific, Woodland, CA), Genipin (Methyl (1S,2R,6S)-2-hydroxy-9-

(hydroxymethyl)-3-oxabicyclo [4.3.0] nona-4,8-diene-5-carboxylate) (Wako Chemicals, Richmond, VA), Lyophilized KOS (Dr. Mark van Dyke, Virginia Tech), Phalloidin 488 (Santa Cruz Biotech, Dallas, TX), Porcine pancreatic elastase (elastase) (Worthington Biochemical Corporation, Lakewood, NJ), Phosphate Buffered Saline (PBS) (Quality Biological, Gaithersburg, MD), and Vectashield Antifade Mounting Medium (Vector Laboratories, Burlingame, CA). Primers (see Table 2.1) and Antibodies (see Table 2.2) were purchased from various companies.

2.3.2 hCSC Isolation and Culture

Briefly, patient heart samples (*i.e.,* atrial appendages) were obtained as discarded tissues from local hospitals. Donor confidentiality was maintained at the hospital's request and no patient identification information or medical history was collected according to the approved protocol. A written consent agreement was obtained for collection of discarded atrial appendages by the hospital and all procedures were approved by the Institutional Review Board (IRB) of Virginia Polytechnic Institute and State University for human subject research. The isolation and culture of hCSCs were previously described (145). Briefly, the isolated cells were cultured in a 37^{o}C incubator (5% CO_2 and 21% O_2) with hCSC medium consisting of Ham's F12, 10% FBS, 10 ng/ml human b-FGF, 0.2 mM L-glutathione, and 0.005 U/ml human EPO. Cells were passaged every 3-5 days and underwent a maximum of 12 passages. Large culture dishes (100 mm dish or T75 flask) were used for cell expansion and maintenance, while middle- or small-well plates (6-well or 12-well plates) containing gelatin- or KOS hydrogel-coated coverslips were used in the specific assays described below.

To examine whether KOS hydrogel altered stemness, hCSCs maintained on regular TCPS culture dishes were transferred on KOS hydrogel-coated dishes and continuously cultured for 3 passages (13 to 15 days in total) in hCSC medium followed by c-kit antibody staining (see *Immunocytochemistry* below), and were compared to the cells passaged only on TCPS dishes.

2.3.3 Keratin Isolation and Hydrogel Formation

KOS was supplied by Dr. Mark Van Dyke's lab at Virginia Tech. Briefly, KOS was extracted and purified from human hair fibers that had been washed with detergent, rinsed,

and dried (50). For 100 g of fibers, 2 L of a 2% (w/v) peracetic acid solution was used to oxidize protein disulfide bonds by heating it at 37°C for 14 hours with gentle rotary stirring. The fibers were recovered by sieve and extracted twice with 4 L of 100 mM Tris base solution. The fibers were separated by sieve and the extract solutions combined, centrifuged to remove suspended particulates, and filtered through No. 4 Whatman filter discs (Thermo Fisher). The protein solution was purified and high molecular weight keratin nanomaterial was isolated by membrane filtration in a custom ultrafiltration system. The membrane cutoff used was 100 kDa and a proprietary buffer solution facilitated separation of the material of interest. After removal of low molecular weight contaminants, the keratin nanomaterial solution was concentrated against dilute buffer using the same 100 kDa membrane, frozen, and lyophilized (50). KOS hydrogel was made with 4.5% lyophilized oxidized keratin (w/w) in PBS 1.5% Genipin (w/w) in various culture plates or coverslips. The KOS hydrogel was plated at a thickness of ~1 mm and let sit for 12 hours to allow the Genipin to crosslink. Hydrogels that were to be used for photomicrographs were produced by making a "sandwich" between glass and plastic coverslips, so removing the glass coverslip after 12 hours produced a flat surface that was ideal for cell imaging. In both cases, hydrogels were then washed 3 times (5 minutes each) in PBS and covered with PBS for 48 hours to remove any residual Genipin from the hydrogels. After the PBS was removed, hCSCs were seeded on top of the KOS hydrogels.

2.3.4 Cell Viability Assays with Calcein-AM/ EthD-1 and Trypan Blue

hCSCs were plated at 1.5×10^5 cells in a regular 60 mm dish (TCPS control) or KOS hydrogel-coated 60 mm dish for 1, 3, and 5 days with hCSC medium. At each time point, medium was collected, and cells were enzymatically detached with 10 U/ml elastase for 3 minutes in a 37°C incubator. All cells (detached and floating dead cells collected from the medium) were pooled together for the Live/Dead assay using Calcein-AM/EthD-1. Briefly, collected cells were washed once with PBS and incubated simultaneously with 2 μM Calcein-AM and 4 μM EthD-1 in a 37°C incubator for 30 minutes. Meanwhile, control wells were subject to a 20 minute treatment with 70% methanol (dead cell controls) or without any treatments (live cell controls) and used to calculate cell viability. Following staining, cells

were collected in PBS by centrifuge and then replated in a 96 well plate at a density of $1x10^4$ cells per well. Six replicates of the experimental group and three replicates of the control group were used to collect data in a SpectraMax M5 plate reader (Molecular Devices).

Trypan blue was also used for evaluating cell death in a separate experimental group. In this case, cells were cultured in a 60 mm dish and elastase enzymatic detachment from the KOS hydrogel was the same as described above. The dead cells (Trypan blue positive) were counted using a Hemocytometer and cell viability (%) was obtained by dividing the number of live cells by the total number of cells. At least 1000 cells were counted in each group and the results were plotted against passage (P) numbers (P1, P2, and P3).

2.3.5 EdU Cell Proliferation Assay

Cells were plated at a density of $2.5x10^4$ cells per well on either gelatin-coated coverslips (Blank control) or KOS hydrogel-coated coverslips in 12-well plates. Cell proliferation was examined at Day 1, 3, and 5. Briefly, cells were incubated with EdU (5-ethynyl-2'-deoxyuridine) at a 1:500 dilution in hCSC medium for 18 hours and then stained by following the manufacturer's protocol included in the Click-iT EdU Cell Proliferation kit. After co-staining with Hoechst 33342, both the TCPS control and KOS hydrogel coverslips were mounted to glass tissue slides using Vectashield Antifade Mounting Medium and sealed with fingernail polish. Fluorescent EdU images were taken with an Olympus IX73 Microscope equipped with an XM10 Camera (Center Valley, PA). The images were then analyzed using ImageJ software (NIH). At least 1000 Hoechst cells were counted on each coverslip to calculate % of EdU positive cells over total number of cells (Hoechst nucleus staining). Statistical analysis and bar graphs were completed using Microsoft Excel 2013 and GraphPad Prism 5.

2.3.6 Cell Morphology Analysis with Phalloidin Staining

hCSCs were cultured at a density of $2.5x10^4$ cells per well on either gelatin-coated coverslips (Blank control) or KOS hydrogel-coated coverslips for 1, 3, and 5 days. The differentiated cells were also used in this assay (see *Cardiac lineage differentiation*). For Phalloidin staining, cells on the TCPS control and KOS hydrogel were fixed in 4% PFA at room temperature (RT) for 30 minutes and washed twice in PBS (5 minutes each) followed by

blocking in 1.5% BSA for 30 minutes. The resulting cells were stained with FITC-conjugated Phalloidin (1:500 dilution from 1000X stock) and Hoechst 33342 (1μM) in PBS for 1 hour at RT followed by 3 additional washes in PBS (5 minutes each). Coverslips were then mounted on tissue slides and fluorescent images were taken with the Olympus IX73 microscope mentioned above. Only cells cultured for 3 days were used for the cell morphological analysis (cell area and ratio of cell length per square of cell area) by Image J (NIH); cells on day 1 and 5 were not selected due to the cell density being either too low or too high to obtain accurate measurements. At least 500 cells in each group were analyzed and the results were plotted as bar graphs.

Furthermore, KOS hydrogels were subject to cryo-sectioning to determine the cell distribution and migration within the hydrogel. To this end, hydrogel samples were fixed in 4% PFA as described above and then embedded and frozen in OCT with 30% sucrose on an aluminum block in liquid nitrogen. Sample blocks were then serially cut at a thickness of 30 μm using a rotating cryostat (Reichert Histostat, Thermo Fisher) and stained with FITC-conjugated Phalloidin (1:500) and Hoechst (1μM) in 1.5% BSA for 1 hour at RT. Fluorescent images were taken using the Olympus IX73 microscope mentioned above with green (Phalloidin), blue (Hoechst 33342), and red (KOS hydrogel auto-fluorescence) filters.

2.3.7 Cardiac Lineage Differentiation of hCSCs

hCSCs were seeded in regular 6-well or 12-well culture dishes as described above. After 2 to 3 days of culture, the hCSC medium was switched to cardiac differentiation medium (DM) containing 89% Ham F12 Nutrient Mixture, 10% FBS, 1% P/S, and 10 μM 5-Aza as described previously (145). After the 3-day treatment with daily medium change, the differentiated cells were maintained in the above DM without 5-Aza up to 28 days with medium changed every other day. The same set of experiments as above were done to examine the effects of KOS hydrogel alone on hCSC differentiation using the same DM but without 5-Aza. In either case, the resulting cells were used for various assays listed below.

2.3.8 qRT-PCR (qPCR)

hCSCs were cultured in 6 well plates at a density of $6x10^4$ cells per well with hCSC culture medium or DM as described above. Total RNA was extracted using TRIzol reagent

Table 2.1 List of qPCR Primers

Primers		Sequence	Supplier
B2M	Forward	CCA GCG TAC TCC AAA GAT TCA	IDT
	Reverse	TGG ATG AAA CCC AGA CAC ATA G	IDT
c-kit	Forward	GTC ATC AGC CAC CAT CCT ATT	IDT
	Reverse	AGT CCA TAC CTC CCT CTC TTT	IDT
Nkx2.5	Forward	CGC ACC CAC CCG TAT TTA T	IDT
	Reverse	GGG TCA ACG CAC TCT CTT T	IDT
cTnI	Forward	GAC AAG GTG GAT GAA GAG AGA TAC	IDT
	Reverse	CTT GCC TCG AAG GTC AAA GA	IDT
vWF	Forward	GTA CAG CTT TGC GGG ATA CT	IDT
	Reverse	GCT CAC TCT CTT GCC ATT CT	IDT
VE-cad	Forward	CCAAAGTGTGTGAGAACGCT	IDT
	Reverse	CGTTTCGTGGTGTTATGTCC	IDT
SMMHC	Forward	TGGGCGAGATGTGGTACAGA	IDT
	Reverse	TCACGCGGGTGAGTATCCA	IDT
GATA6	Forward	AAAGAGGGAATTCAAACCAGGAA	IDT
	Reverse	GAAGTTGGAGTCATGGGAATGG	IDT

Abbreviation: B2M: beta-2-microglobulin; c-kit: Cluster of differentiation 117 (*i.e.*, CD117); cTnI: cardiac troponin I; GATA6: GATA binding protein 6; IDT: Integrated DNA technologies; Nkx2.5: NK2 homeobox 5; SM-MHC: Smooth muscle myosin heavy chain; VE-cad: VE-cadherin or Vascular endothelial cadherin or CD144; vWF: von Willebrand factor.

and RĀA concentration was determined using the NanoDrop 1000 Spectrophotometer (Thermo Scientific). One microgram of total RĀA was reversely transcribed in a 20 ĀL reaction volume using the High Capacity cDĀA Reverse Transcriptase kit according to the manufacturer's protocol. The resulting cDNA was then diluted 2-fold in nuclease-free water (12.5 ng per well) and used as a template for qPCR analysis using Power SYBR Green PCR Master Mix in the StepOnePlus Real-Time PCR System (Thermo Fisher). The following protocol was utilized in all experiments: a 10 minute holding stage at 95^{o}C, followed by 44 cycles at 95^{o}C for 15 seconds and 60^{o}C for 1 minute, then a melting curve stage of 95^{o}C for

15 seconds, 60°C for 1 minute and 95°C for 15 seconds. The primers are listed in Table 2.1. Each target gene was examined in triplicate and the relative expression levels were analyzed using StepOne Software v2.3 provided on the machine. The data are expressed as fold change relative to the Pre-Differentiation (Pre-Diff) after normalization to internal control of beta-2-microglobulin (B2M).

2.3.9 Western Blotting

Cells were cultured at a density of $6x10^4$ cells per well in either the TCPS control or KOS hydrogel-coated 6-well plates using hCSC culture medium or DM as described above. For the TCPS control, cell lysate was directly obtained by adding RIPA buffer, while for the KOS hydrogel-coated wells, cells were first detached using 10 U/ml elastase for 3 minutes and washed once with PBS to remove any residual hydrogel before being treated with RIPA buffer. Protein lysate was quantified using the Bradford assay and then mixed with 4X loading buffer (10% β-ME in laemmli buffer) at a 1:4 dilution and incubated for 5 minutes at 95°C. Samples were then loaded into an SDS-Stacking gel and ran in a Mini Protean Tetra Cell (Bio-Rad) at 100V for 15 minutes followed by 150V for 60 minutes. The protein was then transblotted onto a PVDF -membrane using a Mini Protean Tetra Cell in an ice bath at 95V for 1.75 hours. The transblotted membrane was blocked for 1 hour at RT in 5% milk solution in Tris-Buffered Saline and Tween-20 (TBST) on a plate rocker. Membranes were immunoblotted with specific primary antibodies (c-kit, α-sarcomeric actin "α-SA", CD31, and α-SMA) (see Table 2.2) to identify stem cells, CMs, ECs, and VSMCs, respectively. Beta-actin (Ā-A) was used as an endogenous control. The following optimized conditions were used in the study: 1:500 (c-kit), 1:1000 (Ā-A), 1:500 (CD31), 1:1500 (α-SMA), and 1:20000 (Ā-SA). All antibodies were diluted in 5% milk solution and incubated with PVDF membranes overnight on a plate rocker at 4°C, then washed 3 times (5 minutes each) with TBST solution. The membranes were then incubated with mouse or rabbit secondary antibody conjugated with HRP at 1:10000 for 2 hours at RT on a plate shaker. Films were washed and treated with luminol and images were taken immediately on a Kodak Image Station 400MM.

2.3.10 Immunocytochemistry

Cells were plated at a density of $2.5x10^4$ cells per well on either the Blank coverslips or KOS hydrogel-coated coverslips in a 12-well plate and cultured in hCSC or DM as described above. Four specific primary antibodies (c-kit, α-SA, α-SMA, and CD31) (see Table 2.2) were used to identify stem cells, CMs, ECs, and VSMCs, respectively. Briefly, cells were washed once with PBS, fixed in 4% PFA at RT for 1 hour, and then blocked in 1.5% BSA and 0.2% Tween20 buffer for 30 minutes at RT. The resulting cells were then incubated with 1:200 c-kit, 1:500 CD31, 1:1000 α-SMA, and 1:2000 α-SA primary antibody for 2 hours at RT on a shaker and then washed 3 times with PBS (5 minutes each) and stained with a secondary antibody, either goat anti-rabbit Alexa Fluor 488 or goat anti-mouse Alexa Fluor 488, at a

Table 2.2 List of Primary and Secondary Antibodies

Antibody Name	Antibody Type	Supplier	Catalog Number
c-kit (H300 clone)	Primary Polyclonal Rabbit	Santa Cruz Biotech	sc-5535
CD31 (PECAM-1)	Primary Polyclonal Goat	Santa Cruz Biotech	sc-1506
β-A	Primary Polyclonal Rabbit	BosterBioTech	pa1872
α-SMA	Primary Polyclonal Rabbit	ThermoFisher	PA519465
α-SA	Primary Monoclonal Mouse	Sigma-Aldrich	A2172
Alexa Flour 488	Secondary Goat Anti Mouse	Jackson Lab	115-545-062
Alexa Flour 488	Secondary Goat Anti Rabbit	ThermoFisher	R37116
Alexa Flour 488	Secondary Chicken Anti Goat	ThermoFisher	A21467
Peroxidase-Conjugated	Secondary Goat Anti Rabbit	Jackson Lab	65-6120
Peroxidase-Conjugated	Secondary Goat Anti Mouse	Jackson Lab	115-035-062
Peroxidase-Conjugated	Secondary Mouse Anti Goat	Jackson Lab	205-035-108

Abbreviation: c-kit: Cluster of differentiation 117 (*i.e.*, CD117); β-A: Beta Actin; α-SMA: alpha Smooth Muscle Actin; α-SA: Cardiac alpha Sarcomeric Actin.

concentration of 1:2000 in blocking buffer. An additional set of coverslips were stained with only a secondary antibody as a negative control, and Hoechst 33342 was used in all groups to label cell nuclei. To avoid the auto-fluorescent interference from the KOS hydrogel, cells on the KOS hydrogel were first detached and then cytospun on a glass tissue slide following the antibody staining mentioned above. Fluorescent images of the Blank coverslips (attached cells) and KOS-hydrogel (cytospun cells) were taken using the Olympus IX73 microscope mentioned above. The percentage of positive cells for each cell type was counted and calculated against the total number of nuclei and the results were plotted as a bar graph for statistical analysis.

2.3.11 Statistical Analysis

All experiments were repeated at least 3 times with more than 3 replicates per each group. All data are shown as Mean±Standard Error (SE) unless otherwise stated. Student's t test with a two-tailed distribution was used to compare two groups. One-way analysis of variance (ANOVA) followed by the Bonferroni test was used to compare three or more groups with $p<0.05$ being considered statistically significant. GraphPad Prism 5 and Microsoft Excel 2013 were used for statistical analysis and plotting.

2.4 Results

2.4.1 KOS Hydrogels Maintain Cell Viability and Stemness, but Reduce Cell Proliferation Rate of C-kit Positive hCSCs

To determine whether KOS hydrogel can be used as a delivery vehicle for future stem cell-based therapy, we need to first examine the impact of KOS hydrogel on cell viability and proliferation in the following *in vitro* studies. Briefly, after being enzymatically detached from the TCPS or KOS hydrogel-coated dishes, cells were co-stained with Calcein-AM and EthD-1 and then transferred into 96-well plates for analysis using fluorescent microscopy and a plate reader. The results indicate that most cells are viable after 5 days of culture (Figure 2.1A, green) and only a small number of them appear dead (Figure 2.1A, red). Quantitative analysis shows no statistically significant differences between the TCPS (93.3±0.7%, 96.4±2.3%, 94.3±2.4%) and KOS groups (94.4±1.2%, 93.2±2.2%, 95.4±2.0%) at

Day 1, 3, and 5, respectively (n=4-5, ns, Figure 2.1B). Thus, KOS hydrogel is able to culture and maintain hCSCs well without toxic effects.

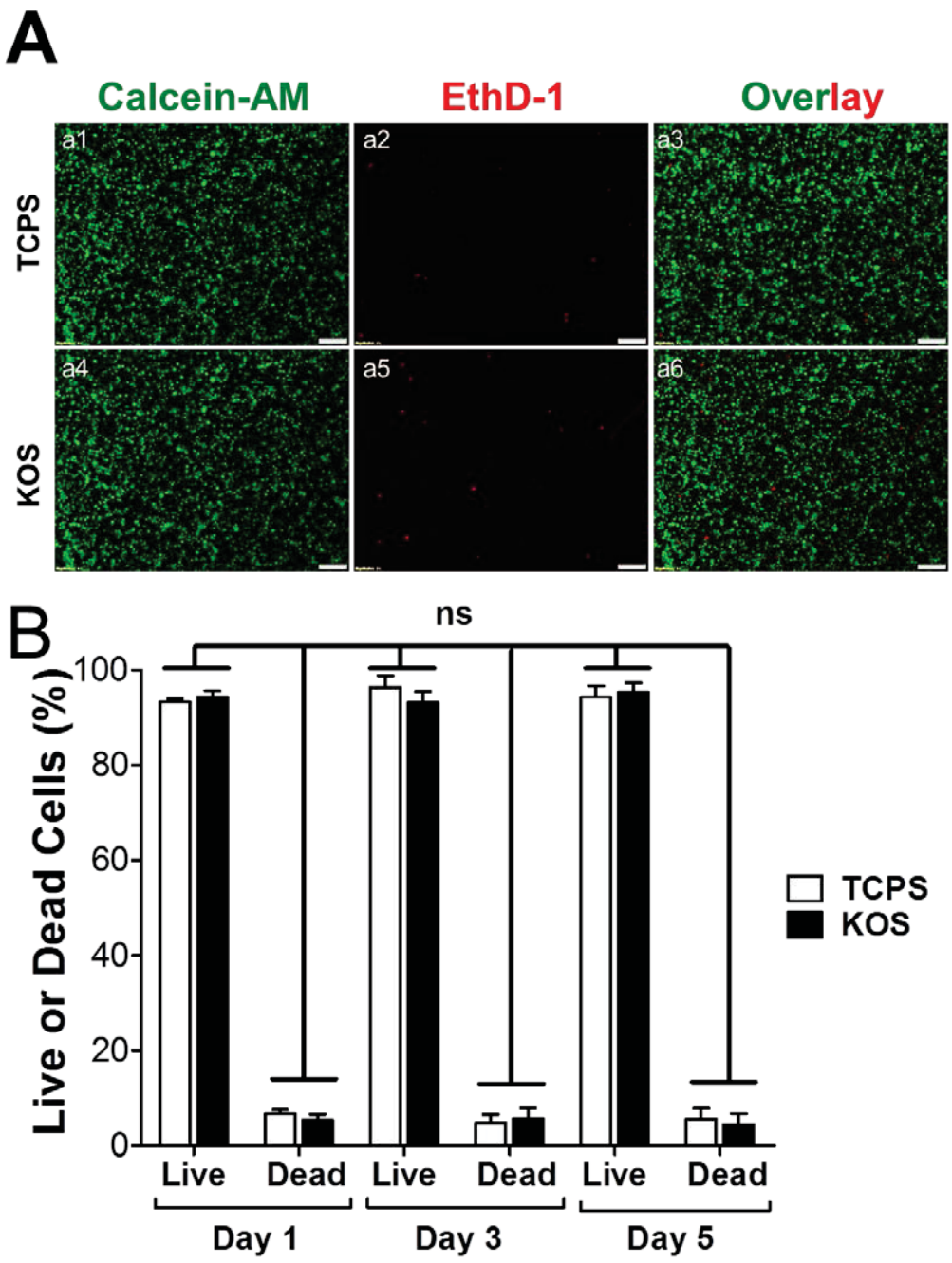

Figure 2.1 KOS hydrogels maintain c-kit$^+$ hCSC viability

Cells from TCPS control dishes or KOS hydrogel-coated dishes co-stained with Calcein-AM and EthD-1 representative day 5 images (A). Average data of percentages of live or dead cells (B). In Panel A, scale bar = 200μm; In Panel B, ns: not significant; n=5.

To determine the "long-term" effect of KOS hydrogel on cell viability, stemness (c-kit expression), and proliferation, a serial passage on KOS hydrogel was performed (Figure. 2.2 and Figure 2.8). Cells were cultured on the TCPS control and the KOS hydrogel-coated dishes

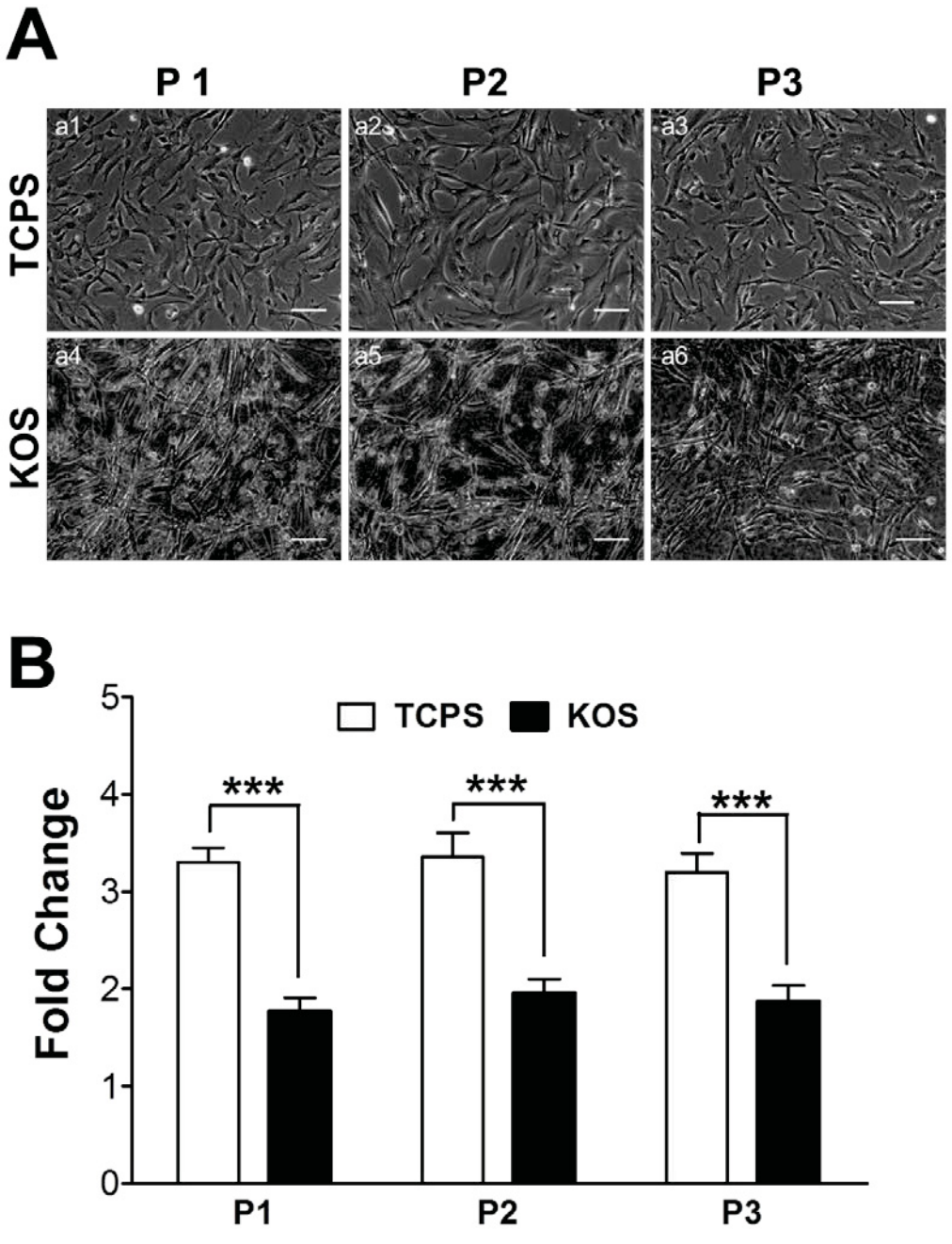

Figure 2.2 Sub-passaging hCSCs on KOS hydrogels

Representative phase contrast images of cultures taken with microscopy on P1, P3, and P5 (A). Fold changes of recovered cell numbers (B). In Panel A, scale bar = 400μm; In Panel B, ***: $p<0.001$; n=5.

for 3-5 days to reach 80-90% confluency before being split for the next passage on a new TCPS or KOS hydrogel-coated dish. Contrast microscopy images indicate that there are no significant differences in overall cellular morphology among passages 1 (P1), P2, and P3 (Figure 2.2A) in both the TCPS and KOS culture conditions, although the imaged cells

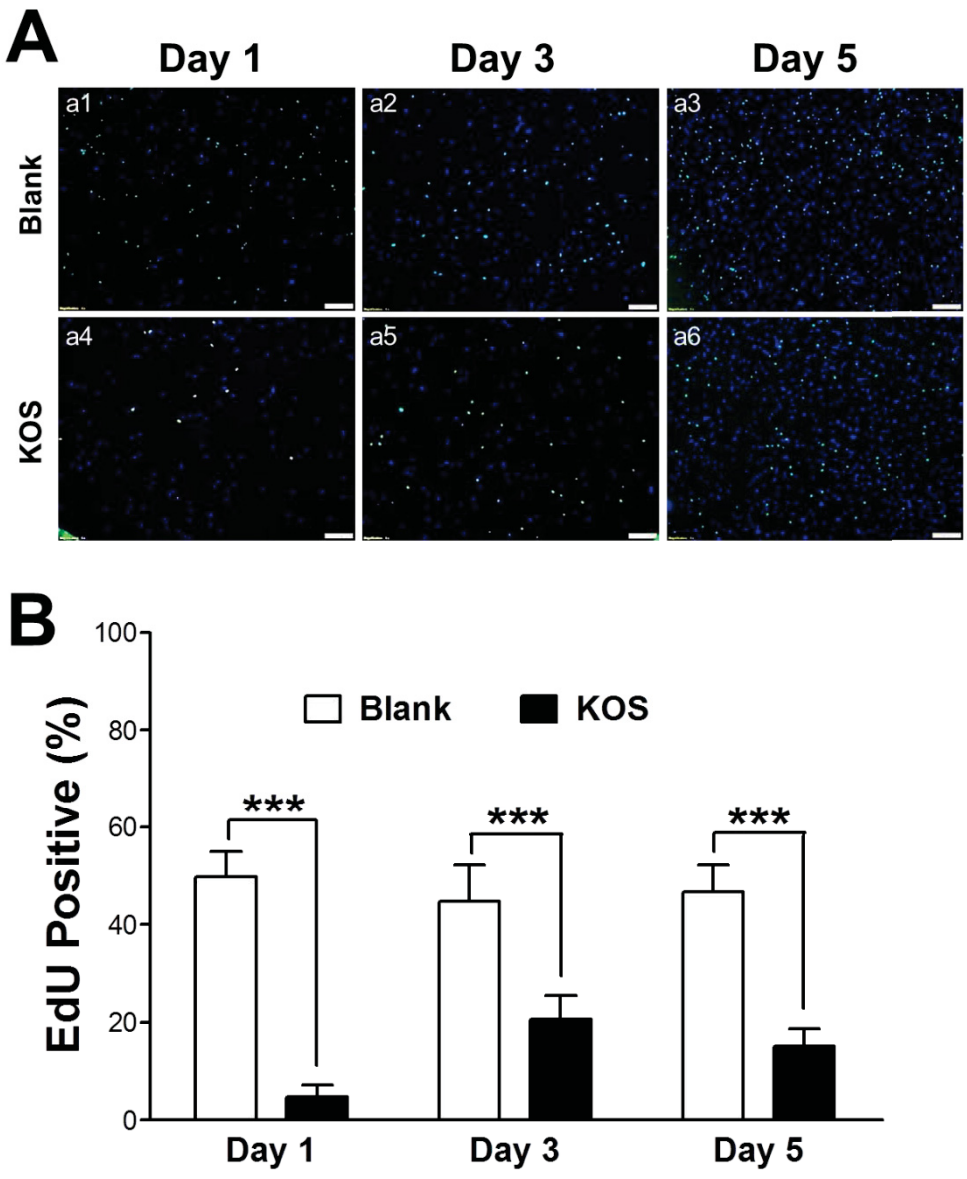

Figure 2.3 KOS hydrogels decrease c-kit$^+$ hCSC proliferation.

EdU positive nuclei in green refers to proliferative cells while Hoechst positive cells represent all nuclei (A). Mean percentages of EdU positive cells from KOS hydrogel and TCPS control dishes were plotted against time (Day 1, 3, and Day 5) (B). In Panel A, scale bar = 200μm; In Panel B, ***: p<0.001, n=6.

cultured on KOS hydrogel appear to be slightly more "narrow" or "bright" (which may be due to the light reflection of the KOS hydrogel). Quantitative analysis using Trypan blue staining demonstrated that the ratio of the number of cells recovered to the number of cells plated is comparable in both the TCPS control (3.31±0.15 in P1, 3.36±0.25 in P2, and 3.21±0.19 in P3) and in the KOS hydrogel culture (1.77±0.14 in P1, 1.96±0.15 in P2, and 1.87±0.16 in P3); however, the total number of cells in the TCPS control condition is significantly higher than that of the KOS hydrogel group across all passages (P1, P2, and P3) (Figure. 2.2B, n=5, $p<0.001$). Meanwhile, c-kit immunostaining demonstrated that KOS hydrogel was able to maintain the stemness of hCSCs well during the 3-passage period within 13 to 15 days at a high comparable expression level of c-kit on KOS hydrogel (90.2±5.8%) versus TCPS control (95.0±2.9%) (Figure 2.8, n=3, ns=not significance). These results imply that cell viability and stemness are well maintained during "long-term" culture, but proliferation rate seems lower in KOS hydrogel than in TCPS culture dishes.

To further confirm the above observation, we performed an EdU assay to quantitatively analyze cell proliferation. Briefly, for the Blank and KOS hydrogel conditions, cells were cultured on coverslips for up to 5 days. EdU staining and Hoechst nucleus co-staining were performed on Day 1, 3, and 5. The stained coverslips were flipped over and mounted on tissue slides and microscopy fluorescent images were taken from the bottom of the slides (to avoid and reduce auto-fluorescence of the KOS hydrogel) using the Olympus IX73 microscope mentioned above. As indicated from Figure 2.2, there indeed appears to be significantly more EdU^+ cells in the TCPS (a1 to a3) compared to the KOS hydrogel (a4 to a6) across each time point examined (Figure 2.3A). Mean percentages of EdU^+ cells in the TCPS (49.7±2.2%, 44.7±3.0%, and 46.7±2.3%) are significantly higher than those in the KOS hydrogel (4.7±1.0%, 20.6±2.0%, and 15.1±1.4%) at Day 1, 3, and 5, respectively (Figure2.3B, n=6, $p<0.001$ in all groups). These findings are consistent with the relatively lower number of cells observed in Figure 2.2B.

2.4.2 hCSCs do not Spontaneously Migrate into KOS Hydrogels, but Form "Endothelial Cell Tube-Like" Microstructures Following Induced Differentiation.

Previous study indicates that porous biomaterials enable cells to migrate into the material (146). To examine whether similar migration occurs in KOS hydrogel, we seeded

hCSCs on the KOS hydrogel and monitored cell location from the top-view (Figure 2.4A, a1 to a4) of a culture dish and the side-view (Figure 2.4A, a5 to a8) of a 30 μm cryosection of the KOS hydrogel following Phalloidin/Hoechst 33342 staining. Interestingly, all cells remained on the surface of the KOS hydrogel during the course of the 5-day culture as indicated in the side-view (Figure 2.4A, a5 to a7), although cell areas appear to become smaller and the ratio of the cell length/cell area is larger on the KOS hydrogel than on the TCPS (Figure 2.4B, n =3, *p<0.01 or p<0.001*, image data not shown). To our surprise, hCSCs on KOS hydrogels formed "endothelial cell tube-like" microstructures, similar to the

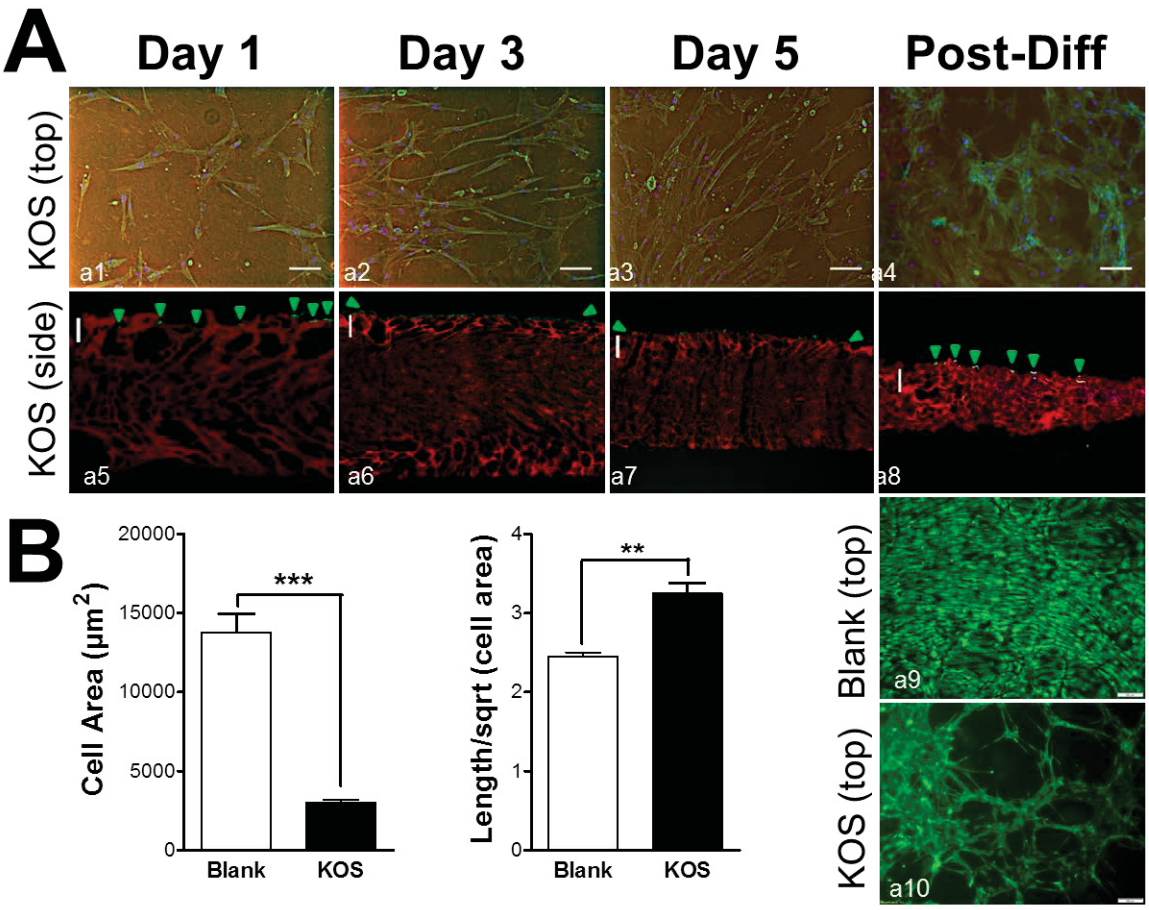

Figure 2.4 Cell distribution and morphology on KOS hydrogel

Phalloidin (a1 to a8) and Calcein-AM (a9 to a10) images of hCSCs taken on TCPS (data not shown) and KOS hydrogel before (Day 1, 3, 5) and Post-Differentiation (a4, a8, a9, a10) (A). Green = cellular F-Actin; Blue = nucleus (Hoechst 33342), and Red = KOS. Horizontal bar = 1000 μm and Vertical bar = 200 μm. The mean data of cell area and length/sqrt (area) is plotted on Panel B (B). n=3; ***p*<0.01; ****p*<0.001.

"endothelial cell tube" typically formed by endothelial cells on Matrigel coated plates (*i.e., in vitro* angiogenesis assay), on days 14 to 28 after induced differentiation (Figure 2.4A, a4, a10), while cells on TCPS culture dishes just appear over-confluent (Figure 2.4A, a9). This finding suggests that KOS hydrogels may promote angiogenesis of VSMCs differentiated from c-kit$^+$ hCSCs.

2.4.3 Predominant c-kit$^+$ hCSCs Become VSMCs after Induced Cardiac Differentiation on KOS Hydrogel

To investigate whether hCSCs tend to become VSMCs on KOS hydrogel compared to the TCPS control, hCSCs were cultured and differentiated as described above, followed by qPCR, Western blot, and Immunocytochemical assays using specific primers and antibodies.

The gene expression analysis using qPCR found that cardiac (ĀK2 Homeobox 5 – Nkx2.5 and Cardiac troponin I - cTnI), endothelial (von Willebrand factor - vWF and Vascular endothelial cadherin - VE-cad, *i.e.*, CD144), and vascular smooth muscle (Smooth Muscle-Myosin Heavy Chain - SM-MHC & GATA Binding Protein 6 - GATA6) markers showed no statistically significant differences between the TCPS control and the KOS hydrogel under the basal condition (Pre-Diff, Figure 2.5). However, these genes are dramatically up-regulated 28 days after 5-Aza-induced differentiation both on the TCPS control and the KOS hydrogel compared to the basal levels. Interestingly, the fold changes of cardiac genes were not different between the TCPS and the KOS hydrogel (Figure 2.5A), but endothelial markers showed statistical significance between the two culture conditions. The fold increases of vWF on the TCPS control (62.3±12.9) are higher than those on the KOS hydrogel (12.0±2.5) (Figure 2.5B, n=4, $p<0.05$) and the fold increase of VE-cad on the TCPS control (7.2±1.8) is lower than that on the KOS hydrogel (11.8±2.4) (Figure 2.5B, n=4, $p<0.05$). To our surprise, two vascular smooth muscle genes (SM-MHC and GATA6) show a robust increase with 19,517±5807 fold changes of SM-MHC and 1,226±390 fold changes of GATA6 on the KOS hydrogel compared to 355±80.4 and 33.4±10.9 fold changes of the same genes on the TCPS control (Figure 2.5C, n=4, $p<0.01$ and $p<0.05$), indicating that KOS hydrogel likely promotes hCSCs toward vascular smooth muscle differentiation.

Āext, we examined the protein levels of stem cell and cardiac lineage markers using immunostaining with specific antibodies. Western blot results (Figure 2.6) appear to agree

well with those in qPCR (Figure 2.5). Figure 2.6A shows that stem cell marker (c-kit) is strongly expressed before differentiation (Pre-Diff), but hard to detect after differentiation (Post-Diff). Interestingly, α-SA was greatly expressed on the TCPS control in contrast to the strong expressions of CD31 and α-SA on the KOS hydrogel (Figure 2.6A). Quantitative

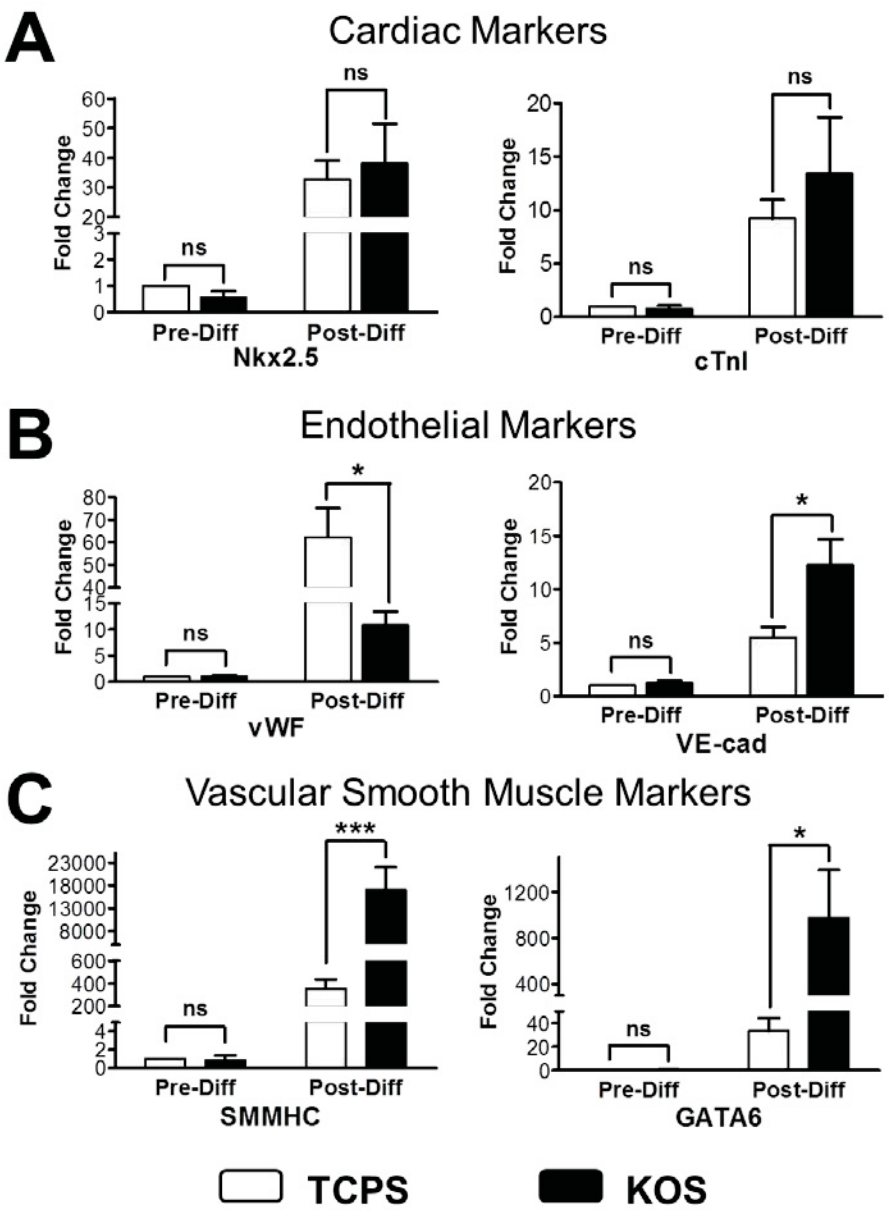

Figure 2.5 KOS hydrogels promote VSMC gene expression

Expression of cardiac (Nkx 2.5 and cTnI) (A), endothelial ((vWF and Ve-cad) (B), and smooth muscle (SM-MHC and GATA6) (C) plotted as Ratios (Pre-Diff RQ TCPS) n=4, ns=not significant, *$p<0.05$, ***$p<0.001$.

analysis of these bands shows 11.54±2.25 fold changes of α-SA on the TCPS control and much less on the KOS hydrogel (2.99±0.45) (Figure 2.6B, n=4-5, *p<0.001*). Additionally, there were 3.03±0.37 and 3.51±0.91 fold changes of CD31 and α-SMA on the TCPS control compared to

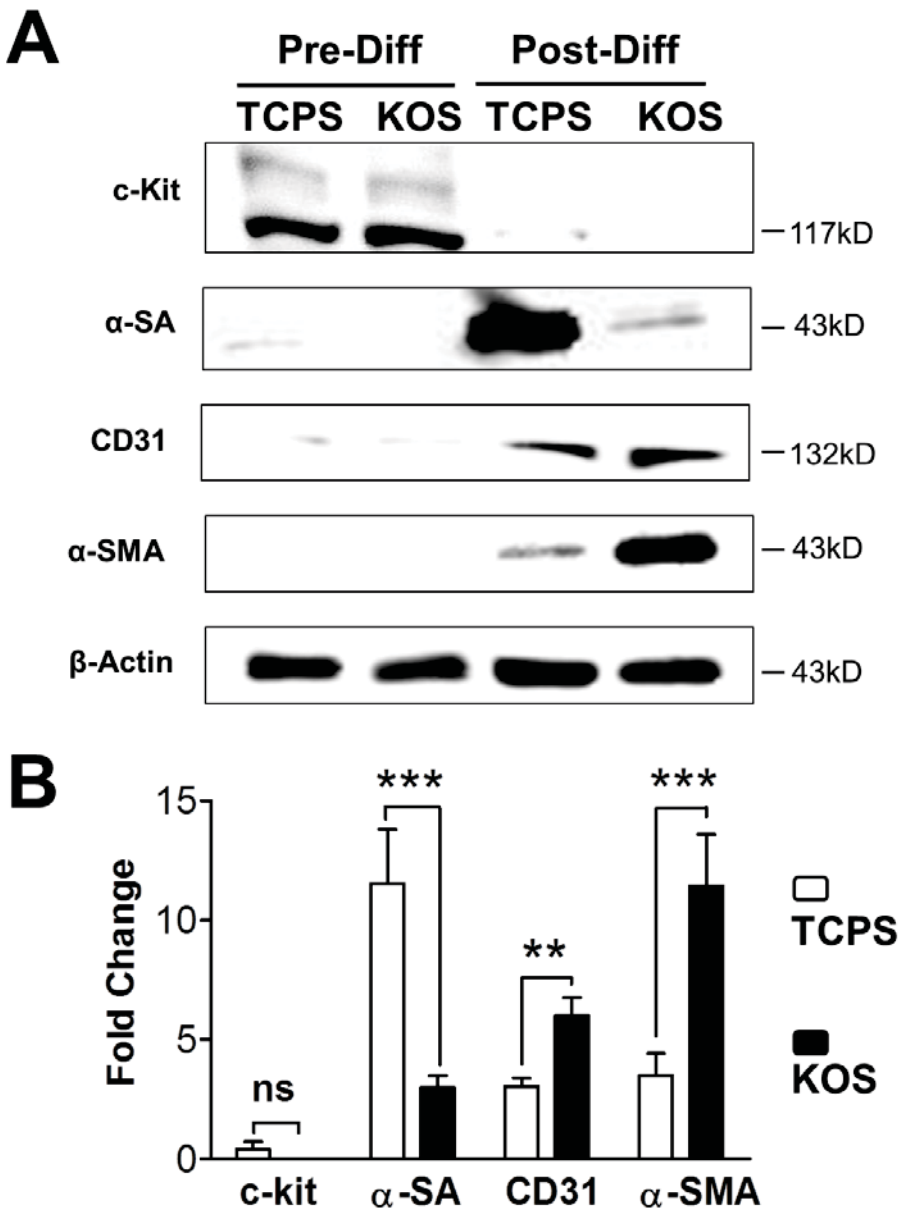

Figure 2.6 KOS hydrogels promote VSMC protein expression - Western blot analysis

Protein expression of stem cell (c-kit), cardiac (α-sarcomeric actin, α-SA), endothelial (CD31), and smooth muscle markers (α-smooth muscle actin, α-SMA) before differentiation induction (Pre-Diff) and 28 day after (Post-Diff) differentiation induction (A). Mean fold change of each protein were obtained by dividing expression levels of Post-Diff versus Pre-Diff following internal normalization with beta-actin of TCPS culture dish (B). n=5, ns=not significant, ***p<0.01,* ****p<0.001.*

6.01±0.75 and 11.45±1.93 fold changes on the KOS hydrogel (Figure 2.6B, n=4-5, *p<0.01,* and *p<0.001*), which confirms our expectation that the KOS hydrogel would enhance vascular smooth muscle differentiation of c-kit^{+} hCSCs.

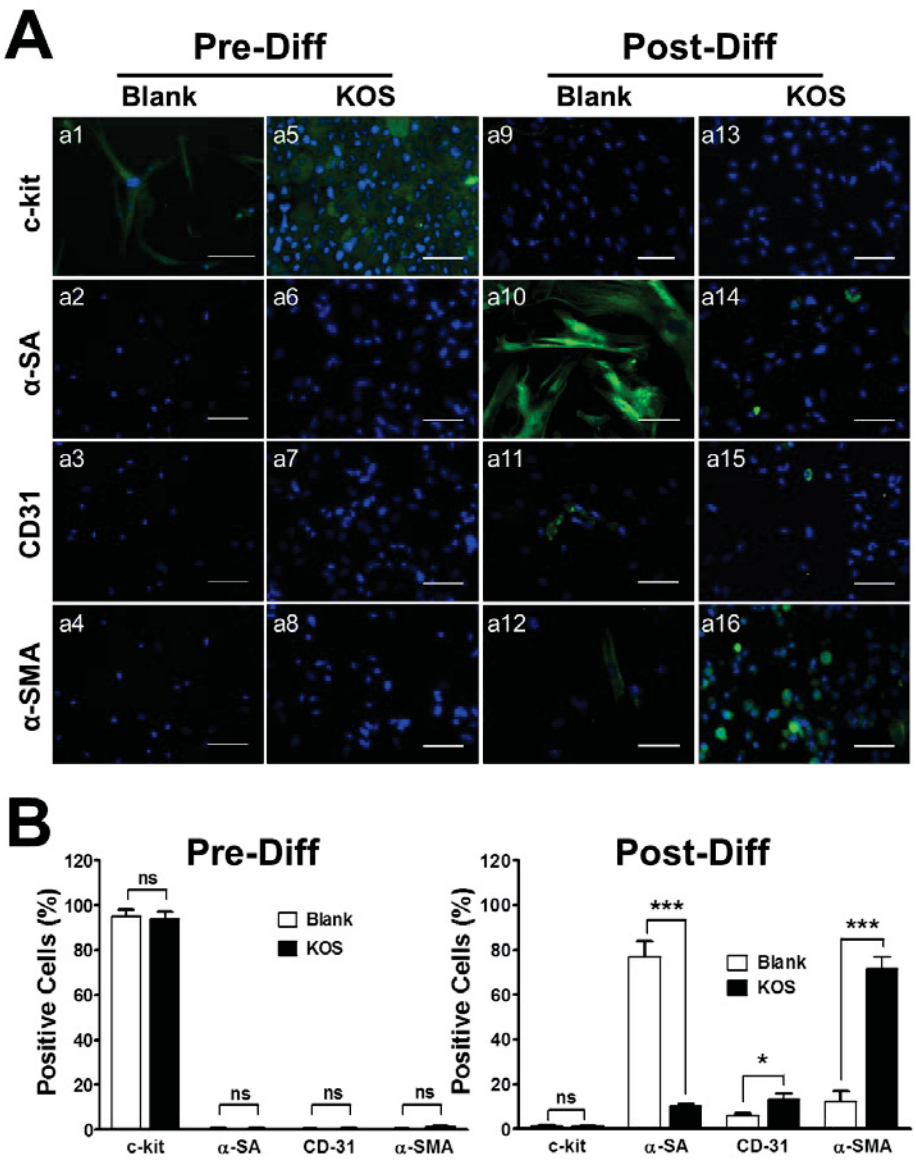

Figure 2.7 KOS hydrogels promote VSMC protein expression - Immunocytochemical staining

Protein expression of stem cell (c-kit), cardiac (α-sarcomeric actin, α-SA), endothelial (CD31), and smooth muscle markers (α-smooth muscle actin, α-SMA) before differentiation induction (Pre-Diff) and 28 day after (Post-Diff) differentiation induction (A). Mean percentages of positive cells counted against the total nucleus before (Pre-Diff) and after (Post-Diff) were plotted in Panel B (B). n=5, ns=not significant, *$p<0.05$, ***$p<0.001$.

Lastly, we used ICC to further confirm our above findings. Due to the interference of auto-fluorescence from the KOS hydrogel under fluorescent microscopy, all cells on the KOS hydrogel were first detached, stained with the specific antibody and then cytospun onto tissue slides before imaging, while cells on the Blank control coverslips were kept for staining and imaging under their "natural" morphology. As it shows in Figure 2.7, before differentiation almost all hCSCs are c-kit positive on both the TCPS control (95.0±2.94%) and the KOS hydrogel (93.9±3.25%), while the other three cardiac lineage markers (α-SA, CD31,

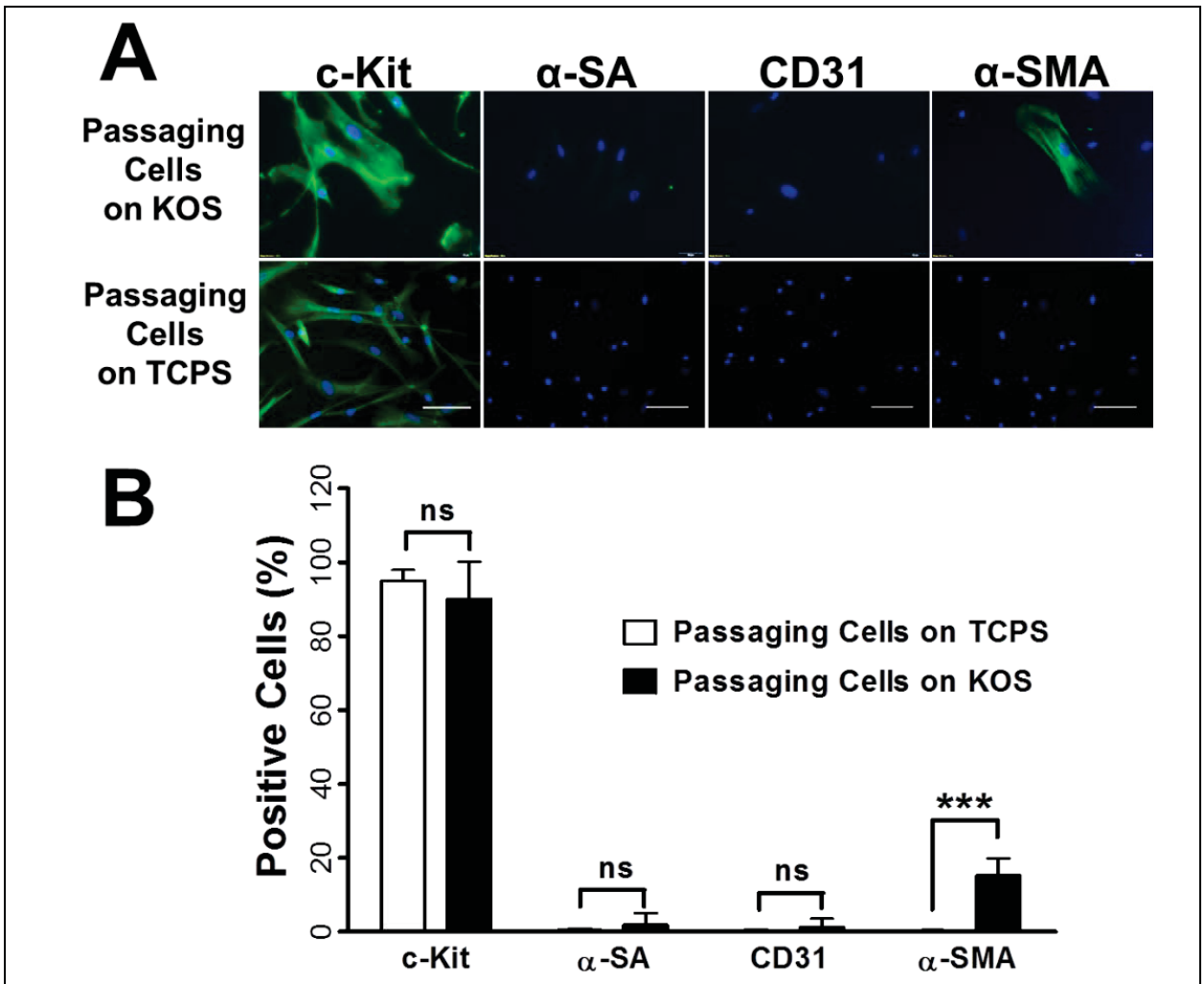

Figure 2.8 Effects of KOS hydrogel cell passaging on c-kit expression

Immunocytochemical staining before (Pre-Diff) TCPS and TCPS Passaged 3 times on KOS hydrogel then plated and stained on TCPS Protein expression of stem cell (c-kit), cardiac (α-sarcomeric actin, α-SA), endothelial (CD31), and smooth muscle markers (α-smooth muscle actin, α-SMA) were determined with specific primary antibodies and all secondary antibodies are conjugated with Alexa flour 488. Scale bar = 100μm (A). Mean percentages of positive cells counted against the total nucleus (B). n=3 or 5, ns=not significant, ****p<0.001.*

and α-SMA) are hardly detected (α-SA: 0.5±0.43% on TCPS vs 0.48±0.42% on KOS; CD31: 0.38±0.34% on TCPS vs CD31 0.33±0.23% on KOS; α-SMA: 0.3±0.23% on TCPS vs 1.27±0.34% on KOS, n=5, all are ns); however, after 28 days of differentiation, c-kit cells are observed on neither the TCPS control (1.58±0.28%) nor the KOS hydrogel (1.29±0.59%) groups; and instead, the majority of c-kit$^+$ cells became cells of cardiac lineages. Mean data shows 76.85±7.12 % α-SA$^+$, 6.26±0.85% CD31$^+$, and 12.45±4.37% α-SMA$^+$ cells on the TCPS control dishes compared to 10.23±1.1% α-SA$^+$, 13.18±2.9% CD31$^+$, and 71.58±5.25% α-SMA$^+$ cells on the KOS hydrogel-coated dishes (Figure 2.7B, n=5, p<0.001, p<0.05, p<0.001, respectively), suggesting that the TCPS culture condition tends to drive hCSCs toward CM differentiation, while the KOS hydrogel mainly drives them to become VSMCs.

2.5 Discussion

In the present study, we investigated the effects of KOS hydrogel on cell viability, stemness, proliferation, cellular morphology, and cardiac lineage differentiation of c-kit$^+$ hCSCs in comparison with cells cultured on regular culture dishes (TCPS control). The results show that both the KOS hydrogel and the regular culture dishes are able to culture and maintain hCSCs well without any observable toxic effects nor reduction of stemness caused by the KOS hydrogel (Figure 2.1, Figure2.2, and Figure2.8); however, cell size, ratio of cell length/size, and cell proliferation rate appear smaller on KOS hydrogel than for those on the TCPS control dishes (Figure 2.3 and 2.4). To our surprise, KOS hydrogel significantly promoted hCSCs becoming VMSCs after differentiation (with or without 5-Aza), in contrast to those cultured on regular culture dishes, in which case most hCSCs differentiated into CMs (Figure 2.5 to 2.7) and also see references (8, 14). Furthermore, differentiated VSMCs appeared to form "endothelial cell tube-like" microstructures (Figure 2.4), similar to the "endothelial cell tube" typically formed by ECs on Matrigel (*i.e.,* in tube-formation or *in vitro* angiogenesis assay) (147). To the best of our knowledge, this is the first report to discover the preferred differentiation of hCSCs toward VSMCs on KOS hydrogel. The innovative methodology by which cells can be recovered from KOS hydrogel through elastase dissociation makes it possible to analyze gene and protein expression without interference

of keratin molecules. Our findings may provide a new and simpler approach to generate a large number of VSMCs for cell-based therapy in cardiovascular diseases.

A number of natural biomaterials, such as collagen, Matrigel, and alginate, have demonstrated the ability to promote and maintain cell viability (35, 148-151). Keratins are naturally derived proteins that can be fabricated into several biomaterial forms including KOS hydrogels (oxidatively derived) (19). These materials are a potential polymeric system for several tissue engineering and regenerative medicine applications due to their ability to support cell attachment, proliferation, and migration (50). Our results show that KOS hydrogels are capable of maintaining high cell viability and stemness after serial passaging without any observable toxic effects, which is consistent with previous studies that used either the same material or different types of stem cells (17, 32, 152). Interestingly, cell proliferation rate is reduced on KOS hydrogel compared to the TCPS control dishes. It is commonly agreed that the physical environment and/or biochemical interaction between the biomaterial and the stem cells are critical mediators of cell behavior (153, 154). Cell proliferation and differentiation appear to be inversely proportional to substrate stiffness (155). Thus, the lower stiffness of KOS hydrogel substrates and/or the potential direct interaction of keratin molecules with β-integrin or Āotch1 signaling in hCSCs may play an important role in modulating hCSC proliferation and differentiation (154-156). Perhaps, a low proliferation rate observed in the present study may reflect the physiological rate of stem cell proliferation to meet the basic needs of homeostasis under normal conditions.

An additional interesting finding in the present study is that both hCSCs (c-kit^{+}) and hCSC-differentiated cells (CMs, ECs, and VMSCs) are unable to migrate into the KOS hydrogel during “long-term” culture and differentiation, showing “immobile” properties. Our findings appear to be different from other published studies, in which the cells (aorta smooth muscle cells and fibroblasts) are able to migrate into the porous hydrogel of various biomaterials (157, 158). The reason remains unknown, but is probably related to the pore size of the hydrogel substrate or cell type (159). Although the pore size of our KOS hydrogel seems larger than the cells in the middle portion under the side-view (Figure2.4A), the surface of the KOS hydrogel seems to form a continuous layer, which may have prevented the cells from migrating into the hydrogel. In addition, the interactions between the cells and the cell/keratin molecules may also play a role in this phenomenon (160, 161).

Tube-formation (also known as *"in vitro* angiogenesis") is a typical *in vitro* Matrigel assay to evaluate the angiogenic properties of ECs or EPCs (162). A surprising observation of the present study was the formation of "endothelial cell tube-like" microstructures from hCSC-differentiated VSMCs on KOS hydrogel, but not on TCPS control dishes. Whether or not this "tube-formation" property of VSMCs facilitates *in vivo* arteriogenesis or collaterogenesis needs to be further investigated using an animal model. The underlying mechanism of the "endothelial cell-like tube" formation remains unknown, although it may be due to the *in vitro* angiogenesis property of the mixed small percent (~13%) of ECs.

Āumerous publications have previously demonstrated that c-kit$^+$ hCSCs can be differentiated into three cardiac lineage cell types (*i.e.,* CMs, ECs, and VSMCs) in both *in vitro* and *in vivo* settings (8, 14, 83-85); however, whether hCSCs are able to differentiate into CMs after transplantation is still under debate (10). In the present *in vitro* study, we discovered for the first time that the majority (~72%) of hCSCs on KOS hydrogel become VSMCs after induced-differentiation (independent from 5-Aza) while for the TCPS control, the majority (~77%) of cells become CMs. The KOS hydrogel seems to switch the myogenic differentiation pattern from CMs on TCPS to VSMCs on KOS hydrogel, whether or not 5-Aza was added in the present study. This important finding may indicate a critical role of KOS hydrogel in modulating hCSCs toward vascular smooth muscle differentiation. However, the mechanism underlying the preferred-VSMC differentiation on KOS hydrogel remains to be determined. A good number of published studies implicated that TGF-β signaling might be a cause of VSMC differentiation from various types of stem cells, such as embryonic stem cells, bone marrow mesenchymal stem cells, adipose stem cells, and multipotent adult progenitor cells (163-166). It has been shown that keratin is able to enhance angiogenesis or cell differentiation through up-regulation of TGF-β signaling pathways (19, 36, 138, 156); while 5-Aza, as a demethylating epigenetic reagent, is known to be capable of promoting cardiac differentiation from various types of stem cells (167-170). Certainly, 5-Aza plays a critical role in the differentiation of hCSCs on TCPS control, but it is not necessary for the VSMC differentiation observed on KOS hydrogel (Figure 3.1). In the experiments where we simply induced differentiation by removing growth factors (bFGF and EPO) from hCSCs cultured on KOS hydrogels, we discovered nearly the same percentage of VSMCs (~71%) with or without the addition of 5-Aza. Moreover, the present study used FBS in DM, and FBS is known to

contain various growth factors, including TGF-β; thus we could not exclude the potential role of FBS-TGF-β on KOS-promoted VSMC differentiation (138). Interestingly, platelet derived growth factor (PDGF) and integrin signaling pathway were also found in mediating smooth muscle differentiation from pluripotent stem cells, scal-1$^+$ stem cells, and hair follicle stem cells, probably through a mechanotransduction signaling pathway (130, 131, 136). Thus, the complex interactions among keratin molecules and TGF-β, PDGF and the Integrin pathway may play a critical role in the preferred-VSMC differentiation (171-173).

2.6 Conclusions

In conclusion, our present study demonstrates that KOS hydrogels are able to well maintain cell viability and stemness, produce "endothelial cell tube-like" microstructures (similar to the "endothelial cell tube"), and significantly promote vascular phenotypes, especially VSM differentiation (independent from 5-Aza), from c-kit$^+$ hCSCs. These findings offer new methods, which are not only useful for generating a robust number of VSMCs from hCSCs by simply differentiating hCSCs on KOS hydrogel, but also for providing a practical therapeutic platform with an injectable stem cell-based KOS hydrogel in treating cardiovascular diseases. However, the present study is limited by a lack of mechanistic data. The complex biological interactions between cellular receptors and KOS hydrogel is a critical area to be further explored in understanding the cellular and molecular signaling pathways underlying the KOS-preferred VSMC differentiation. Future studies should examine the individual effects of KOS hydrogel, TGF-β, PDGF, and the Integrin pathway in a defined medium (*e.g.,* KnockOut™ Serum Replacement to replace FBS) in the presence and absence of pathway specific inhibitors. Studies showing a coherent and coordinated stage-specific sequence of gene and protein expression should also be performed. The transplantation of hCSC-differentiated VSMCs into ischemic animal models (*e.g.,* MI or hind limb ischemia) would be an important future study to determine the therapeutic roles of these cells in repairing damaged organs.

CHAPTER 3: ROLE OF TGF-β IN KOS HYDROGELS DIFFERENTIATION OF C-KIT$^+$ HUMAN CARDIAC STEM CELLS

3.1 Abstract

Previous work in our lab showed that c-kit$^+$ hCSCs cultured on KOS hydrogels promoted smooth muscle gene and protein expression. In this study, we plan to expand upon this work to determine how KOS promoted this differentiation pattern. Experiments were conducted by culturing c-kit$^+$ hCSCs on KOS hydrogels, TCPS, and collagen hydrogels. We investigated the time course of VSMC differentiation, cell contractility, inhibition of VSMC differentiation, and measured protein expression of TGF-β_1 and its associated proteins. Cell contractility was measured using a collagen lattice contraction assay. Expression of three VSM markers α-SMA, calponin, and SMMHC were monitored with IF prior to differentiation, 14, and 28 days after differentiation induction. VSM differentiation was inhibited with A83-01 on TCPS and KOS hydrogels, and TGF-β NAB on KOS hydrogels. Production of TGF-β_1 was measured using ELISA the day before and after differentiation induction, and every 7 days throughout the 28 day differentiation protocol. TGF-β associated proteins, LTBP-1, and LAP were measured prior to differentiation induction, then 14 and 28 days after induction using western blot. KOS hydrogel differentiated hCSCs significantly increased expression for all three VSM markers compared to TCPS differentiated cells. Additionally, KOS differentiated hCSCs were significantly more contractile than cells differentiated on TCPS. RhTGF-Ā1 was able to induce VSM differentiation on TCPS. VSM differentiation was successfully inhibited using TGF-β NABs and A83-01. ELISA analysis revealed that both TCPS and KOS hydrogel differentiated cells produced TGF-β_1, with higher levels being measured at early time points on TCPS and latter time points on KOS hydrogels. Results from supplementing rhTGF-β_1 to TCPS and KOS hydrogels revealed that KOS seems to interact with TGF-β to a greater extent. Western blot results revealed that LTBP-1 and LAP had elevated levels early during differentiation. Further, the levels of LTBP-1 and LAP were higher on KOS differentiated hCSCs than TCPS hCSCs. This study reaffirms previous results of a VSM phenotype observed on KOS hydrogels, and provides a strong evidence for TGF-β_1 inducing VSM differentiation on KOS hydrogels. Additionally, results from ELISA and western blot provide evidence that

KOS plays a direct role in this pathway via interactions with TGF-β_1 and its associated proteins, LTBP-1 and LAP.

3.2 Introduction

Heart Disease is the leading cause of mortality in the United States, accounting for 1 out of every 4 deaths at a cost exceeding 200 billion dollars annually. CAD is the most common type of heart disease killing over 370,000 people each year (174). To have any chance to regenerate intermediate sized vasculature of the heart it is necessary to produce and abundant source of VSMCs. Previously published data conducted in our lab has shown that c-kit$^+$ hCSCs differentiated on the keratin-based biomaterial KOS show a high percentage (~72%) of cells positive for smooth muscle marker α-SMA indicating potential vascular smooth muscle (VSM) differentiation (24). The etiology of this differentiation was unknown and for this reason, we chose to further investigate c-kit$^+$ hCSC differentiation on KOS hydrogels. Several processes have been described to produce VSMCs *in vitro* including; small molecules such as ascorbic acid (175), matrix proteins (176, 177), cyclic mechanical strain (178), and stimulation by various growth factors (PDGF-AA, PDGF-BB, TGF-β_1) (134, 179, 180).

Of the various methods used to induce smooth muscle differentiation *in vitro* TGF-β_1 signaling is certainly among the most commonly reported (111, 114, 120-122, 181). TGF-β_1 has been reported to produce VSMC differentiation in ESCs and somatic stem cells (111, 119, 123, 124), by increasing expression of VSMC contractile proteins and producing a corresponding contractile phenotype (125-127). TGF-β_1 is translated as an inactive form known as Pro-TGF-β_1 (182) which consists of the LAP and TGF-β_1. This pro-peptide is packaged and processed in the rough endoplasmic reticulum and Golgi apparatus (182) to form the SLC composed of LAP + TGF-β_1 bound by noncovalent bonds. This complex is further bound to LTBP-1 and to the LAP via a covalent bond to form the LLC (113). After formation LLC is then excreted from the cell and then is bound by fibrillin and fibronectin in ECM (113). This complex can release TGF-β_1 via various mechanisms (*e.g.* mechanical stretch or proteolysis) (99-101). After TGF-β_1 is released from LLC the free TGF-β_1 is available to

bind TGF-β receptor I/TGF-β Receptor II complex (TGFBRI/TGFBRII) (113). This activates the SMAD2/3 co-SMAD canonical TGF-β_1 signaling pathway (113-117).

Keratin biomaterials (including KOS hydrogels) are a new comer in biomedical research but have found a wide range of applications in a relatively short period of time. KOS hydrogels have been used in drug release and cell delivery (25, 28, 50, 51, 59), several models of nerve injury (32-35), and a study examined the use of KOS hydrogels in a rat model of MI (36). These studies have shown excellent biocompatibility, a range of biomedical applications, and potential as a therapeutic for cardiac regeneration. Keratin based biomaterials like KOS also offer distinct advantages over other biomaterials. For instance, KOS is not susceptible to enzymatic digestion by collagenases (183), and also contains cell binding motifs (19) that are not present in polysaccharide based biomaterials like alginate or chitosan. Compared to the alternative keratin biomaterial KTĀ KOS has a lower thiol content due to the method of extraction via oxidative chemistry versus reductive chemistry (18, 19). The oxidative process of protein extraction is ideal for applications requiring hydrogel formulations but comes with the trade-off that KOS has a lower capacity to spontaneously self-assemble via disulfide covalent crosslinking. This issue can be resolved by using chemical crosslinkers like genipin (24) which imparts greater mechanical strength to the material.

The objective of this study is to understand the molecular signaling behind VSM differentiation of c-kit$^+$ hCSC on KOS hydrogels. Based upon previously published data and preliminary evidence, we hypothesize that TGF-Ā1 is integral in the differentiation pattern observed on KOS hydrogels. To validate our hypothesis, we established a differentiation protocol to produce VSMCs from c-kit$^+$ hCSCs on TCPS, and KOS hydrogels. We then examined the differentiation time-course of cells prior to induction, 14 and 28 days after induction on KOS hydrogels and TCPS with a TGF-β_1 antagonistic small molecule (A83-01), and a pan TGF-β neutralizing antibody using immunofluorescence (IF) examining three markers for VSM differentiation (Table 3.2). Additionally, cell contractility was measured using a collagen lattice contraction assay. We then examined the cellular production of TGF-β_1, LAP, and LTBP-1 to determine how KOS interacts with TGF-β_1 and its associated proteins. The level of TGF-β_1 was measured prior to and after induction, and then every 7 days

throughout differentiation using a TGF-β_1 ELISA. LAP and LTBP-1 were measured from cell lysate prior to induction, 14 and 28 days after induction using Western blot.

3.3 Materials and Methods

3.3.1 Reagents

All chemicals used in the present study are listed below unless stated elsewhere: 30% bis-acrylamide, clarity ECL Western blotting substrate and Laemmli buffer (all from Bio-Rad), 5-Aza, β-mercaptoethanol, BSA, Bradford reagent, EPO, A83-01, l-glutathione, PFA, and peracetic acid (all from Sigma-Aldrich), Hoechst 33342 (Hoechst), Page Ruler Prestained Protein Ladder, P/S, RIPA buffer, Glacial Acetic Acid, SDS, sucrose S5-500, TRIzol, Tris base, Trypan blue, Knockout SR, Calcein-AM, and Tween-20 (all from Life Technologies), b-FGF (Pepro-Tech), ethanol (Decon Laboratories), FBS (JR Scientific), genipin (methyl (1S,2R,6S)-2-hydroxy-9-(hydroxymethyl)-3-oxabicyclo [4.3.0] nona-4,8-diene-5-carboxylate) (WakoChemicals), lyophilized KOS (Dr. Mark Van Dyke, Virginia Tech) porcine pancreatic elastase (elastase) (Worthington Biochemical Corporation), phosphate-buffered saline (PBS) (Quality Biological), and Vectashield antifade mounting medium (Vector Laboratories), TGF-β_1 ELISA (Biolegend Inc), rhTGF-β_1 (Biolegend Inc).

3.3.2 hCSC Isolation and Cell Culture

Patient heart samples (*i.e.,* atrial appendages) were obtained as discarded tissues from local hospitals. Donor confidentiality was maintained at the hospital's request and no patient identification information or medical history was collected according to the approved protocol. A written consent agreement was obtained for collection of discarded atrial appendages by the hospital and all procedures were approved by the IRB of Virginia Polytechnic Institute and State University for human subject research. The isolation and culture of hCSCs were previously described (50).

3.3.3 Keratin Isolation and Keratose Hydrogel Formation

KOS was supplied by Dr. Mark Van Dyke's laboratory at Virginia Tech. Briefly, KOS was extracted and purified from human hair fibers that had been washed with detergent,

Table 3.1. Stem Cell Culture and Differentiation Medium (all contains 89% HAM/F12)

MAIĀTENANCE MEDIUM	COMPOĀEĀTS	FUĀCTIOĀS
A. hCSC (FBS)	FBS (10%), L-Glutathione (200μM),rhbFGF (10ng/mL), rhEPO (0.005units/mL)	Maintain hCSCs as stem cells
B. hCSC (SR)	KnockOut™ SR (10%), L-Glutathione (200μM), rhbFGF (10ng/mL), rhEPO (0.005units/mL)	Maintain hCSCs as stem cells and avoid addition of TGF-β from FBS
DIFFEREĀTIATION MEDIUM	**COMPOĀEĀTS**	**FUĀCTIOĀS**
A. Cardiac Induction	FBS (10%), P/S (1%), 5-Aza (10μM)	Induce cardiomyocyte differentiation
B. TCPS VSMC (FBS+5-Aza)	FBS (10%), P/S (1%), 5-Aza (10μM), rhTGF-β_1 (5ng/mL)	Induce VSMC differentiation and measure effect of 5-Aza on VSMC differentiation
C. TCPS VSMC (SR+5-Aza)	KnockOut™ SR (10%), P/S (1%), 5-Aza (10μM), rhTGF-β_1 (5ng/mL)	Induce VSMC differentiation without additional TGF-β from FBS, and measure effect of 5-Aza on VSMC differentiation
D. TCPS VSMC (FBS)	FBS (10%), P/S (1%), rhTGF-β_1 (5ng/mL)	Induce VSMC differentiation
E. TCPS VSMC (SR)	KnockOut™ SR (10%), P/S (1%), rhTGF-β_1 (5ng/mL)	Induce VSMC differentiation without additional TGF-β from FBS
F. KOS VSMC (SR+5-Aza)	KnockOut™ SR (10%), P/S (1%), 5-Aza (10μM)	Measure effect of 5-Aza on KOS VSMC differentiation
G. KOS VSMC (FBS)	FBS (10%), P/S (1%)	Measure effect of TGF-β from FBS on KOS VSMC differentiation
H. KOS VSMC (SR)	KnockOut™ SR (10%), P/S (1%)	Induce VSMC differentiation on KOS hydrogels
I. TGF-β_1 Inhibition 1	KnockOut™ SR (10%), P/S (1%), A83-01 (500nM)	Inhibit TGF-β_1 signaling on KOS hydrogel differentiation
J. TGF-β_1 Inhibition 2	KnockOut™ SR (10%), P/S (1%), rhTGF-β_1 (5ng/mL) A83-01 (500nM)	Inhibit TGF-β_1 signaling on TCPS differentiation
K. TGF-β_1 Inhibition 3	KnockOut™ SR (10%), P/S (1%), TGF- β ĀAB (25μg/mL)	Measure effect of TGF-β removal from KOS hydrogel differentiation

rinsed, and dried. For 100 g of fibers, 2 L of a 2% (w/v) peracetic acid solution was used to oxidize protein disulfide bonds by heating it at 37°C for 14 h with gentle rotary stirring. The fibers were recovered by sieve and extracted twice with 4 L of 100mM Tris base solution. The fibers were separated by sieve and the extracted solutions were combined, centrifuged to remove suspended particulates, and filtered through No. 4 Whatman filter discs (Thermo Fisher). The protein solution was purified and high-molecular-weight keratin nanomaterial was isolated by membrane filtration in a custom ultrafiltration system. The membrane cutoff used was 100 kDa and a proprietary buffer solution facilitated separation of the material of interest. After removal of low molecular-weight contaminants, the keratin nanomaterial solution was concentrated against dilute buffer using the same 100 kDa membrane, the material was then frozen and lyophilized (50).

KOS hydrogel was made with 4.5% lyophilized oxidized keratin (w/w) in PBS and 1.5% genipin (w/w) in various culture plates or coverslips. The KOS hydrogel was plated at a thickness of ~0.5 mm, and let to sit for 12 hours to allow the genipin to crosslink. Hydrogels that were to be used for photomicrographs were produced by making a ''sandwich'' between parafilm and glass coverslips, so removing the glass coverslip after 12 hours produced a flat surface that was ideal for cell imaging. In both cases, the hydrogels were then washed three times (5 min each) in PBS and covered with PBS for 48 hours to remove any residual genipin from the hydrogels. After the PBS was removed, hCSCs were seeded on top of the KOS hydrogels

3.3.4 TCPS and KOS Hydrogel Vascular Smooth Muscle Differentiation

VSMC differentiation was induced with two different protocols, one for TCPS and one for KOS hydrogels. For TCPS, hCSCs were plated at a density of $6.3x10^3$ cells/cm^2 and cultured with maintenance medium B (Table 3.1) using Knockout Serum Replacer (SR) in place of FBS for 3 days, changing the medium 24 hours after plating. To induce a VSMC phenotype differentiation medium E was used (Table 3.1). The medium was changed every 48 hours for a 28 day differentiation period.

For KOS hydrogels, hCSCs were plated at a density of $1.2x10^4$ cells/cm^2 and cultured with maintenance medium B (Table 3.1) with SR in place of FBS for 3 days, changing the

medium 24 hours after plating. To induce differentiation for hCSCs on KOS hydrogels we used differentiation medium H (Table 3.1). The hCSCs were maintained in the differentiation culture condition for 28 days changing the medium every 48 hours.

3.3.5 Immunocytochemistry

One primary antibody was used to identify stem cells (c-kit) and three antibodies were used to identify VSMCs (α-SMA, calponin and Myh-11 see Table 3.2). Due to autofluorescence of genipin-crosslinked KOS hydrogels, cells were detached with elastase or TrypLE, then washed with PBS, and allowed to attach to glass coverslips for 2 hours or cytospun. Cells were then fixed in 2% PFA at RT for 30 minutes and then blocked in 1.5% BSA buffer containing 0.2% Tween20 for 30 minutes at room temperature. The resulting cells were then incubated with either 1:200 c-kit, 1:300 α-SMA, and 1:1000 calponin, and 1:30 Myh-11 primary antibody overnight at 4^{o}C on a plate-shaker and then washed 3 times with PBS (5 minutes each) and stained with a secondary antibody, either goat anti rabbit Alexa Fluor 488 (c-kit+Myh-11) or goat anti mouse Alexa Fluor 594 (Ā-SMA+ calponin), at a concentration of 1:2000 in blocking buffer. An additional set of coverslips were stained only with a secondary antibody as a negative control, and Hoechst was used in all groups to label cell nuclei. Fluorescent images of the TCPS and KOS-hydrogel cultured cells were taken using an Olympus IX73 microscope. The intensity of fluorescence was calculated against the total number of nuclei and the results were plotted as a bar graph for statistical analysis.

3.3.6 Collagen Lattice Contraction Assay

Contractility of hCSCs was measured for cells differentiated on TCPS with or without 5ng/mL rhTGF-β_1, or on KOS hydrogels for 28 days. Mice tails were collected from 6-12 week old NSG mice and stored in -80^{o}C until an adequate number had been collected (~40tails). Mouse tails were then thawed in 70% ethanol for 15 minutes. Using wire strippers, ~1 centimeter sections of the tail were stripped starting at the thinnest section to remove tendons. Tendons were then transferred to an ice cold 0.1% acetic acid solution at a ratio of about 100 ml of acetic acid solution per gram of tendon. The solution was placed in in the 4^{o}C refrigerator for 2 days and mixed every half day. After the tendons dissolved the solution was transferred to high speed centrifuge tubes and spun at 8800 x g for 90 minutes

Table 3.2 List of Primary and Secondary Antibodies

Antibody Names	**Antibody Type (Usage)**	**Company (Catalog Number)**
α-SMA	Mouse Monoclonal (Immunofluorescence)	Āovus Biologics **(NBP2-32808)**
SMMHC (Myh-11)	Primary Polyclonal Rabbit (Immunofluorescence)	Sigma-Aldrich (**HPA015310)**
Calp	Primary Monoclonal Mouse (Immunofluorescence)	Sigma-Aldrich (**C2687)**
LAP	Primary Polyclonal Goat (Western Blot)	R+D Biologics (**AF-246-NA**)
TGF-β_1	Primary Polyclonal Rabbit (Neutralizing antibody)	R+D Biologics (**AB-100-NA)**
LTBP-1	Primary Monoclonal Mouse (Western Blot)	R+D Biologics (**MAB399**)
β-A	Primary Monoclonal Mouse (Western Blot)	ThermoFisher(**MA1140**)
Alexa Flour 594	Secondary Goat Anti Mouse (Immunofluorescence)	ThermoFisher(**A11005**)
Alexa Flour 488	Secondary Goat Anti Rabbit (Immunofluorescence)	Jackson Lab (**115-545-062**)
Peroxidase-Conjugated	Secondary Goat Anti Rabbit (Western Blot)	Jackson Lab (**65-6120)**
Peroxidase-Conjugated	Secondary Goat Anti Mouse (Western Blot)	Jackson Lab (**115-035-062)**
Peroxidase-Conjugated	Secondary Mouse Anti Goat (Western Blot)	Jackson Lab (**205-035-108)**

Abbreviation: β-A: Beta Actin; α-SMA: alpha Smooth Muscle Actin; SMMHC: Smooth Muscle Myosin Heavy Chain; Calp: Calponin-1; LAP: Latency Associated Peptide; TGF-β_1: Transforming Growth Factor Beta 1; LTBP-1 Latent TGF-β Binding Protein-1

at 4^o C. The supernatant was transferred to new conical tubes and frozen at -20^{o}C for 2 hours and then transferred to -80^{o}C overnight. The next day the frozen samples were lyophilized until dry. Cells were mixed with collagen to form a 3% collagen solution with a cell

concentration of 3.75x10^5 cell/mL and allowed to cross-link for 1 hour. Contraction was observed over a 48 hour period of time measuring at 6 hours, 24 hours, and 48 hours. Contractility was measured as a ratio of the initial size of gel at time=0 hours.

3.3.7 Carbachol Induced Cell Contraction

Cells were allowed to spontaneously differentiate for a standard 28 day protocol on KOS hydrogels and compared against undifferentiated cells on collagen hydrogels. After differentiation, cells were washed with Krebs solution containing 118mM ĀaCl, 4.7mM KCl, 1.2mM KH_2PO_4, 1.2mM $MgSO_4$, 25mM $ĀaHCO_3$, 1.25mM $CaCl_2$, and 110mM glucose. Then the Krebs solution was removed and replaced with Krebs containing 1mM carbachol. Subsequently photomicrographs were taken every 90 seconds over a 15-minute interval. These images were used to create brief time lapse videos for each condition using ImageJ analysis software.

3.3.8 TGF-β ELISA Assay

Cells were cultured on TCPS or on KOS hydrogels and allowed to spontaneously differentiate using differentiation medium H (Table 3.1). During differentiation cell culture medium was collected at the time of medium change 1 day before differentiation induction, 1 day after differentiation induction, and then every 7 days throughout the 28 day differentiation time-course. Six replicates were collected for each cell culture time-point and each replicate was run in triplicates. The assays were carried out following the manufacturer's protocol (LEGEND Max Free Active TGF-β_1 ELISA kit). Additionally, differentiation medium E (Table 3.1) containing free rhTGF-β_1 was measured on TCPS and KOS hydrogels without cells to determine if there was an interaction with TCPS or KOS hydrogels that could potentially deplete levels of free TGF-β_1 measured from conditions with cells. Levels of rhTGF-β_1 were measured at various time intervals (0, 12, 24, 48 hours) during the typical 48 hour interval in which cell culture medium would be changed.

3.3.9 Western Blotting

Cells were cultured on TCPS or on KOS hydrogels and allowed to spontaneously differentiate using differentiation medium H (see Table 3.1). For the TCPS control, the plate

was washed with PBS and then cell lysate was directly obtained by adding RIPA buffer. For the KOS hydrogel-coated wells, cells were first detached using 7 U/ml elastase for ~1 minute and washed once with PBS to remove any residual hydrogel before being treated with RIPA buffer. Protein lysate was quantified using the Bradford assay and then mixed with 4X loading buffer with or without β-ME (10% β-ME in laemmli buffer) at a 1:4 dilution and incubated for 5 minutes at 95°C. Samples were then loaded into a 4-20% gradient SDS-Stacking gel and ran in a Mini Protean Tetra Cell (Bio-Rad) at 100V for 15 minutes followed by 150V for ~60 minutes. The protein was then transblotted onto a PVDF membrane using a Mini Protean Tetra Cell in an ice bath at 90mA for 16 hours. The transblotted membrane was blocked for 1.5 hours at RT in 3% milk solution in TBST on a plate rocker. Membranes were immunoblotted with specific primary antibodies (LAP, or LTBP-1 see Table 3.2) to determine the amount of TGF-β_1 associated proteins that were present prior to differentiation induction, 14 days, and 28 days post differentiation induction. β-A was used as an endogenous control. The following optimized conditions were used in the study: 1:100 (LAP), 1:5000 (Ā-A), and 1:500 (LTBP-1). All antibodies were diluted in 1% milk solution and incubated with PVDF membranes overnight on a plate rocker at 4°C, then washed 3 times (5 minutes each) with TBST solution. The membranes were then incubated with mouse or goat secondary antibodies conjugated with HRP at 1:10000 for 2 hours at RT on a plate shaker. Films were washed and treated with ECL and images were taken immediately on a Kodak Image Station 400MM.

3.3.10 Inhibition of TGF-β Signaling

To determine if TGF-β_1 signaling could be inhibited, hCSCs were cultured on either TCPS or KOS hydrogels and induced with differentiation medium E on TCPS or with differentiation medium H (Table 3.1) on KOS hydrogels.

3.3.10.1 A83-01 Small Molecule Inhibition

TGF-β_1 was inhibited on TCPS and KOS hydrogels with a TGFBR1 inhibiting small molecule A3-01. TCPS VSM differentiation was inhibited with differentiation medium J and KOS hydrogels were inhibited with differentiation medium I (Table 3.1), both containing

500nM A83-01. Differentiation was induced for 28 days and followed by immunostaining with α-SMA and secondary antibody conjugated with Alexa flour 488.

3.3.10.2 TGF-β Neutralizing Antibody Inhibition

While A83-01 is a potent inhibitor of TGF-β_1 it can interact with other signaling pathways (184). To eliminate the possible crosstalk with other signaling pathways we elected to inhibit TGF-β_1 signaling using a neutralizing antibody specific to TGF-β to inhibit differentiation. In these experiments we inhibited differentiation on KOS hydrogels using either differentiation medium H to induce VSMC differentiation or medium K to inhibit VMSC differentiation. Differentiation inhibition was maintained for 21 days (changing the medium every 48 hours) and for the remaining 7 days of differentiation cells were cultured with medium H until day 28. Following differentiation cells were stained for VSM markers (α-SMA, calponin, and SMMHC) and corresponding secondary antibodies as described previously.

3.3.11 Statistical Analysis

All experiments were repeated at least three times with more than three replicates per group. All data are shown as mean ± standard error of mean unless otherwise stated. Student's t-test with a two-tailed distribution was used to compare two groups. Two-way ANOVA followed by the Bonferroni test was used to compare three or more groups with $P < 0.05$ being considered statistically significant. GraphPad Prism 5 and Microsoft Excel 2013 were used for statistical analysis and plotting.

3.4 Results

3.4.1 5-Aza Does Not Play a Significant Role in KOS hydrogel Differentiation

To determine whether 5-Aza is necessary for KOS hydrogel-induced VSMC differentiation, we repeated the above differentiation experiments using the DM with or without 5-Aza. The results demonstrated that hCSCs did spontaneously differentiate into VSMCs on KOS hydrogel using the DM without 5-Aza (Figure 3.1). Unexpectedly, the percentage (71.6±2.23%) of VSMCs in the presence of 5-Aza is almost the same as in the

absence of 5-Aza (70.5±+3.3%, n=4-5, no significant difference) when differentiated on KOS hydrogel. This indicates that KOS hydrogel alone is able to differentiate hCSCs into VSMCs without 5-Aza, and addition of 5-Aza seemed not to generate significant effects. In addition, "long-term" hCSCs cultured on KOS hydrogel maintained high expression level of c-kit stem cell marker (similar to those in TCPS control dish, Figure 2.8), a good portion (15.3±2.7%) of hCSCs still spontaneously differentiated into VSMCs in hCSC medium, which suggests a strong biological regulatory effect of KOS on hCSC differentiation.

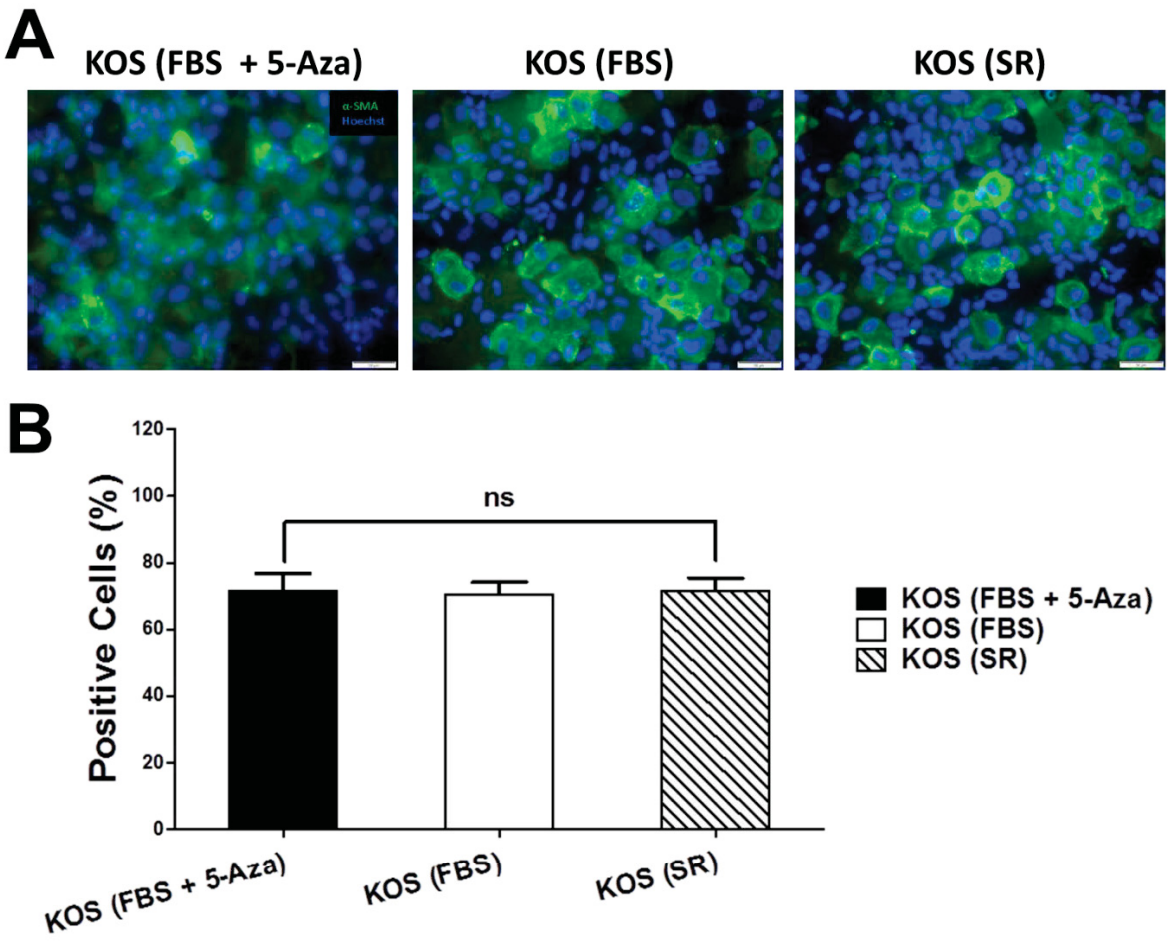

Figure 3.1 Effects of FBS, 5-Aza, and SR on VSMC differentiation

Immunocytochemical staining of α-SMA (Post-Diff) differentiation of hCSCs on KOS hydrogel Representative fluorescent images were taken from cytospun cells (A). Mean percentages of positive cells counted against the total nucleus (FBS+5-Aza), (FBS) and (KnockOut™) were plotted in Panel B (B). Scale bar = 50μm. n=4-5, ns=not significant.

3.4.2 TGF-β_1 Induces VSM Differentiation of c-kit$^+$ hCSCs on TCPS

Since our previous results demonstrated that c-kit$^+$ hCSCs were expressing high levels of VSM genes and protein markers for cells cultured on KOS hydrogels (24), we wanted to know if this could also be induced on TCPS. To determine if this would be the case we induced differentiation with rhTGF-β_1 at a concentration of 5ng/mL and maintained the cells for 28 days changing the culture medium every 48 hours. At the end of the period we examined α-

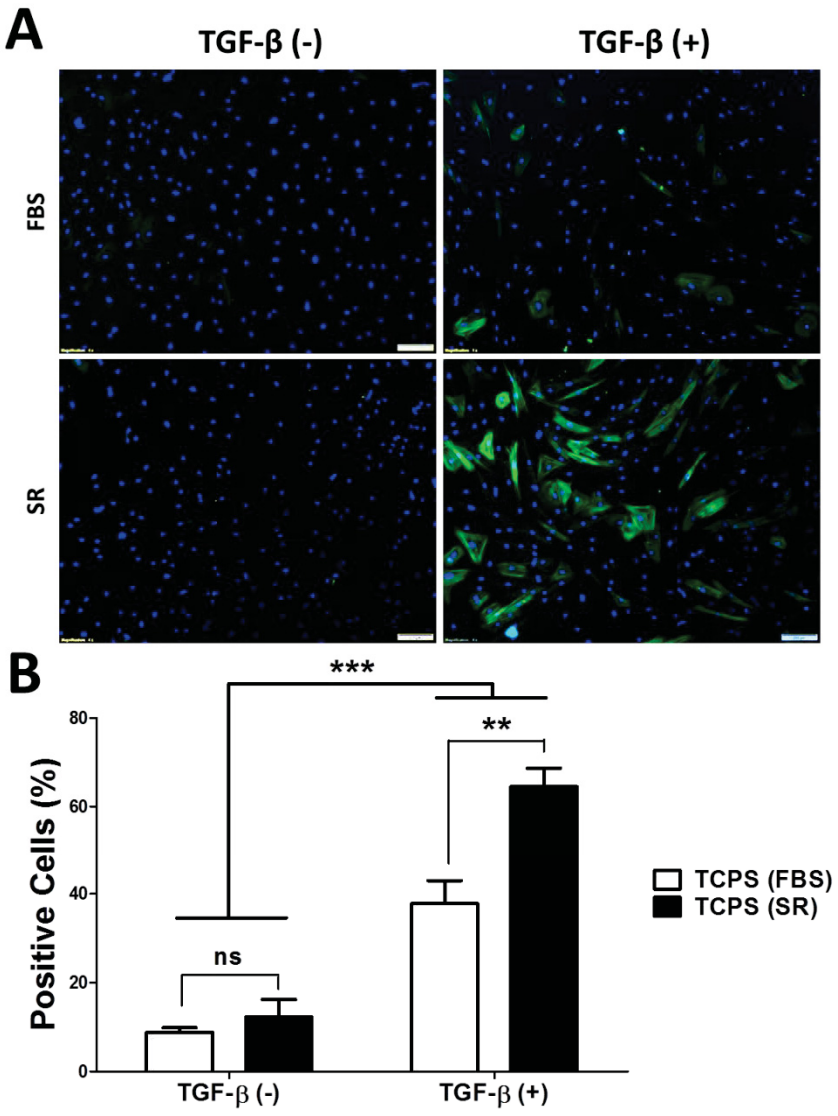

Figure 3.2 TGF-β promotes smooth muscle differentiation on TCPS

Representative fluorescent images were taken from TCPS dishes with attached cells on coverslips for microscopy imaging (A). Mean percentages of positive cells counted against the total nuclei (B). Scale bar=200μm. ns= not significant, ** $p< 0.01$, *** $p< 0.001$, n = 4

SMA expression using IF. We also examined the effect of FBS, and SR on the differentiation profile. Our results demonstrated a statistically significant increase in α-SMA positive cells for both groups that were supplemented with rhTGF-β_1 compared to the conditions where TGF-β was not supplemented (Figure 3.2) FBS (36.49±2.89% with rhTGF-β_1 vs 8.91±0.78% without TGF-β_1 n=4 p<0.001) and SR (64.49±4.22% with rhTGF-β_1 vs 12.54±2.79% n=4 p<0.001). Additionally, there was a statistically significant increase of α-SMA positive cells cultured in SR with rhTGF-β_1 compared to cells cultured in FBS with rhTGF-β_1 (64.49±4.22 vs 36.49±2.89 n=4 p<0.01). Interestingly, the percentages of α-SMA positive cells was very similar to levels seen for the SR TCPS group supplemented with growth factor compared to cells cultured on KOS hydrogels in our previous study (~65% vs ~70%)(24).

3.4.3 KOS Hydrogels Differentiation Significantly Increases Smooth Muscle Phenotype

To determine the differentiation time-course of c-kit$^+$ hCSCs we monitored the expression of 3 different markers that are indicative of VSM differentiation: α-SMA, Calponin, and SMMHC (111, 185-187). Differentiation was induced by removal of b-FGF, EPO and l-glutathione from hCSC maintenance medium B (see Table 3.1). Cells were monitored prior to differentiation induction, 14, and 28 days after induction. To measure the level of protein expression, fluorescent intensity was normalized to the number of nuclei and then to the level of TCPS pre-induction. Prior to differentiation induction levels of all 3 markers were similar (Figure 3.3) for TCPS and KOS hydrogel cultured cells: α-SMA (TCPS 1.00±0.10 n=5 vs KOS 0.74±0.10 n=4), calponin (TCPS 1.00±0.15 n=4 vs KOS 1.00±0.34 n=4), and SMMHC (TCPS 1.00±0.28 n=4 vs KOS 0.88±0.26 n=4) there was no significant difference between any of the groups. For day 14 all markers increased compared to pre-induction, but only calponin saw a significant difference between the KOS hydrogel and TCPS (TCPS 3.24±0.34 n=4 vs KOS 7.54±0.61 n=4 p<0.001), levels for α-SMA (TCPS 3.40±0.77 n=4 vs KOS 5.38±1.22 n=4 p=0.0921) and SMMHC (TCPS 2.20±0.37 n=4 vs KOS 4.92±0.61 n=4 p=0.0998) were not significantly different from each other. By day 28 after differentiation induction KOS differentiated cells had significant increases for all three markers compared to TCPS at the same time-point, α-SMA (TCPS 2.26±0.61 n=5 vs KOS 19.37±1.17 n=4 p<0.001), calponin

(TCPS 2.44± n=4 vs KOS 9.33±1.12 n=4 p<0.001), and SMMHC (TCPS 1.58±0.21 n=4 vs KOS 10.86±1.99 n=4 p<0.001).

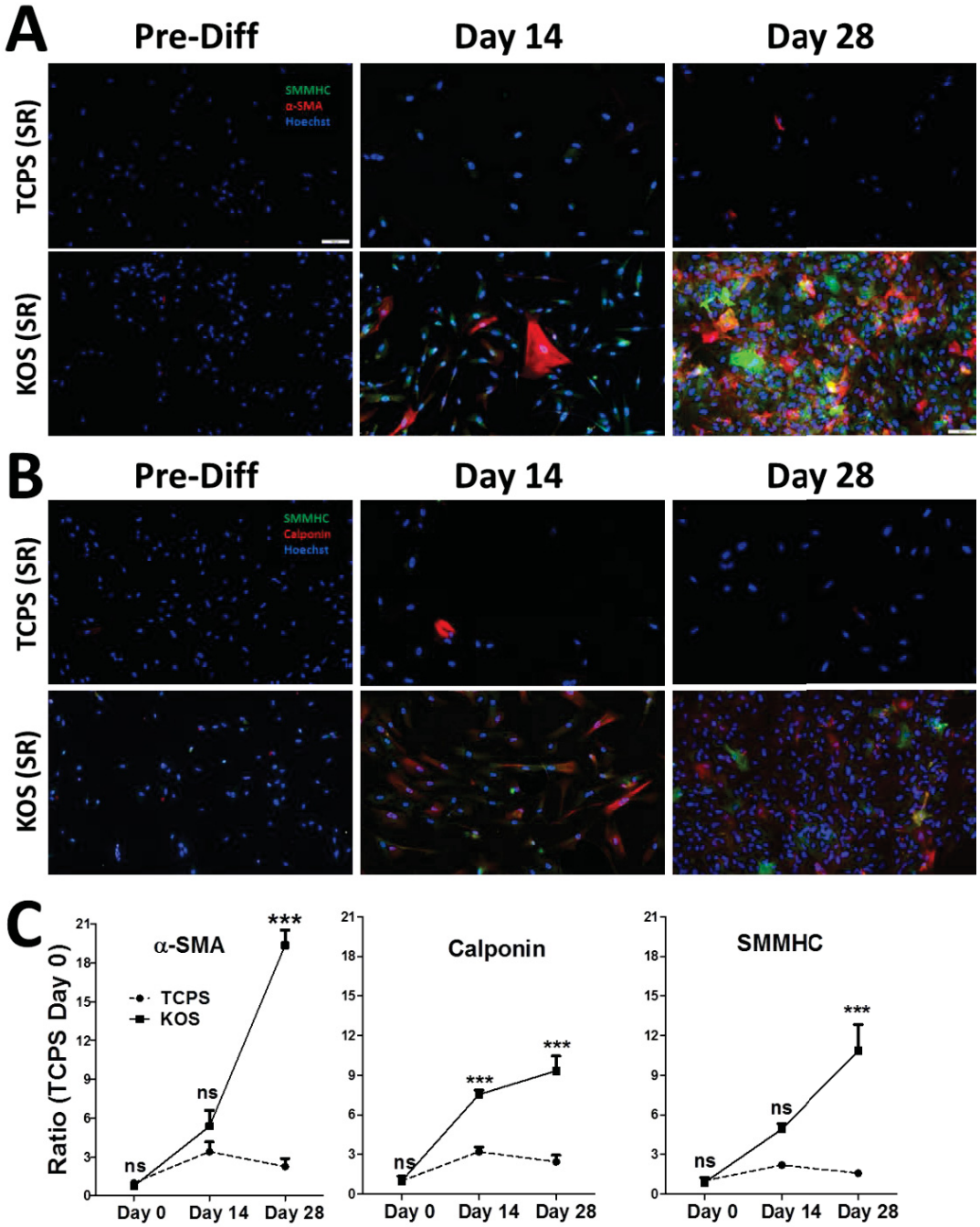

Figure 3.3 VSMC differentiation time course on KOS hydrogels

Representative images of cells stained with α-SMA (red) and SMMHC (green) (A). Representative images of cells stained with Calponin (red) and SMMHC (green) (B). Mean data (>1000 cells per replicate) of fluorescent intensity normalized to cell number and Pre-Diff TCPS (C). Scale bar=100μm. ns=not significant, *** p< 0.001, n = 4

3.4.4 VSMC Differentiation is Consequence of KOS Hydrogels not an Effect of Hydrogel Cell Culture

To determine if a protein based biomaterial was able to induce VSM differentiation cells were differentiated on collagen hydrogels, and collagen hydrogels crosslinked with genipin using differentiation medium H. (Table 3.1). After a 28-day differentiation induction cells were stained for the same 3 VSM markers (α-SMA, calponin, and SMMHC). IF results demonstrated that the level of protein expression was significantly lower for collagen and genipin cross linked collagen compared to KOS (Figure 3.4) for all 3 VSM markers: α-SMA ($9.29x10^5 \pm 3.24x10^4$ vs $1.68x10^5 \pm 2.79x10^4$and $1.02x10^5 \pm 5.94x10^4$ n=4 $p<0.001$), calponin

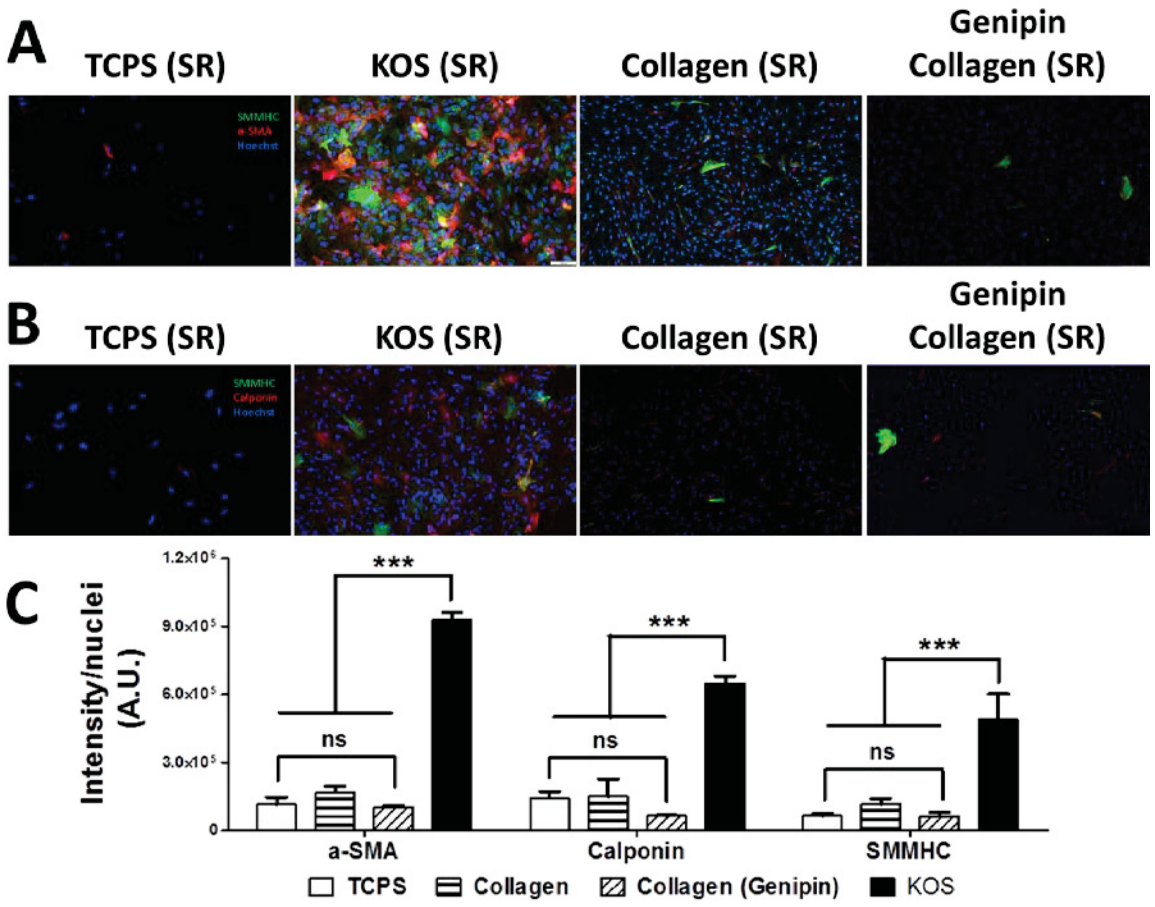

Figure 3.4 Collagen hydrogels exhibit lower levels of VSMC protein expression than KOS hydrogels

Representative images of cells stained with α-SMA (red) and SMMHC (green) (A). Representative images of cells stained with Calponin (red) and SMMHC (green) (B). Mean data (>1000 cells per replicate) of fluorescent intensity normalized to cell number and Pre-Diff TCPS (C). Scale bar=100μm. ns=not significant, *** $p< 0.001$, n = 4

($6.47x10^5 \pm 3.38x10^4$ vs $1.50x10^5 \pm 7.73x10^4$ and $6.40x10^4 \pm 4.53x10^3$ n=4 $p<0.001$), and SMMHC ($4.19x10^5 \pm 1.06x10^5$ vs $1.16x10^5 \pm 2.54x10^4$ and $6.07x10^4 \pm 1.85x10^4$ n=4 $p<0.001$).

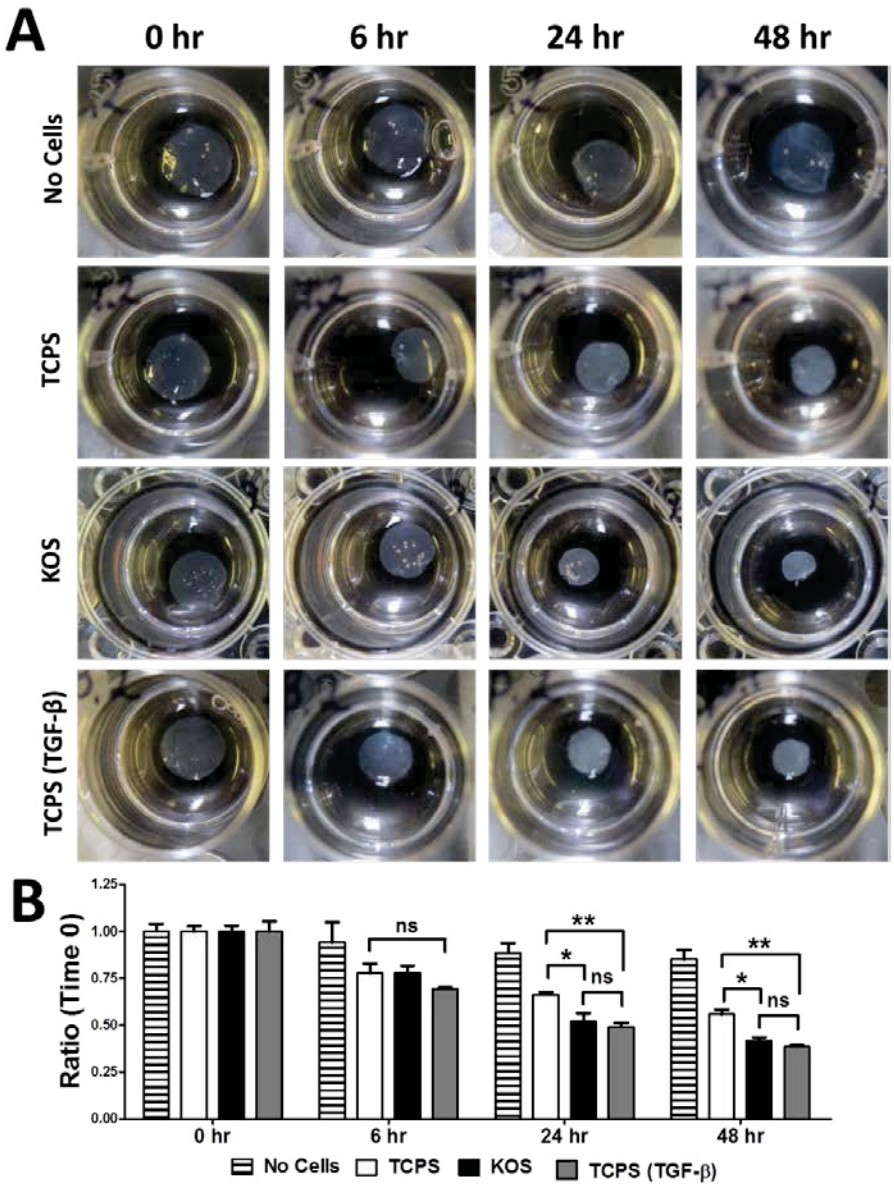

Figure 3.5 KOS hydrogel differentiated cells are more contractile that TCPS differentiated cells: Collagen lattice contraction assay

hCSCs were differentiated on TCPS with or without 5ng/mL rhTGF-β_1 or on KOS hydrogels for 28 days then detached and the mixed with collagen at a concentration of 3.75x10^5 cell/mL and allowed to cross-link. Contraction was measured over a 48 hour period of time. Panel A shows representative images of collagen hydrogels (A). Mean data of ratio of initial size at each time-point measured (B). Scale bar=200μm. ns=not significant, * $p< 0.05$, ** $p< 0.01$, n = 6

There was also no statistical difference for any of the collagen groups compared to the TCPS control α-SMA ($1.15x10^5$ ±$3.08x10^4$ vs $1.68x10^5$±$2.79x10^4$and $1.02x10^5$±$5.94x10^4$, n=4, ns), calponin ($1.43x10^5$ ±$2.97x10^4$ vs $1.50x10^5$±$7.73x10^4$ and $6.40x10^4$±$4.53x10^3$, n=4, ns), and SMMHC ($6.58x10^4$ ±$9.05x10^3$ vs $1.16x10^5$±$2.54x10^4$ and $6.07x10^4$±$1.85x10^4$, n=4, ns).

3.4.5 Cell Contractility

In an effort to measure the functional contractility of KOS hydrogel differentiated cells we used a collagen lattice contraction assay. Contractility was measured for 3 different cell treatment groups, TCPS differentiated cells, KOS hydrogels differentiated cells, and TCPS cells differentiated with rhTGF-β_1. Our results showed greater contraction of collagen for KOS hydrogel differentiated cells than TCPS differentiated cells at 24-hour (TCPS=0.66±0.01 n=6 vs KOS=0.52±0.04 n=6 p<0.05) and 48-hour (TCPS=0.56±0.02 n=6 vs KOS=0.42±0.02 n=6 p<0.05) time-points. Additionally, the rhTGF-β_1 stimulated hCSCs were also significantly more contractile than the standard TCPS cultured hCSCs at 24-hour (TCPS=0.66±0.01 n=6 vs TCPS+TGF-β=0.49±0.02 n=6 p<0.01) and 48-hour (TCPS=0.56±0.02 n=6 vs KOS=0.39±0.01 n=6 p<0.05) time-points. Additionally, we found that carbachol (an M3 muscarinic agonist (188)) stimulated cell contraction of hCSCs differentiated on KOS hydrogels while undifferentiated cells on collagen hydrogels did not (data not shown).

3.4.6 Dynamic Change of TGF-β and Associated Peptides Concentrations

VSM differentiation observed on KOS hydrogels without the supplementation of TGF-β_1 was an interesting finding since the cell culture medium should be free of any TGF-β_1 because SR does not contain TGF-β. If this was the case we needed to determine if the cells were producing TGF-β_1. To do so we measured free TGF-β_1 and its associated proteins (LAP and LTBP-1) using TGF-β_1 ELISA and western blotting to monitor the levels of these proteins in cell culture medium, and cell lysate at periodic intervals before and after differentiation induction. Additionally, we measured levels of rhTGF-β_1 plated on KOS hydrogels and TCPS without cells over an interval of 48 hours (typical time of medium change) to determine if TGF-β_1 was binding to either KOS or TCPS in a way that might interfere with ELISA measurements.

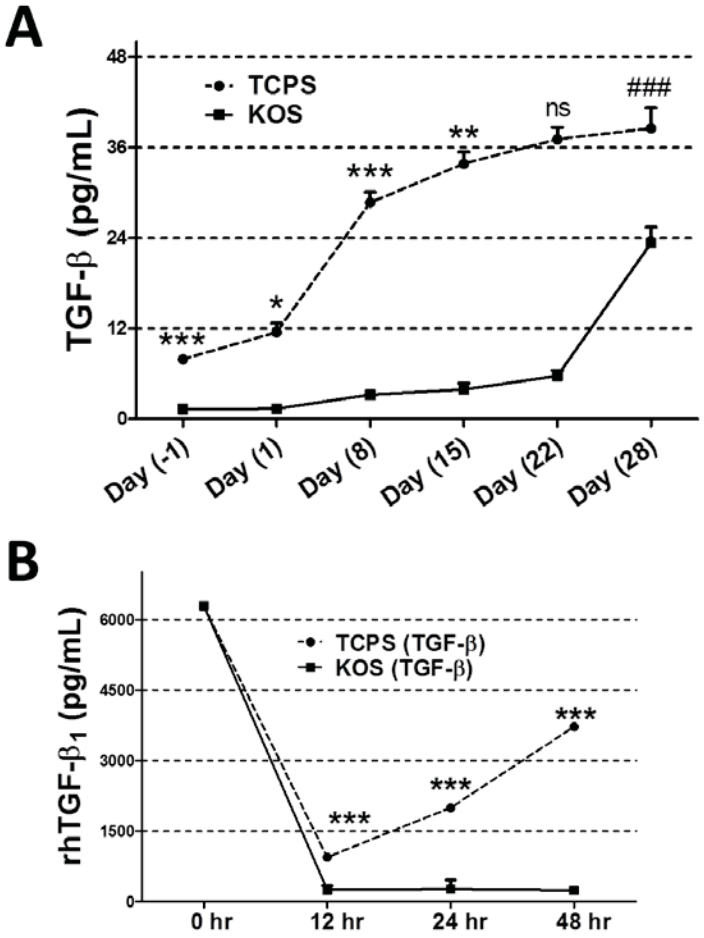

Figure 3.6 C-kit⁺ hCSCs secrete TGF-β_1: TGF-β_1 ELISA assay

Mean data of TGF-β_1 measured from cell culture supernatant (A). Mean data of rhTGF-β_1 measured from cell free supernatant (B). * when TCPS>KOS, # when TCPS<KOS , ns=not dignificant, *p<0.05, **p<0.01, ***p<0.001, ###p<0.001 n=4.

The results of ELISA experiments demonstrated that cells on KOS hydrogels and TCPS both produced TGF-β_1 during the course of differentiation, but the highest measurements were at early time-points (pre-induction to day 8 post induction) for TCPS cells and late time-points (post induction day 22 to day 28) for KOS cells (Figure 3.6A). The highest level of TGF-β_1 was measured on day 8 post induction (17.20±2.38 pg/mL, n=4) for TCPS cells, and on day 28 post induction (17.61±2.08pg/mL n=4) for cells on KOS hydrogels. This trend was also statistically significant when comparing TCPS to KOS. At early time points: day 1 pre-induction (TCPS=7.93±0.26pg/mL vs KOS=1.35±0.28 pg/mL p<0.001), day 1 post-induction (TCPS=3.58±2.38pg/mL vs KOS=0.03±0.28pg/mL p<0.05), day 8 post-induction

(TCPS=17.20±2.38pg/mL vs KOS=1.86±0.48pg/mL $p<0.001$), and day 15 post-induction (TCPS=5.13±1.55pg/mL vs TCPS=0.69±0.83pg/mL $p<0.01$) TGF-β_1 was higher for TCPS cells, and at later time-points the trend reverses and TGF-β_1 is higher for KOS cells at day 28 (TCPS=1.43±2.74pg/mL vs KOS=17.61±2.08pg/mL $p<0.001$).

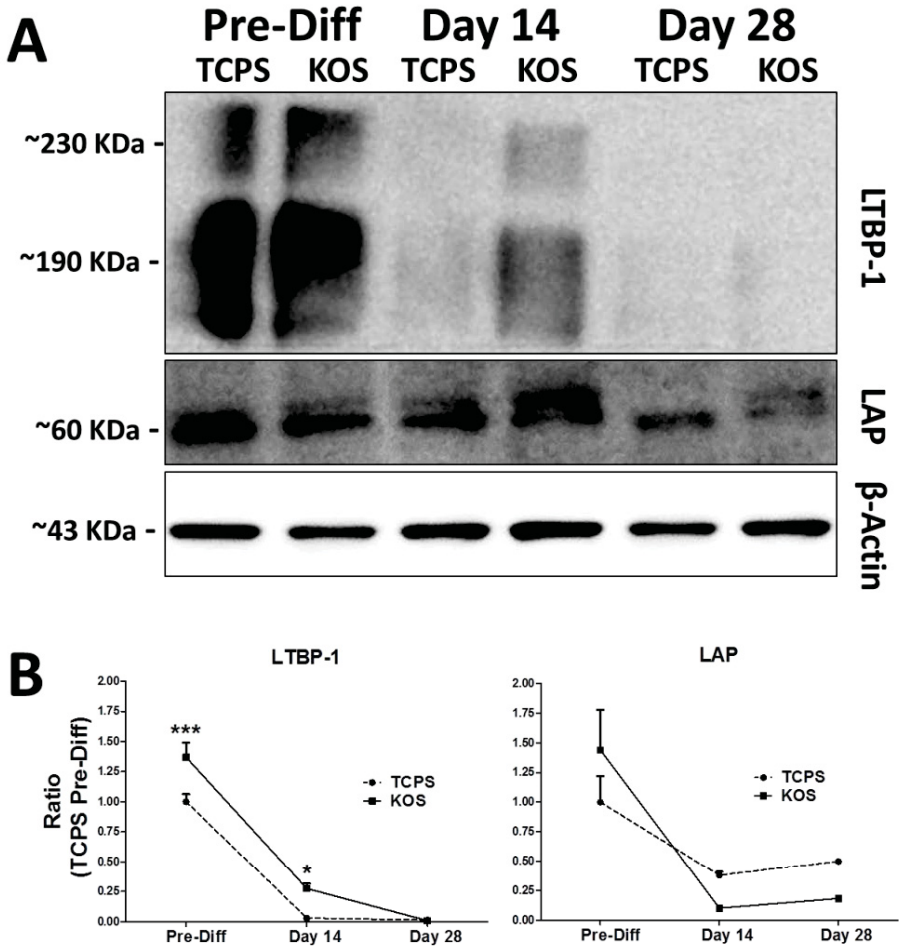

Figure 3.7 Protein expression of TGF-β associated peptides: Western blot analysis

Protein expression of LTBP-1, and LAP, were measured at prior to differentiation induction, 14, and 28 days after differentiation induction. Western blot images from TCPS and KOS (A). Mean data of each protein normalized to amount of Beta Actin from TCPS Pre-Diff (B). n=4, ns=not significant, *$p<0.05$ ***$p<0.001$

Western blot results demonstrated that LAP and LTBP-1 expression levels were higher at early time-points for both KOS hydrogels and TCPS cultured hCSCs (see Figure 3.7B). Surprisingly, the levels of LTBP-1 were significantly higher on KOS hydrogels than

TCPS prior to induction (KOS=1.370±0.122 vs TCPS=1.000±0.064 n=4 p<0.001), and Day 14 post-induction (0.274±0.041vs 0.028±0.007 n=4 p<0.05). This result was interesting because neither LTBP-1 nor LAP western blot measurements for KOS hydrogels (see Figure 3.7) corresponded to the measurements of free TGF-β_1 using ELISA (see Figure 3.6A). On the other hand, the results were consistent between western and ELISA on TCPS both revealing higher levels at early time-points.

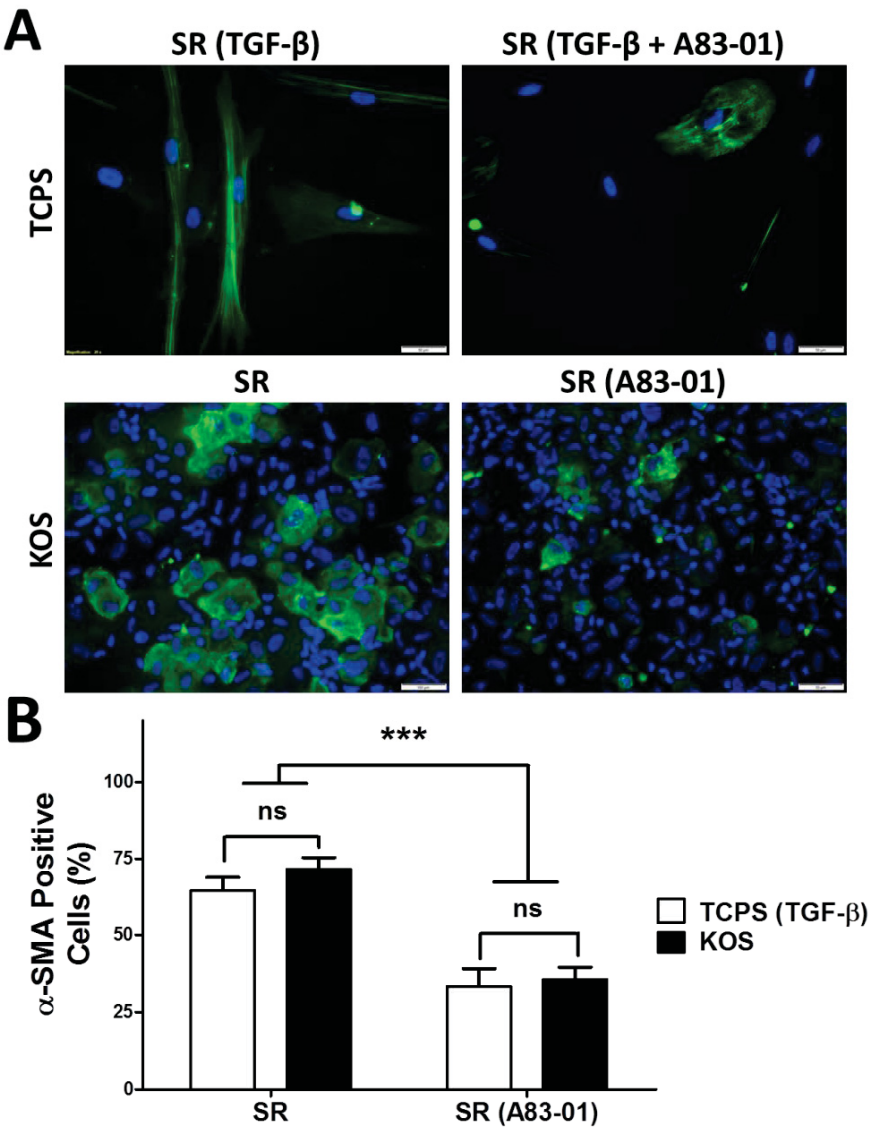

Figure 3.8 A83-01 inhibition of TGF-β decreases VSM differentiation on TCPS and KOS
Representative images of α-SMA IF staining of cells differentiated under various treatments (A). Mean data of IF staining (B). ns=not significant, *** p<0.001, n = 4.

Therefore, additional ELISA experiments were needed to clarify this seemingly contradictory result. To determine if KOS was potentially interacting with TGF-β_1, we ran an additional ELISA. In this experiment, we added cell culture medium supplemented with rhTGF- β_1 on KOS hydrogels and TCPS for a 48-hour interval without cells. This experiment demonstrated that free TGF-β_1 levels were very low (Figure 3.6B) for medium plated on KOS hydrogels compared to TCPS. Prior to adding the medium to KOS hydrogels or TCPS plates the levels were identical (0-hour TCPS=6288±35pg/mL n=4), but for all later time-points KOS was significantly lower (12-hour TCPS=944±47pg/mL vs KOS=249±91pg/mL, n=4 p<0.001, 24-hour TCPS=1996±40pg/mL vs KOS=268±194pg/mL n=4 p<0.001, 48 hour TCPS=3716±38 pg/mL vs KOS=239±73pg/mL n=4 p<0.001). This depletion of rhTGF-β_1 from medium on KOS hydrogels provides a potential explanation for the lower numbers observed for the cell culture supernatant (see Figure 3.6A).

3.4.7 A83-01 and TGF-β NAB Inhibited KOS Hydrogel VSM Differentiation

After determining that rhTGF-β_1 was able to induce VSM differentiation from c-kit$^+$ hCSCs on TCPS and that KOS hydrogels were able to produce a similar differentiation pattern without supplementing TGF-β_1, our next goal was to see if this process could be inhibited with antagonistic small molecules and neutralizing antibodies. We chose A83-01 as a small molecule antagonistic drug, and a pan TGF-β neutralizing antibody to inhibit TGF-β_1 signaling. A83-01 is a potent TGF-β receptor 1 (TGFBR1) inhibitor that blocks phosphorylation of SMAD-2 in the canonical TGF-β_1 signaling pathway (189). IF results revealed that A83-01 significantly inhibited α-SMA protein expression (Figure 3.8) for both rhTGF-β_1 supplemented TCPS (TCPS+TGF-β_1=64.49±4.22% n=4 vs TCPS+TGFβ_1+A83-01=23.17± 2.15% n=4 p<0.001) and KOS hydrogel (KOS=71.7±3.72% n=4 vs KOS+A83-01=26.75±5.16% n=4 p<0.001).

While the A83-01 is a potent inhibitor of TGF-β_1 signaling, it also inhibits ALK4 and ALK7 (190). Therefore, we wanted to use a neutralizing antibody (pan TGF-β antibody) to minimize interaction with other signaling pathways. The TGF-β ĀAB was able to produce a strong inhibition for all three VSM markers (Figure 3.9): α-SMA (KOS= $9.29x10^5$±$1.35x10^5$ n=4 vs KOS+TGF-β ĀAB=$1.08x10^5$±$4.80x10^4$ n=4 p<0.001), calponin

(KOS=6.47x10^5±3.38x10^4 n=4 vs KOS+TGF-β ĀAB=9.09x10^4±1.15x10^4 n=4 p<0.001), and SMMHC (KOS=4.19x10^5±1.06x10^5 n=4 vs KOS+TGF-β ĀAB=5.74x10^4±1.73x10^4 n=5 p<0.01).

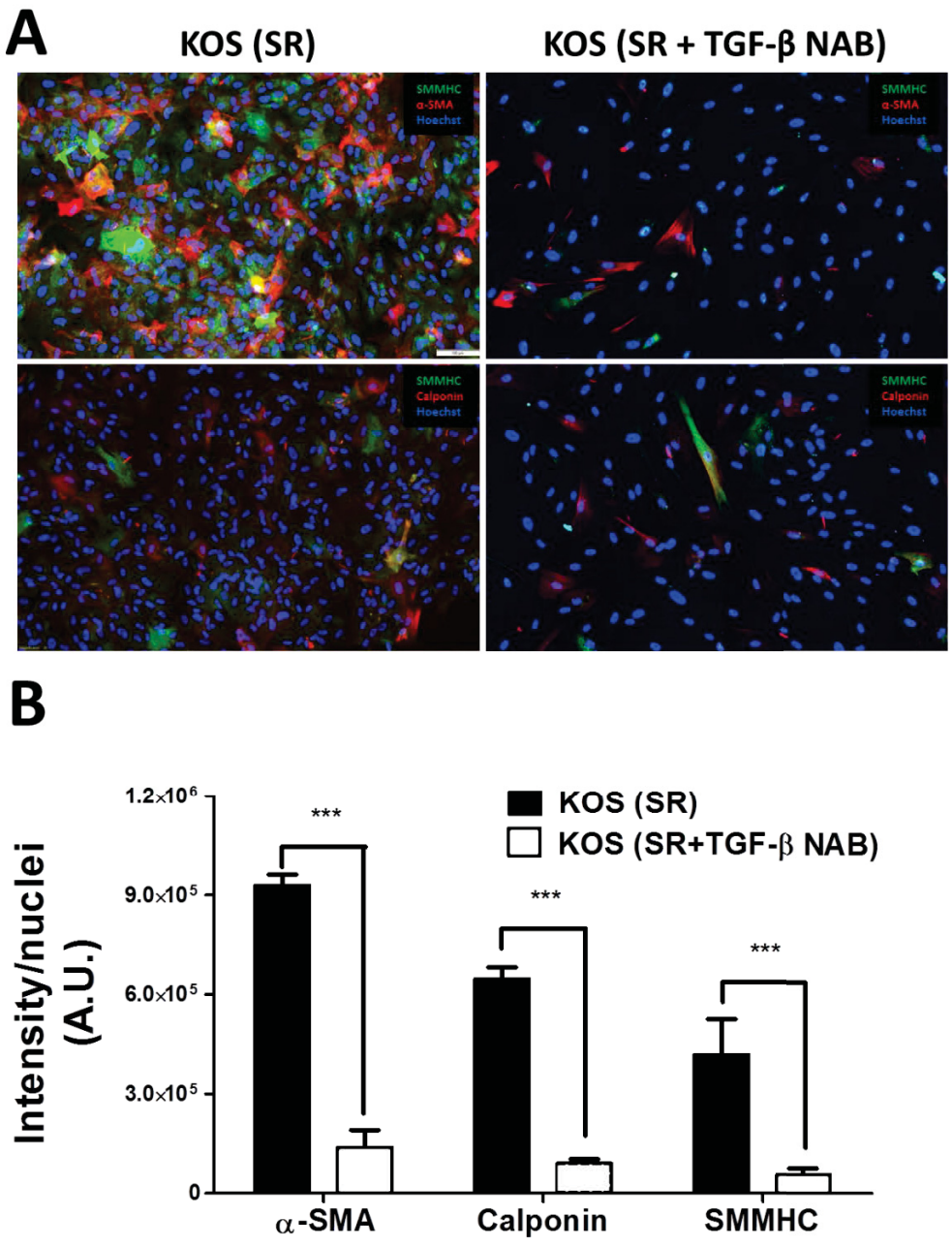

Figure 3.9 TGF-β neutralizing antibody inhibits VSM differentiation on KOS hydrogels.
Panel A shows represntatiive images of cells stained for three VSMC protein markers (α-SMA Calponin and SMMHC) and corresponding secondary antibodies conjugated with either Alexafluor 488 or Alexafluor 594 (A). Scale bar=200μm. Mean data of intensity per nuclei (B). n=4 ***p<0.001.

3.5 Discussion

In the present study, we developed a protocol to induce VSM differentiation of c-kit$^+$ hCSC on TCPS, and observed the differentiation time-course on TCPS and KOS hydrogels. We then monitored the production of TGF-β_1 and its associated proteins, LAP and LTBP-1. Additionally, we investigated the potential role of TGF-β_1 in the observed VSM differentiation pattern of these cells on KOS hydrogels by inhibiting differentiation using a TGF-β_1 inhibitory small molecule and neutralizing antibody. The results show that supplementing rhTGF-β_1 on TCPS was able to produce similar cell characteristics to the VSM phenotype produced on KOS hydrogels (Figures 3.2, 3.3, 3.5). Additionally, we found that there was no need to use 5-Aza to induce VSM differentiation on KOS hydrogels (Figure 3.1) and the observed differentiation pattern on KOS hydrogels was not observed on collagen hydrogels or collagen crosslinked with genipin (Figure 3.4). Collagen lattice assays and carbachol induced contraction revealed that cells differentiated on KOS hydrogels, and cells supplemented with rhTGF-β_1 were significantly more contractile than hCSCs differentiated on TCPS (Figure 3.5). Production of TGF-β_1 and its associated pro-peptides LAP and LTBP-1 was enhanced on KOS hydrogels compared to TCPS (Figure 3.6 and 3.7). Furthermore, we found that use of TGFBR1 inhibitory small molecule A83-01 was able to reduce expression of α-SMA on both TCPS and KOS hydrogels (Figure 3.8), and that a pan TGF-β ĀAB was able to significantly reduce three different VSM markers on KOS hydrogel differentiated hCSCs (Figure 3.9).

Several methods have been developed to produce VSMCs from various types of stem cells (111, 114, 120-122, 181). Our described method of generating VSMCs using c-kit$^+$ hCSCs differentiated on KOS hydrogels presents a simple, effective, and novel method to produce these cells without the addition of growth factors. The drastic increase of all three VSM markers (Figure 3.3), increased contractility of the cells (Figure 3.5), and previously published data showing reduced proliferation of hCSCs on KOS hydrogels (24). These results offer convincing evidence of a cell phenotype consistent with contractile VSM that has been reported via TGF-β_1 differentiation induction (130, 191-193). Yet this differentiation pattern was achieved without supplementing rhTGF-β_1 and was free of any exogenous TGF-β_1 from FBS since the medium used SR in place of FBS (Figure 3.6B). Additionally, we found that c-kit$^+$ hCSCs were responsive to rhTGF-β_1 (Figure 3.2 and 3.5). These results also demonstrate

that TGF-β_1 can induce a similar differentiation pattern seen on KOS hydrogels, making this a plausible signaling pathway candidate warranting further investigation of TGF-β signaling in KOS hydrogel differentiation. Since many other studies have already explored the mechanisms of intercellular signaling as it relates to VSM differentiation (100, 117, 194-198), we chose to take a closer look at the interaction between the hCSCs and the KOS hydrogel.

Since we confirmed that TGF-β_1 was not present in the cell culture medium to induce VSM differentiation of hCSCs, we hypothesized that TGF-β_1 was produced by the cells. To test this assumption, levels of TGF-β_1 and its associated proteins were monitored throughout differentiation. Free TGF-β_1 was measured from cell culture supernatant using an ELISA kit, and associated peptides LAP and LTBP-1were measured using western blots of cell lysate. Results of the TGF-β_1 ELISA demonstrated that hCSCs cultured on TCPS and KOS hydrogels produced TGF-β_1 with higher levels for TCPS measured prior to and during initial stages of differentiation (Figure 3.6A). Cells cultured on KOS hydrogels saw a different trend with the highest levels of TGF-β_1 measured at day 22 to day 28 after differentiation induction (Figure 3.6A). To confirm these results, we ran additional experiments examining the levels of proteins from the SLC (LAP) and LLC (LTBP-1) using western blot. Outcomes from both western blot and TGF-β_1 ELISA of TCPS cultured cells demonstrated consistent results. These findings showed higher levels of TGF-β_1, LAP and LTBP-1 at the earliest time-point measured and decreasing levels thereafter. Interestingly, the western blot and TGF-β_1 ELISA results from KOS hydrogel cultured cells were not in agreement (see Figure 3.6A and 3.7B). ELISA measurements revealed higher levels of TGF-β_1 at later time-points, while western blot measurements showed levels of LAP and LTBP-1 were higher at the earliest time-point. Since TGF-β_1, LAP and LTBP-1 are all excreted from the cell in complex we would expect that ELISA and western blot measurements would be consistent. These seemingly contradictory results lead us to take a closer look at the ELISA.

Therefore, to examine this contradiction, we performed an additional TGF-β_1 ELISA measuring levels of rhTGF-β_1 that had been supplemented to cell culture medium and then placed on either a TCPS dish or on KOS hydrogel both without cells. Results showed an initial decrease for both groups at the 12-hour time point, but the level of rhTGF-β_1 increased on TCPS at 24 and 48-hour time points, but not for KOS hydrogels (Figure 3.6B). Additionally,

the levels of TGF-β_1 were significantly lower at all three time-points after being plated on KOS compared to TCPS (Figure 3.6B). Taken together with the results of cells cultured on TCPS and KOS hydrogels, our findings indicate differential interactions with KOS and TGF-β. Perhaps this is due to differential proteolysis of the SLC via deglycosolation of LAP and/or traction activation of the LLC to produce free active TGF-β (199, 200). In either case, results of ELISA and western blot provide sufficient evidence that either TGF-β_1 or LTBP-1 and KOS have some level of binding affinity similar to the interactions between LTBP-1 and fibrillins or free TGF-β and type IV collagen (200). Additionally, increased levels of LTBP-1 on for hCSCs cultured on KOS hydrogels may explain the increased VSM differentiation pattern seen on this material.

Because there is a chance that the differentiation pattern observed on KOS hydrogels is due to interactions between the proteinaceous biomaterial and TGF-β_1 or its associated peptides, we decided that another biomaterial control was necessary to see if this effect was unique to KOS hydrogel. To do so we used a collagen based biomaterial and a genipin crosslinked collagen biomaterial. We selected a protein based biomaterial because of its similarity to KOS, and there is a possibility that this could play a key role in VSM differentiation by concentrating TGF- β_1 at the cell surface as seen in collagen type IV found in the ECM of vascular tissue (201-203). We also wanted to eliminate the possibility that residual un-crosslinked genipin could be covalently binding growth factors and proteins excreted during initial stages of cell culture creating locally high concentrations of growth factors like TGF-β_1 (204-207). Our results from the biomaterial controls (Figure 3.4) indicate that this is not the case suggesting that the VSM differentiation pattern seen on KOS hydrogels is a unique process specific to our KOS hydrogels.

While results confirmed that TCPS and KOS hydrogel cultured cells do produce TGF-β_1 and its associated proteins LAP and LTBP-1, it does not necessarily confirm that TGF-β_1 is responsible for the differentiation pattern seen on KOS hydrogels. Using a TGFBR1inhibitory small molecule A83-01, we measured VSM protein expression with IF. Results from A83-01 inhibition (see Figure 3.8) confirmed a significant decrease in α-SMA for both the positive control rhTGF-β_1 induced hCSCs on TCPS (~65% vs ~23% $p<0.001$) and, hCSCs differentiated on KOS hydrogels (~72% vs ~27% $p<0.001$). Small molecule inhibition offered compelling evidence that TGF-β_1 plays a role in VSM differentiation observed on KOS

hydrogels, but A83-01 has been reported to inhibit other signaling pathways (184). Using a TGF-β NAB is a more conclusive test to implicate the role of TGF-β_1 in KOS hydrogel VSM differentiation. Additionally, this experiment examined IF of three VSM markers (Figure 3.9). Results showed robust inhibition of all three markers: α-SMA ($9.29x10^5$ vs $1.08x10^5$ $p<0.001$), calponin ($6.47x10^5$ vs $9.09x10^4$ $p<0.001$), and SMMHC ($4.19x10^5$ vs $5.74x10^4$ $p<0.001$). This offers conclusive evidence that TGF-β_1 plays an integral role in the VSM differentiation seen on KOS hydrogels.

3.6 Conclusions

In this study we provide evidence that KOS hydrogels promote VSM differentiation of c-kit$^+$ hCSC through TGF-β_1 signaling. Expression of VMSC contractile proteins and cell contractility were enhanced by KOS hydrogel differentiation. Small molecule inhibition and antibody neutralization of TGF-β_1 signaling lead to significant decreases in expression of contractile proteins for KOS hydrogel differentiated c-kit$^+$ hCSCs. Additionally, we found evidence that TGF-β_1 and its associated proteins interact with KOS hydrogels. Findings in our study provide evidence for potential mechanisms that may direct VSMC differentiation of c-kit$^+$ hCSC through interaction between KOS, TGF-β_1, and proteins of the LLC. Results of this study have implications for potential signaling and differentiation patterns and therapeutic mechanisms of c-kit$^+$ hCSCs in clinical trials.

CHAPTER 4: KERATOSE HYDROGEL-DERIVED VASCULAR SMOOTH MUSCLE CELLS PROMOTE ANGIOGENESIS IN MURINE HIND LIMB ISCHEMIA

4.1 Abstract

Peripheral artery disease (PAD) is a commonly studied disorder with many disease models including CLI. Additionally, many cell based therapies have been investigated to treat this disorder clinically and pre-clinically, but very little of this research has focused on the use of VSMCs as a therapy. The main goal of this study is to determine the therapeutic potential of KOS hydrogel-derived VSMCs (Cells from KOS). We induced hind limb ischemia in 3 groups (n=15/group) of adult mixed gender NSG mice by excising the femoral artery (FA) and femoral vein (FV), and then treated the mice with PBS (PBS-treated), Cells differentiated on TCPS (Cells from TCPS), or Cells from KOS. Blood perfusion of the hind limbs was measured immediately before and after surgery, then 14, and 28 days after surgery using Laser Doppler analysis. Tissue vascularization, cell engraftment, and skeletal muscle regeneration were measured using immunohistochemistry, DiL vessel painting, and H&E pathohistological staining. During the 4-week period, both cell treatment groups showed significant increases in blood perfusion compared to the PBS-treated control, and at day 28 the Cells from KOS group had significantly better blood flow than the Cells from TCPS group. Additionally, the Cells from KOS group demonstrated a significant increase in the ratio of DiL positive vessels, capillary density, and a greater number of small diameter arterioles density compared to the PBS-treated group. Further, both cell-treated groups had similar levels of engraftment into the host tissue. We conclude that Cells from KOS therapy increases blood perfusion in an NSG model of CLI, but does not lead to increased cell engraftment compared to other cell based therapies.

4.2 Introduction

PAD is a common vascular disorder caused by atherosclerosis or thrombosis, which either narrows or completely blocks blood perfusion to organs or the extremity of limbs (*e.g.* legs). The risk of PAD increases with age and approximately 4-8 million people are affected in the United States, and 50,000-80,000 experience CLI which has an associated mortality rate of 20-25% (208). Over a five year period approximately 5% of individuals suffering from PAD had to have part of the affected limb amputated (2, 209). Current therapies for CLI include antithrombotic medication and angioplasty with or without stenting (2). Additionally, there are several completed clinical trials using BMMĀCs, angiogenic cell precursors, mesenchymal stem cells, and various other cell based therapies to treat CLI (210-217).

Various studies in animal models of hind limb ischemia have also extensively studied cell based therapies for CLI. In mice models of hind limb ischemia, mesenchymal stem cells (218, 219), cord blood cells (220), ESCs (221), peripheral blood stem cells (222), dental pulp stem cells (223), EPCs (224), iPSCs (225), and many other cell types have been investigated. Interestingly, to our knowledge only one other animal study has examined the use of VSMC to recover blood flow in mice after induced CLI (226). A more in-depth understanding of the potential role that VSMCs play in the recovery of an acute hind limb ischemia model is a key step in developing more robust tissue engineering approaches for revascularization of ischemic tissues.

In the present study, we utilize resection of the femoral-saphenous artery and vein to induce unilateral CLI in NSG mice to compare the efficacy of c-kit$^+$ human cardiac stem cell (hCSC)-derived VSMCs via KOS hydrogel differentiation versus the same cells differentiated on TCPS and a saline injection at regenerating vascularity and blood perfusion to the ischemic limb. Functional outcomes were measured using Laser Doppler Imaging and pathophysiological analysis. By studying the NSG mouse model, we expect that our results will have implications for the use of VSMCs as a therapeutic for ischemic disorders such as PAD and CAD.

4.3 Materials and Methods

4.3.1 Hind limb Ischemia

All animal protocols were approved by the Virginia Tech IAUCUC committee. Forty-five adult NSG mice between 8-12 weeks of age were used for the study. There were 15 mice per group (PBS-treated vs. Cells from TCPS vs. Cells from KOS). The mice were kept in bio secured and environmentally controlled rooms at the Virginia Maryland College of Veterinary Medicine. Same-gender mice were labeled with ear tattoos for identification purposes and were also housed in the same cage (Chen *et al.*, 2016). Mice had access to food and water ad libitum. Cages, bedding, water and aspen wood shavings were changed weekly. Ambient temperature and humidity were kept at 22-23˚C and 50-70%, respectively. Illumination was kept at a 12 hr/day night cycle with lights on at 7 am.

To induce ischemia mice were anesthetized with 3-4% isoflurane using an ez-7000 anesthesia system (Euthanex, Palmer, PA) and maintained at 1-2% for the duration of the procedure. The mouse body temperature was maintained at 37°C using a water-heated pad and monitored with a TC-1000 temperature controller (Euthanex). The FA and FV were dissected from the femoral nerve to avoid injury to the nerve. After dissection of the FA and vein from the nerve, unilateral ischemia was induced by excision of the FA inferior to the pudendoepiggastric trunk and superior to the popliteal bifurcation on the left limb using an electrocoagulator (HIT0) with a micro sharp tip (Fine Science Tools, Foster City, CA). 2 mm of FA between both ends were removed for complete excision. After the surgery, skin incisions were closed with a 5-0 silk suture and mice were returned to the animal facility following recovery from anesthesia. The right limb served as an internal control for comparison when obtaining blood flow ratios of the ischemic limb, because it did not undergo surgical procedures.

4.3.2 Cell Culture and Delivery to the Ischemic Limb

Treatments were administered to each group (PBS-treated, Cells from TCPS, and Cells from KOS) following surgery and Laser Doppler scans. C-kit$^+$ hCSCs were isolated, cultured, and differentiated as previously described (24). Briefly, c-kit$^+$ hCSCs were isolated from the right atrial appendage in patients with ischemic cardiomyopathy, and then frozen and

banked for later usage. Cells were seeded onto KOS hydrogels or TCPS, and cultured in hCSC medium consisting of Ham's F12 (Thermofischer), 10% FBS (JR Scientific), 10ng/ml FGF (Peprotech), 0.005 U/ml EPO (Sigma), and 0.2mM L-glutathione (sigma). Differentiation was induced by removal of growth factors and supplementing with 10 μM 5-Aza for 3 days, followed by a 28-day period of culture without 5-Aza or growth factors.

Later, differentiated cells were harvested from TCPS and KOS hydrogels and suspended in PBS at a concentration of $4.0x10^7$ cells/mL. Cells were injected into 3 locations in the midpoint gastrocnemius muscle measured with a ruler. Injection sites were marked with tattoo ink (to aid in locating cells after euthanizing the mice) and were injected to a depth of ~2mm using a 28 ½ gauge insulin syringe. Each injection administered 10 μL of cell suspension containing $4x10^5$ cells for a total of $1.2x10^6$ cells per each of the cell-treated mice. The PBS-treated negative control mice were administered in the same manner as the two cell groups.

4.3.3 Laser Doppler Imaging

Blood flow images for both paws were measured before and after surgery on days 0, 14 and 28 using a non-invasive MoorLD12-HIR Laser Doppler imager (Moor Instruments, Wilmington, DE). Blood flow was calculated as a function of image intensity and normalized to the control limb for each mouse using Laser Doppler Imager Software (v 5.3, Moore Instrument) or NIH ImageJ v2. All animals were kept at 37^0C on a water-heated pad for 15 minutes before and during the scanning procedure to minimize the potential impact of body temperature on blood flow. After conducting the imaging 3 times per mouse, the measurements were averaged. A string aligned with the fourth metatarsal pads of each paw was used as a reference line to select the region of interest for post-analysis (ROI). The same region, size, and mean pixel intensities of all three experimental groups were obtained using the imaging software. Imaging colors ranging from blue to red were used to represent increased blood flow and were defined by "heat map." Averages of pixel intensity accounted for the size variation between mice. The ischemic paw measurements were divided by those on the control paw for natural ratios.

4.3.4 Vascular Density Measurements

4.3.4.1 Capillary Density Analysis

Both gastrocnemius muscles (ischemic and non-ischemic) for each experimental group were harvested, fixed overnight in 4% PFA, and embedded in optimum cutting temperature (OCT) freezing medium. Serial tissue sections were cut at 5 μm thick and one out of 18-24 consecutive sections were selected for IHC staining using anti-mouse CD31 antibody (R&D systems, Minneapolis, MĀ). Sections were blocked with 3% BSA in PBST (PBS plus 0.1% tween-20) and stained with primary antibody at 1:200 dilutions overnight at 4℃. Afterwards, sections were washed with PBS and incubated with Alexa Fluor 488-conjugated 2° antibody of chicken anti-goat (Thermofischer sci.) at 1:1000 dilutions and Hoechst 33342 (Thermofischer sci) at 1:5000 dilution for 1h at RT. Slides were mounted with a glass coverslip using Vectashield anti-fade medium and sealed with nail polish for post-analysis. The CD31 tissue samples were analyzed in ImageJ, and we selected for < 10 μm for CD31.

4.3.4.2 Arteriole and Venule Density Analysis

Gastrocnemius muscles from each group were in the same manner as previously described for cryosectioning. One out of 18-24 consecutive sections were selected for IHC staining using a goat anti-mouse α-smooth muscle antibody (R&D systems, Minneapolis, MĀ). Sections were blocked with 1.5% BSA in TBST (TBS plus 0.1% tween-20) and stained with α-SMA primary antibody at 1:300 dilutions (Āovus, catalog #: NBP2-32808-0.2MG) overnight at 4℃. Sections were then washed with PBS and incubated with Alexa Fluor 488-conjugated 2° antibody of goat anti-mouse (Thermofischer sci.) at 1:1000 dilutions and Hoechst 33342 (Thermofischer sci) at 1:5000 dilution for 1h at RT. Slides were mounted with a glass coverslip using Vectashield anti-fade medium and sealed with nail polish for post-analysis. Tissue samples stained with α-SMA antibody were analyzed in ImageJ. Tissues with diameters of 10-25 μm, 25-50 μm, >50 μm were selected for α- smooth muscle.

4.3.5 Gastrocnemius Vessel Painting

On day 28, mice were euthanized by CO_2 inhalation followed by cervical dislocation. The mouse's chest was opened and its heart was perfused with an anti-clotting, vessel dilating buffer that contains 3% sodium citrate and 1mM sodium nitroprusside (Sigma

Aldrich, St. Louis, MS), 12 μM DiL (Santa Cruz, Dallas, TX) in 5% glucose dissolved in PBS (pH 7.4), and 4% PFA in PBS at RT. The muscle was then cut into 5 μm thick tissue sections. Images were taken using an Olympus ckx4 fluorescent microscope and the density of DiL perfused tissue was measured as a ratio of the control limb. Image analysis was performed using ImageJ software.

4.3.6 Skeletal Muscle H&E Staining

The gastrocnemius skeletal muscles from both limbs were harvested on day 28 after tissue perfusion. All tissue samples were fixed for 48 hrs in 4% PFA in PBS at RT before it was processed in an automatic Shandon Citadel 2000 tissue processor. Tissue processing was followed by paraffin wax embedding using a Leica eg1160 tissue embedding station (Buffalo Grove, IL). The gastrocnemius muscle was cut into 5 μm tissue sections in the middle of the gastrocnemius muscle proximal to the injection location using a Leica RM 2125 microtome (Buffalo Grove, IL). Sections were stained using an H&E kit (Scytek Laboratories, West Logan, UT). Stained sections were imaged using an Olympus Vanox-t light microscope equipped with an Olympus dp70 camera and CellSense software (Olympus). Images were analyzed to collect the number of central nuclei and adipose cells per image using ImageJ. The cells were counted for each area of measurement and plotted for comparison.

4.3.7 Xenograft Analysis

As a baseline, 1.2 million cells were injected into three sites within the gastrocnemius muscle of the NSG mouse. The mouse was then euthanized and the muscle was harvested 1 hr later. The three injection locations were marked using green tattoo ink to aid in localizing tissue to examine for cell density. Tissues were fixed for 48 hrs in 4% PFA, and then embedded in OCT, and tissue sections were cut at a 5 μm thickness. One hundred twenty serial sections were cut and 1 out of every 18 sections was used to measure total number of cells by co-localization of nuclei with human mitochondrial stain using ImageJ software. Sections were blocked in 3% PBTA for 2 hrs and then stained overnight with a 1:800 dilution with 1° mouse anti-mitochondria monoclonal antibody (Abcam catalog number: ab9284). The following day, tissue sections were stained 1:1000 dilution with a goat anti-mouse 2°

antibody (Jackson ImmunoResearch West Grove, PA) for 1 hr at RT. This data was used as a Day 0 baseline to compare with Day 28 values and calculate the percentage of surviving cells.

4.3.8 Statistical Analysis

Data are expressed as a mean +/- standard error of the mean (SEM) unless otherwise stated. T-test or two-way AĀOVA followed by Bonferroni post-test to compare two or three

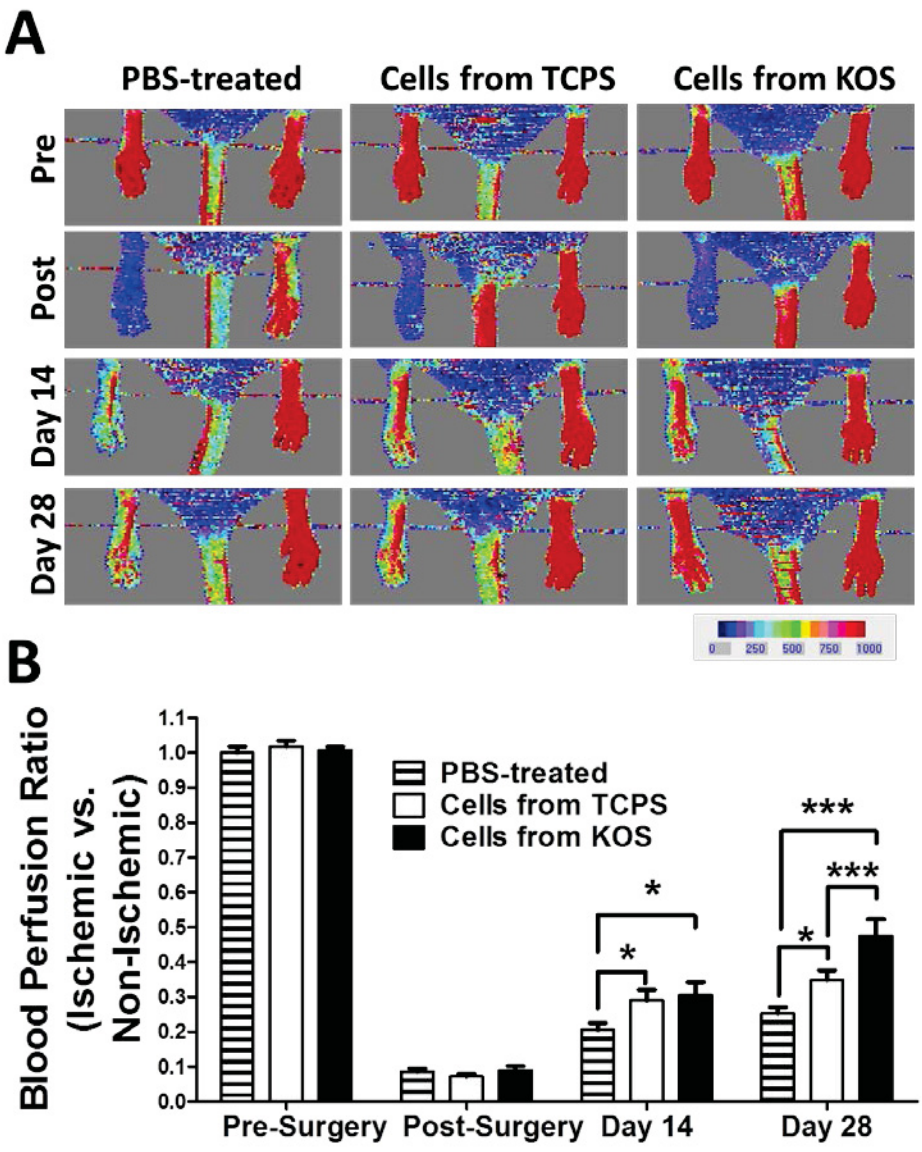

Figure 4.1 VSMCs from KOS hydrogels significantly increase blood perfusion in CLI mice

Representative laser Doppler images before (Pre) and serially (Post, D14, and D28) after ligation of femoral artery and vein (A). Mean data of CLI blood perfusion; ratio of ischemic vs. non-ischemic (B). N = 14-15, *p<0.05 and *** p<0.001.

groups, respectively. A p value <0.05 was considered statistically significant. Graphpad Prism 5.0 and MS excel were used for statistical analysis and plotting.

4.4 Results

4.4.1 Laser Doppler Analysis: Demonstrates Increased Blood Perfusion for Cells from KOS-Treated Mice

Using the Laser Doppler, we examined how each treatment group (PBS-treated, Cells from TCPS, and Cells from KOS) affected the rejuvenation of blood flow on the ischemic limb (see Figure 4.1). During pre-surgery, the mean blood flow ratio was comparable across all treatment groups (1.00±0.018 for PBS-treated, 1.018±0.01.7 for Cells from TCPS and 1.007±0.01 for Cells from KOS). After ligation, the Laser Doppler analysis on the ischemic limb was reduced to ~0.09 ± 0.02 across treatment groups. Blood flow gradually improved in the ischemic limb post-surgery. By day 14, there was a statistically significant increase in average blood flow between the cell-treated groups (0.29±0.03 in Cells from TCPS n=14 and 0.304±0.038 in Cells from KOS n=13) versus PBS-treated (0.205±0.021 n=13 pĀ0.05). Additionally, on Day 28, the mean blood flow ratio for Cells from KOS was significantly higher than PBS-treated and Cells from TCPS (25.2 ± 1.8%, 34.8 ± 2.8% and 47.4 ± 4.9% on Day 28 for PBS-treated, Cells from TCPS and Cells from KOS, respectively). These results demonstrate that the Cells from KOS treatment induced the most blood flow in the ischemic limb.

4.4.2 Vessel Density

4.4.2.1 IHC Analysis of α-SMA and CD31 Show Increases of Capillary Density in Mice treated with Cells from KOS Hydrogel

Increased blood flow from Laser Doppler analysis indicates greater vascularization of the lower limb of mice for the two cell-treated groups. We measured capillary and arteriole density using CD31 (see figure 4.2) and α-SMA (see figure 4.3) IHC stains on frozen tissue sections from the ischemic and non-ischemic gastrocnemius muscle of each treatment group (PBS-treated vs Cells from TCPS vs Cells from KOS). There was a significantly higher density of capillaries with a luminal diameter of less than 10 μm for mice treated with cells

differentiated on KOS compared to PBS-treated (1132.1±93.9/mm^2 n=4 Cells from KOS vs 738.3±113.8/mm^2 n=5 PBS-treated p<0.01). Capillary density was higher for the Cells from

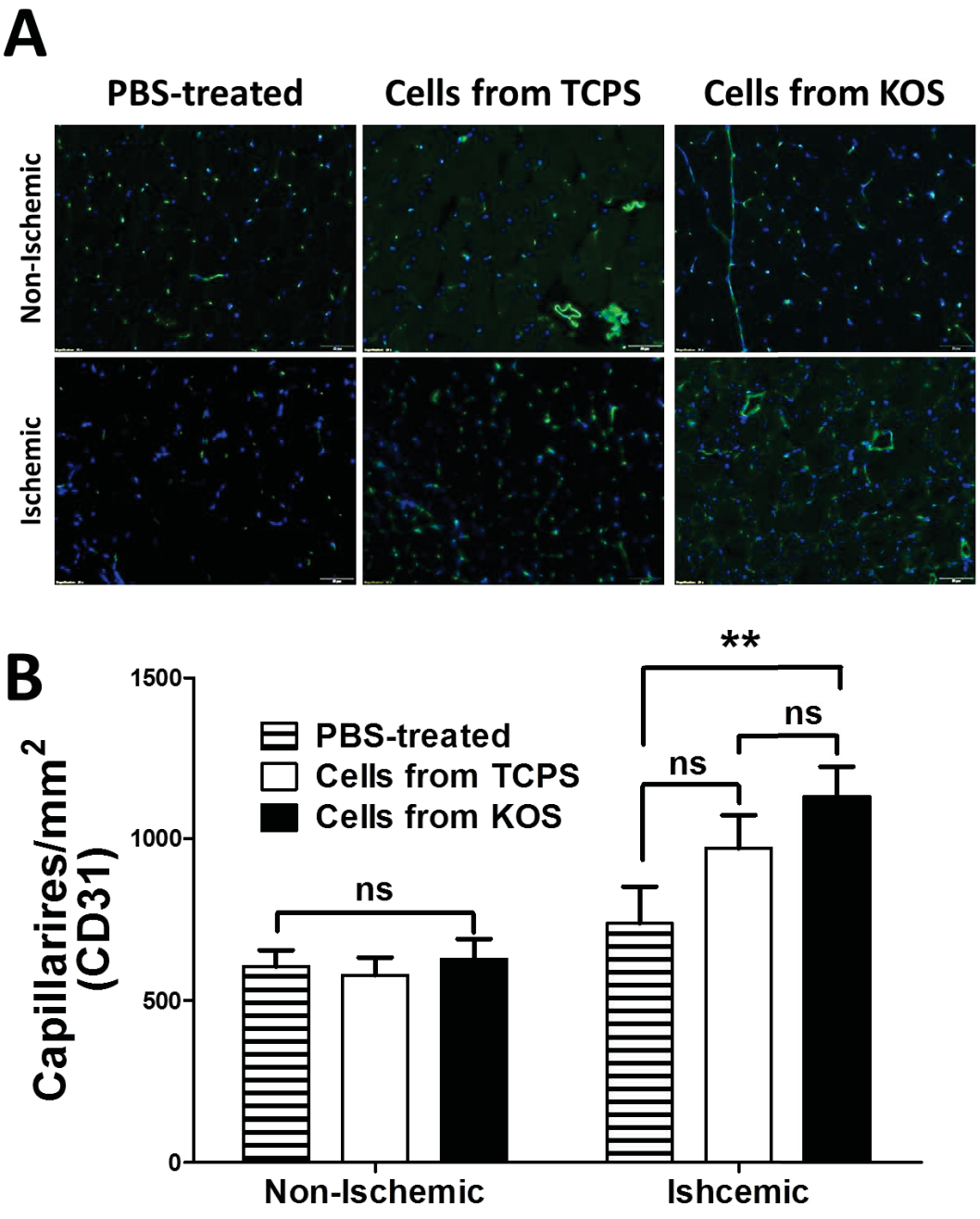

Figure 4.2 Cells from KOS hydrogels significant increase capillary density in treated mice : CD31 IHC

Representative photomicrograph of CD31 (Green) positive vascular tissue and Hoechst (Blue) nuclear stain were taken at Day 28 after euthanizing the mice (A). Mean data of the density (per mm^2) of CD31 positive vascular tissues smaller than 10μm in diameter from Control and Ischemic limb (B). Scale Bar=50μm, n=4 or 5, ns=not significant *p<0.01.

TCPS (970.8±102.2 capillaries/mm^2 n=5 Cells from TCPS vs 738.3±113.8/mm^2 n=5 PBS-treated p=0.091), but it was not statistically significant.

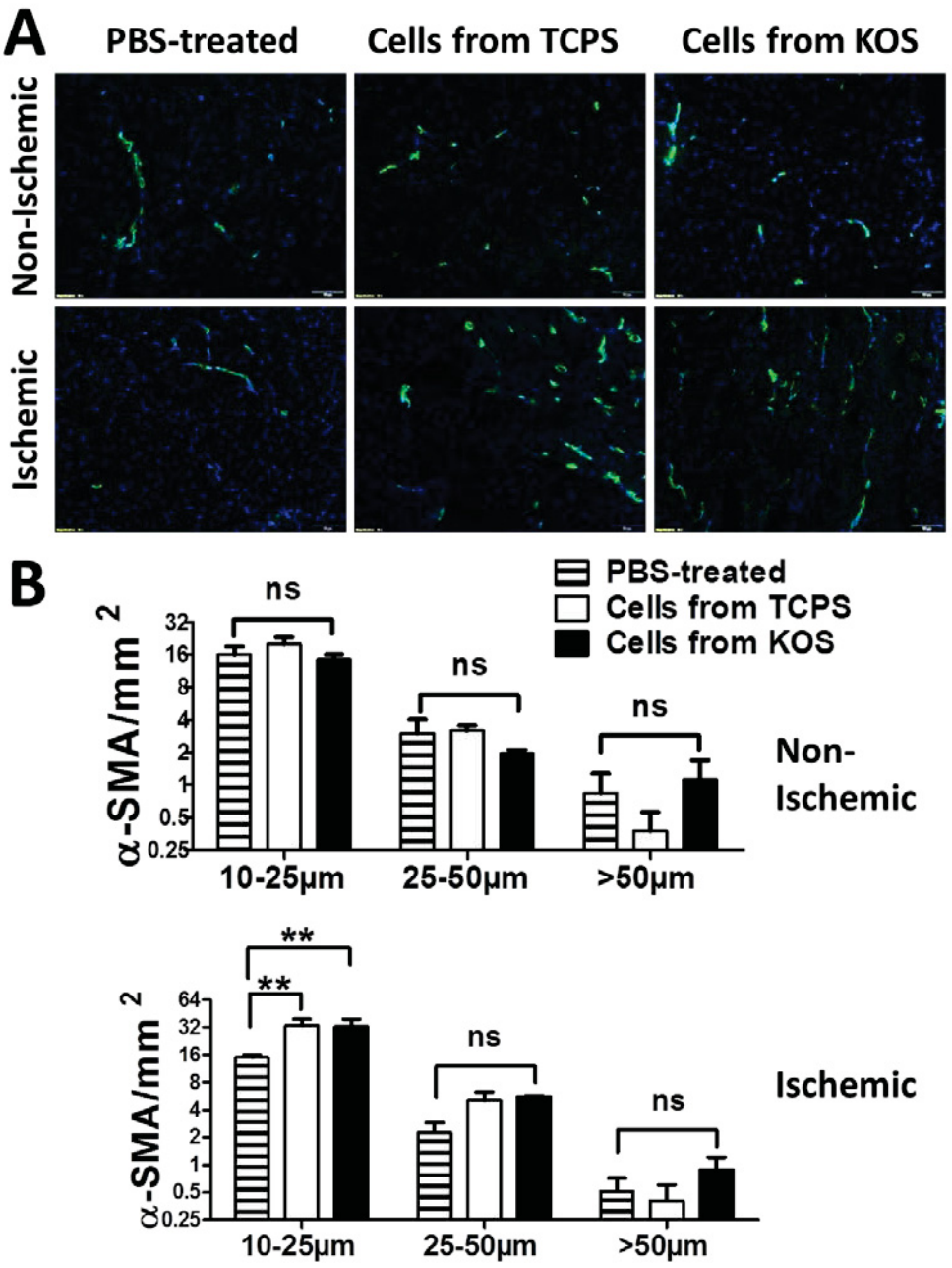

Figure 4.3 Cells from KOS hydrogels significantly increase density of small diameter vascular tissue in treated NSG Mice: α-SMA IHC

(A) Representative photomicrograph of α-Smooth Muscle Actin (Green) positive vascular tissue and Hoechst (Blue) nuclear stain were taken at Day 28 after euthanizing the mice. (B+C) Mean data of the size and density (per mm^2) of α-Smooth Muscle Positive Vascular tissue from Control and ischemic limb. Scale Bar=100μm, n=3 or 4, ns=not significant **p<0.01.

Arteriole density was measured from frozen sections stained with α-SMA and split into three size categories for luminal diameter: 10-25 μm, 20-50 μm, and >50 μm (see figure 4.3). For the non-ischemic limb there was no significant difference between any of the groups. For the ischemic limb there was a significant difference in density for the 10-25 μm diameter arterioles for both Cells from KOS-treated (Cells from KOS 32.97±6.34/mm^2 n=4 vs PBS-treated 15.01±0.94/mm^2 n=4 p<0.01), and Cells from TCPS-treated (Cells from TCPS 33.49±5.85 n=5 vs PBS-treated 15.01±0.94/mm^2 n=4 p<0.01) compared to PBS-treated. There was no significant difference for the 25-50 μm sized vessels nor the >50μm sized vessels.

4.4.2.2 DiL Analysis of Vessel Density Reveals Treatment with Cells from KOS Increases Gastrocnemius Perfusion

DiL is a lipophilic carbocyanine dye that, when incorporated into the phospholipid bilayer of endothelial cells, produces a vibrant fluorescent orange-red color. Cardiac perfusion with aqueous DiL solution is a simple and efficient method to visualize vascular tissue (227). Using this method, we were able to measure the level of tissue perfusion in each mouse post ligation. Results were measured as a ratio of perfused vessels of the ischemic limb to the non-ischemic limb (see figure 4.4). The data demonstrated that the Cells from KOS treatment group had the greatest ratio of perfused vascular tissue in the ischemic limb (0.793±0.196 n=4) versus PBS-treated (0.518±0.077 n=4) and Cells from TCPS (0.606±0.095 n=4). Statistical analysis revealed a significant difference between the PBS-treated and Cells from KOS (p<0.05). The TCPS treatment group however, did not reach significance when compared to the PBS-treated group. Additionally, although the ratio was higher for the Cells from KOS group (0.793) compared to the Cells from TCPS group (0.606), the difference was not statistically significant.

4.4.3 H&E Analysis Reveals Skeletal Muscle Preservation for both Cell-Treated Groups

The presence of the central nucleus and development of adipose tissues within the gastrocnemius muscle are one of the few quantifiable markers for skeletal muscle differentiation. The tissue samples were stained with H&E in order to examine the ratio of

central nuclei and adipose tissue per treatment group (see figure 4.5). Our results show that the central nuclei and adipose cell ratios in the ischemic limb were higher than those in the

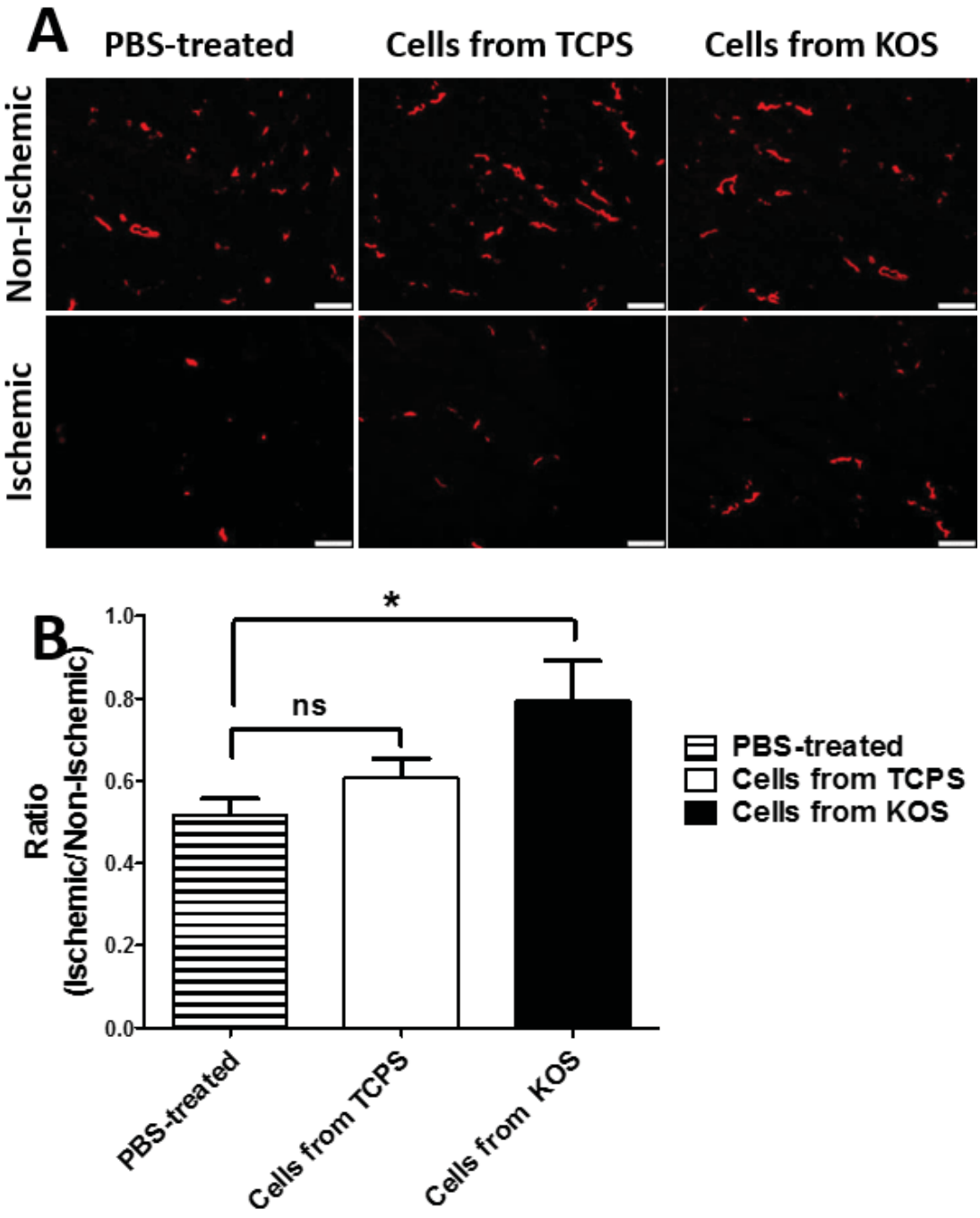

Figure 4.4 Dil-stained vessel densities is significantly higher in Cells from KOS compared to control (PBS-treated)

Panel A shows the representative photomicrograph of DiL positive (Red) vascular tissue Day 28 after euthanizing the mice. (B) Mean data of ratio of ischemic limb vs control limb. Scale Bar=100μm, n=4 or 5, ns=not significant *p<0.05.

control limb. The central nuclei mean ratios for the ischemic limb were as follows: 0.544±0.009 n=4 (PBS-treated), 0.311±0.028 n=5 (Cells from TCPS), and 0.322±0.054 n=5

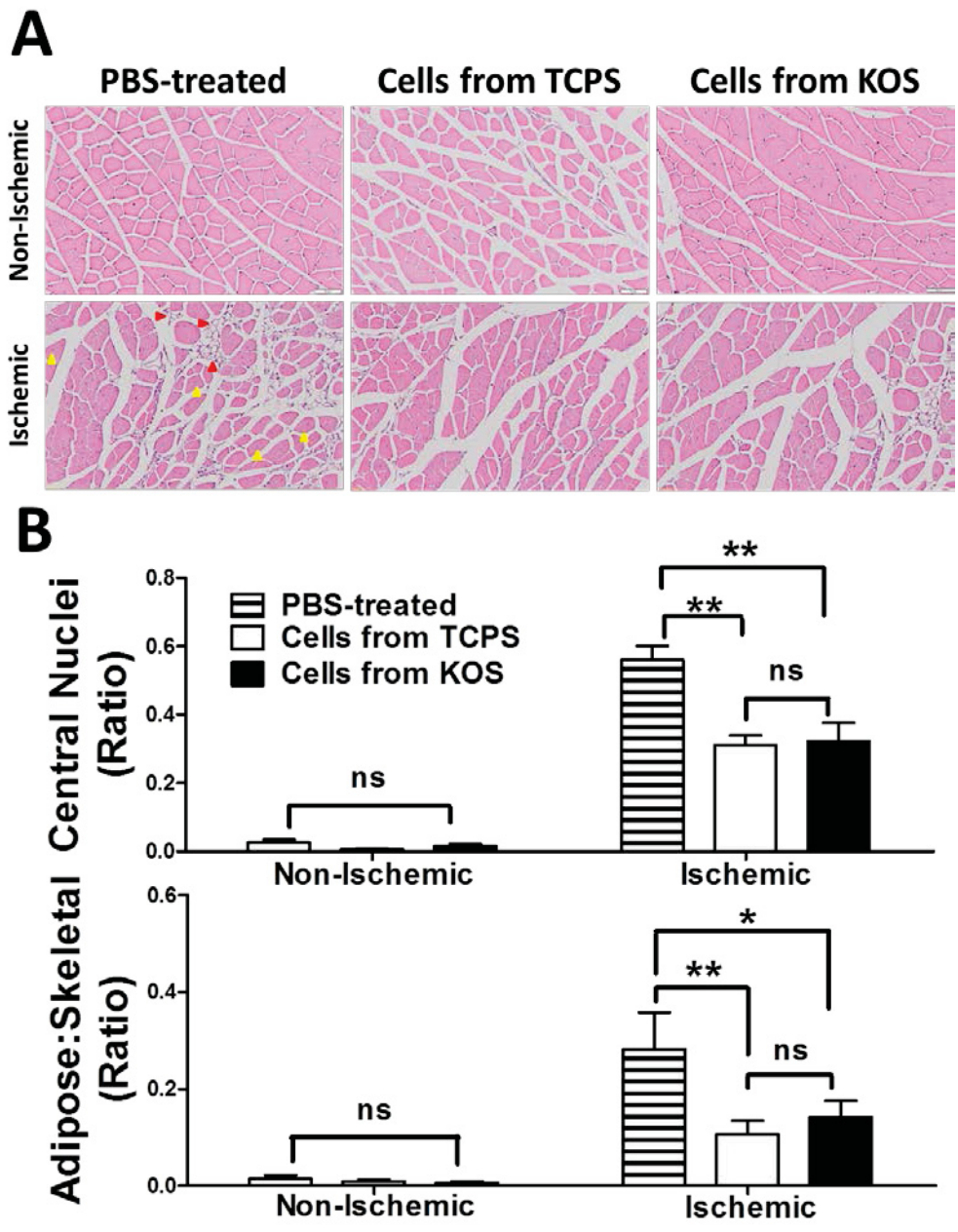

Figure 4.5 Cells from KOS hydrogel and Cells from TCPS preserve skeletal muscle microstructure: H&E analysis

Representative photomicrograph of H&E stained gastrocnemius muscle Day 28 after euthanizing the mice (A). Mean data of ratio of ischemic limb vs control limb (B). Yellow arrow heads= central nuclei, red arrow heads=adipocytes Scale Bar=50μm, n>5, ns=not significant *p<0.05 **p<0.01

(Cells from KOS), versus 0.025± 0.009 n=5 (PBS-treated), 0.006±0.003 n=5 (Cells from TCPS) and 0.016±0.007 n=5 (Cells from KOS) for the control limb. Additionally, the adipose cell

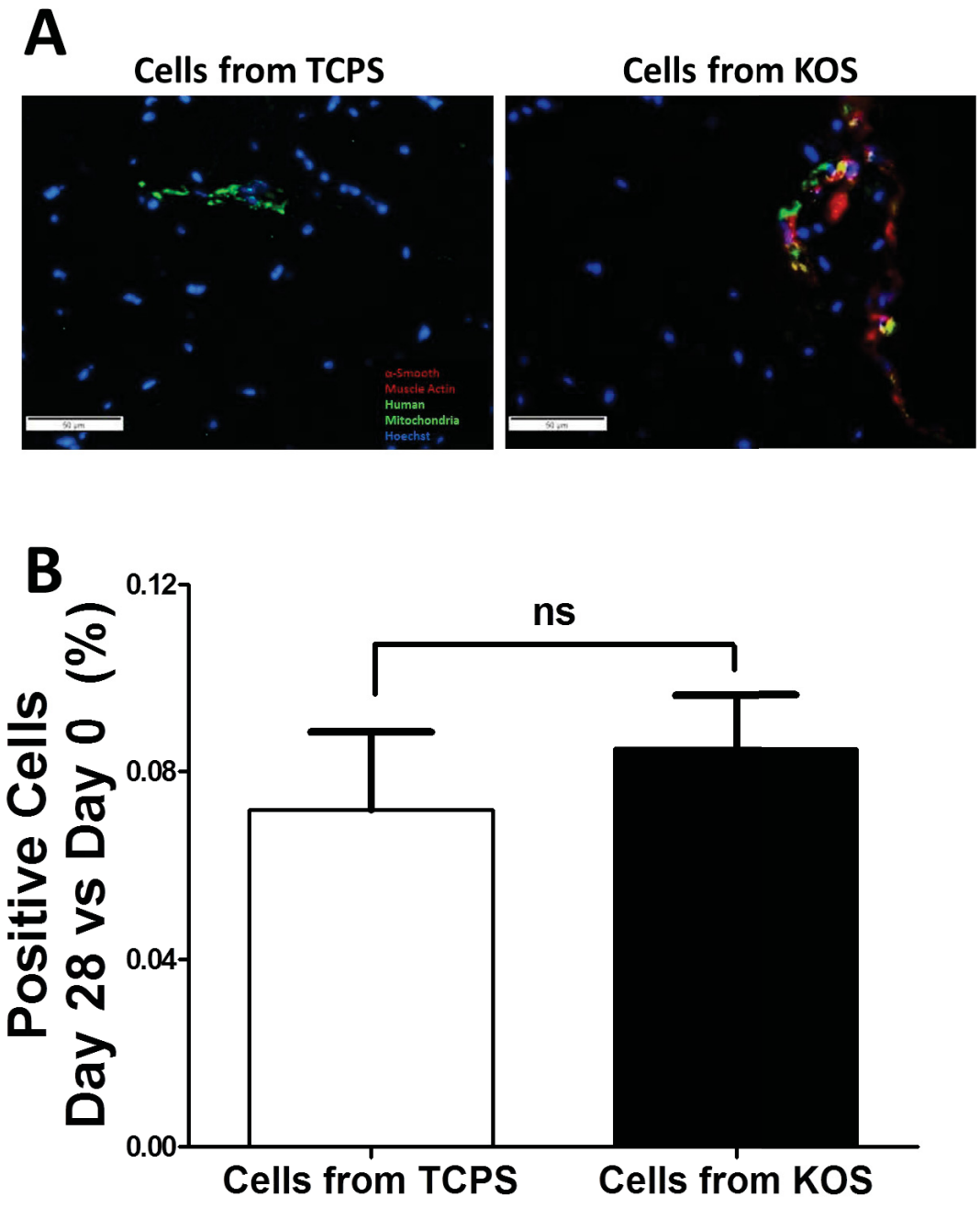

Figure 4.6 No significant increase of tissue incorporation with Cells from KOS

Representative photomicrograph of α-Smooth Muscle Actin (Red) and Human Mitochondria (Green) at Day 28 after euthanizing the mice (A). Mean data of percentage of cells present at Day 28 vs cells present at Day 0 (B). Scale Bar=50μm, n=3 to 4, ns=not significant.

ratios were: 15.5±5.4% (PBS-treated), 11.3±4.8% (Cells from TCPS), and 10.9±1.5% (Cells from KOS) versus the adipose cell ratios in the non-ischemic limb, which were 1.5±0.7% (PBS-treated), 0.9±0.3% (Cells from TCPS) and 0.6±0.3% (Cells from KOS). Both cell-treated groups had statistically significant lower numbers of skeletal muscle cells with central nuclei (pĀ0.001). Additionally, both cell-treated groups had lower numbers of adipose tissue within the ischemic limb compared to the PBS-treated group (Cells from TCPS pĀ0.01) and (Cells from KOS pĀ0.05).

4.4.4 Xenograft Cell Incorporation had no Significant Increase for Cells from KOS Compared to Cells from TCPS

Another reason that the Cells from KOS-treated group could have better blood flow could be better cell engraftment compared to the Cells from TCPS group. Mice were injected with cells differentiated on KOS and TCPS. We stained frozen tissue sections with a human specific mitochondrial stain to calculate the percentages of cells that incorporated into the tissue of the gastrocnemius muscle (see figure 4.6). We found that approximately the same number of cells incorporated into the host tissue for both TCPS (0.072±0.017%) and KOS (0.085±0.012%) differentiated cells (n=4, p=0.5659). The same tissue sections were also stained for α-SMA and we found that the KOS cells were positive for α-SMA, but the Cells from TCPS were not.

4.5 Discussion

In the present study, we investigated the ability of KOS hydrogel-derived VSMCs to recover blood perfusion of NSG mice in an ischemic hind limb model. Our results provide evidence that c-kit$^+$ hCSC-derived VSMCs on KOS hydrogel promote vascular regeneration in a murine hind limb ischemia model. Laser Doppler analysis showed that these mice had better recovery of blood perfusion than both the PBS-treated and TCPS-differentiated hCSC-treated mice. Additionally, mice treated with Cells from KOS significantly increased capillary density compared to PBS-treated, but the Cells from TCPS group did not. Analysis of cell incorporation of both KOS and Cells from TCPS revealed that there was a low level of engraftment for both cell types, but only cells differentiated on KOS were positive for α-SMA.

The use of VSMCs is rare, therefore this is only the second study to examine the regenerative capabilities of VSMCs in an ischemic hind limb model (226). While there is extensive inquiry for the use of ECs in many regenerative medicine applications, very little research has examined the use of VSMCs as a cell based therapy. Ischemic hind limb animal model have been used to examine ECs from various sources (222, 228-232), administration of growth factors with cells (233), genetically modified ECs (233, 234), and various other methods to improve EC-based therapy (235, 236). Interestingly, very little research has examined the regenerative capabilities of VSMCs, and when they are used it is often in conjunction with ECs (237, 238), or smooth MPCs (238). Since we had previously found that c-kit$^+$ hCSCs differentiated on KOS hydrogels could easily produce significant quantities of VSMCs (24), we were interested in testing the therapeutic capacity of these cells.

Our Laser Doppler results showed that mice treated with Cells from KOS had better foot perfusion than both PBS-treated and Cells from TCPS groups (Figure 4.1). This was consistent with the finding of Foubert *et al.* which also showed that smooth MPCs increased blood perfusion compared to PBS-treated mice (226). This result also demonstrates that the effect on perfusion was greater than the TCPS cell control, indicating that the effect was not simply a paracrine effect that would result from injecting any cell type, but instead likely a result of unique exosomal profile of the KOS derived VSMCs. Further, CD31 IHC staining within the gastrocnemius muscle of mice treated with KOS derived VSMCs had a significantly higher capillary density compared to PBS-treated (Figure 4.2 $p<0.05$ n=5), but mice treated with cells differentiated on TCPS did not reach significance compared to the PBS-treated group. Small diameter arterioles stained for α-SMA also had a significant increase in density for both cell-treated groups compared to PBS-treated (Figure 4.3 $p<0.01$ n=4). Our results are consistent with many other studies that show cell based therapy does increase angiogenesis in CLI models (239-242), but unlike Foubert *et al.*, we found the VSMCs did increase capillary density (226). This could be a result of different experimental conditions, most likely time point examined or mouse strain (NSG vs athymic nude mice). Additionally, we demonstrated that there was an added benefit of using KOS derived VSMCs compared to the TCPS cell control, which seems to indicate that VSMCs provide paracrine effect unique to this cell type. This is a new finding which merits further investigation of the role that VSMCs play in angiogenesis and arteriogenesis.

While we did demonstrate that the blood flow was increased using Laser Doppler measurements, and that greater angiogenesis occurred based on cell type used, we still needed to measure gastrocnemius blood flow since Laser Doppler only penetrates the outer layer of skin (243, 244). To directly measure the amount of vascular tissue receiving blood we perfused mice with the vessel painting lipophilic dye DiL. Vessel painting results demonstrated that mice treated with KOS derived VSMCs significantly increased vascular density compared to the PBS-treated control (Figure 4.4), and again the TCPS cell control failed to significantly increase the number of vessels stained with DiL dye. This result agreed with our earlier findings that mice treated with KOS derived VSMCs had superior perfusion and angiogenesis compared to PBS-treated and cell controls (Figures 4.1, 4.2, and 4.3). Again, this agreed with previous literature examining cell based therapies used in hind limb models of CLI, which demonstrate ability to increase vascular density measured by various methods of angiography (245, 246). While these results provide evidence of vascular regeneration future studies need to examine map arterioles and the origins of capillaries within the gastrocnemius and superficial adductor muscle using more quantitative methods precisely measure formations of capillary networks such as x-ray micro computed tomography (247-249).

Histological analysis of ischemic tissue using H&E staining revealed better preservation of tissue in both cell-treated groups compared to the PBS-treated control (Figure 4.5). H&E staining revealed that mice treated with Cells from KOS or Cells from TCPS had significantly fewer central nuclei (Cells from TCPS vs PBS-treated $p<0.01$ and Cells from KOS vs PBS-treated $p<0.001$) and less adipocytes ($p<0.01$ Cells from TCPS vs PBS-treated, $p<0.05$ Cells from KOS vs PBS-treated) compared to the PBS-treated control. The lower number of actively regenerating muscle fibers and decreased adipocyte infiltration both indicate that Cells from KOS and Cells from TCPS improved outcomes compared to the PBS-treated control.

To determine if effects on blood flow and angiogenesis were related to greater engraftment for KOS derived VSMCs, we performed a xenograft analysis of tissue proximal to the cell's injection site in the gastrocnemius muscle. We stained for an antihuman mitochondrial monoclonal antibody as a general marker for any human cells present in the gastrocnemius muscle and calculated the number of cells present at day 28 versus 1 hr after

injection (Figure 4.7.). Our results demonstrated that there was no significant difference in engraftment for KOS derived VSMCs compared to the TCPS control (Figure 4.6). The level of engraftment was low for both cell types (0.085% for KOS vs 0.072% for TCPS). These cell engraftment numbers were consistent with other published research (220, 226). While there was no difference in the level of engraftment, we did find that KOS derived VSMCs stably expressed α-SMA, and TCPS derived cells did not. This result indicates that the KOS derived VSMCs stably expressed smooth muscle marker, α-SMA. Additionally, the results from Laser Doppler, IHC, and vessel painting demonstrate a more robust effect on blood flow for KOS derived VSMCs compared to the TCPS Cell control. The improvements of limb blood flow following cell transplantation are probably due to paracrine effects, but the greater effect observed in VSMCs from KOS hydrogel may indicate additional mechanisms related with KOS hydrogel. Due to the increased capillary density observed in mice treated with KOS derived VSMCs future work should take a closer look at proangiogenic growth factors such as bFGF and VEGF (250-252) and determine how these growth factors play a role in tissue preservation.

4.6 Conclusions

In this study we provide evidence that KOS hydrogel-derived VSMCs increased blood perfusion in a unilateral murine CLI model via paracrine mediated angiogenesis. Increased limb perfusion was confirmed by Laser Doppler analysis and DiL tissue perfusion, both demonstrating higher blood flow than the PBS-treated and TCPS-differentiated control. Angiogenesis was confirmed using IHC staining of CD31 and α-SMA in the gastrocnemius muscle, both stains indicating significantly higher densities of small diameter vascular tissue for the KOS-VSMC-treated mice compared to the PBS-treated control. Additionally, analysis of cell incorporation of both Cells from KOS and Cells from TCPS revealed a low level of engraftment for both cell types, indicating that the increased angiogenesis seen with Cells from KOS was a result of an unknown paracrine effect of these cells. Of further note Cell from KOS that did incorporate into host tissue stably expressed α-SMA while Cells from TCPS did not. H&E histological staining revealed better preservation of the skeletal muscle on the ischemic limb, which displayed less adipogenesis, and fewer skeletal muscle cells with

central nuclei. Both results indicate better preservation of skeletal muscle in Cells from KOS-treated mice than the PBS-treated control.

CHAPTER 5: OVERALL CONCLUSIONS AND FUTURE WORK

5.1 Overall Conclusions

The overall goal of this work was to investigate the impact of KOS hydrogel on c-kit$^+$ hCSCs *in vitro,* determine the signaling pathway(s) behind the observed differentiation pattern, and measure the therapeutic capability of differentiated hCSCs to repair ischemia *i*n *vivo*. Two studies were conducted *in vitro* to determine how culturing c-kit$^+$ hCSCs on KOS hydrogels effects several parameters of these stem cells. The first *in vitro* study was designed to investigate the effects of KOS hydrogel on cell viability, stemness, proliferation, cellular morphology, and cardiac lineage differentiation of c-kit$^+$ hCSCs. KOS hydrogels can culture and maintain hCSCs well without any observable toxic effects or reduction of stemness caused by the KOS hydrogel; however, cell size, ratio of cell length/size, and cell proliferation rate appear smaller on KOS hydrogel than for those on the TCPS. Interestingly, KOS hydrogel significantly promoted hCSC expression of VMSC genes and proteins (with or without 5-Aza), in contrast to those cultured on TCPS, in which case most hCSCs differentiated into CMs. Furthermore, differentiated VSMCs appeared to form "endothelial cell tube-like" microstructures, similar to the "endothelial cell tube" typically formed by ECs on Matrigel (*i.e.,* in tube-formation or *in vitro* angiogenesis assay). The innovative methodology by which cells can be recovered from KOS hydrogel through elastase dissociation makes it possible to analyze gene and protein expression without interference of keratin molecules.

In the second study (Chapter 2), we developed a protocol to induce VSMC differentiation of c-kit$^+$ hCSCs on TCPS, observed the differentiation time-course on TCPS and KOS hydrogels, investigated the potential role of TGF-β_1 in the observed VSMC differentiation pattern of these cells on KOS hydrogels, and attempted to inhibit this differentiation using a TGF-β_1 inhibitory small molecule and neutralizing antibody. A VSM phenotype was produced on KOS hydrogels and on TCPS using rhTGF-β_1 (Figures 3.2, 3.3, and 3.5). Additionally, the observed differentiation pattern on KOS hydrogels was not observed on collagen hydrogels or collagen hydrogels crosslinked with genipin (Figure 3.4). Collagen lattice assays revealed that cells differentiated on KOS hydrogels, and cells supplemented with rhTGF-β_1 were significantly more contractile than hCSCs differentiated

on TCPS (Figure 3.5). Cells cultured on both KOS hydrogels and TCPS produced TGF-β_1 and its associated pro-peptides LAP and LTBP-1, but was enhanced on KOS hydrogels compared to TCPS (Figure 3.6 and 3.7). Also, we found that the use of inhibitory small molecule A83-01 was able to reduce expression of VSM marker on both TCPS and KOS hydrogels (Figure 3.8), and that a TGF-β NAB both significantly reduced VSM contractile protein expression on KOS hydrogel differentiated hCSCs (Figure 3.9).

Given the considerable evidence that our cells were exhibiting a phenotype consistent with VSMCs, the third study was designed to evaluate the capability of these cells to regenerate ischemic tissue. In this study, we investigated the ability of KOS hydrogel-derived VSMCs to recover blood perfusion and regenerate vascular tissue in a critical hind limb ischemia model using ĀSG mice. Animals were treated with either PBS-treated, cells differentiated on TCPS, or VSMCs differentiated on KOS hydrogels. Blood flow measurements using Laser Doppler demonstrated better recovery of blood perfusion for the KOS hydrogel differentiated cell treatment group than for both the PBS-treated and TCPS differentiated cell-treated mice. KOS hydrogel derived VSMCS also promoted significantly higher angiogenesis than PBS-treated, but Cells from TCPS did not. H&E analysis revealed that both cell treatment groups resulted in significantly less intermuscular adiposity and a lower central nuclei ratio, indicating that both cell treatment groups resulted in better preservation of tissue. Cell incorporation of both KOS and Cells from TCPS revealed that there was a low level of engraftment for both cell types, but only cells differentiated on KOS were positive for α-SMA indicating preservation of cell phenotype, and that observed angiogenesis was a result of paracrine effect of the cells and not a result of cell engraftment.

5.2 Future Work

The long-term goal of this work is to characterize the effects of keratin based biomaterials on c-kit$^+$ hCSCs to understand the underlying mechanisms behind its modulation of cell phenotype. Using this information, we plan to devise new cardiovascular regenerative medicine strategies using a combined stem cell and biomaterial therapy. Extensions of this work would involve: (1) thorough investigation of potential binding interactions of KOS hydrogels and TGF-β_1 and its associated peptides; (2) the role that

integrin signaling material stiffness of KOS hydrogels plays on cell differentiation; and (3) animal studies to examine the use of KOS derived VSMCs in AMI rodent models.

Perhaps the most obvious extension of our research is to quantitatively investigate protein binding interactions of KOS hydrogels and the peptides of the LLC (TGF-β_1, LAP, and LTBP-1). Results from ELISA experiments in Chapter 3 show indirect evidence that rh-TGF-β_1 interacts with KOS hydrogels (see Figure 3.6B). While this experiment provides interesting results, more quantitative analysis is needed to determine if there is any protein to protein binding between KOS hydrogels and any of the components of the LLC. Experiments to measure interactions between these components should include both biophysical and biochemical methods. The first step would be to screen for broad interaction between proteins in KOS hydrogels and cell lysates. These interactions could be relatively weak and transient; therefore a biochemical test such as a crosslinking protein analysis should be used. Using this method, we could screen interactions for all components of the LLC (TGF-β_1, LAP, and LTBP-1) with KOS. If these experiments reveal any interactions with KOS, then we would further investigate the interactions using biophysical methods such as surface plasmon resonance (SPR) to measure association and dissociation constants of the components that do interact.

Another area of investigation we are interested in examining is integrin activation of TGF- β_1. Traction mediated activation of TGF- β_1 has been reported in many studies (122, 199, 253) and could be a likely mechanistic candidate to explain our observed VSMC differentiation on KOS hydrogels. Of particular interest would be mechanical activation of TGF-β_1 by $\alpha v\beta 6$, $\alpha v\beta 5$, and $\alpha v\beta 3$ integrins, all of which have been reported to activate Latent TGF-β_1 (254). These studies would focus on small molecule inhibition of cell contractility and inhibition of RGD cell binding motifs that are essential for binding of the integrins to the LAP portion of the LLC (199).

Extensive research has investigated the use of stem cells and stem cell derived CMs and ECs (75, 80, 255-258), but comparatively there are very few studies examining the role of VSMCs for cardiac repair. Positive results showing increased revascularization from our hind limb ischemia model (see Figure 4.1 to 4.4) provide meaningful data to pursue further studies investigating the application of our KOS hydrogel derived VSMCs to treat AMI in rodent models. Additionally, other hind-limb ischemia studies (226) and AMI models (259)

have shown some positive results: improved LV function, less ventricular dilation, greater number of blood vessels, and a smaller infarct area. Despite these positive findings, few studies have investigated the use of VSMC in the treatment of cardiovascular disorders. Such studies should investigate: the contribution of c-kit^{+} hCSCs into vascular tissue of AMI, the use of differentiated cells vs stem cells, and the use of VSMCs alongside ECs or EPCs.

REFERENCES

1. Heart Disease Fact Sheet [updated 6/16/2016; cited 2017 4/7/2017]. Available from: https://www.cdc.gov/dhdsp/data_statistics/fact_sheets/fs_heart_disease.htm.
2. Di Minno G, Spadarella G, Cafaro G, Petitto M, Lupoli R, Di Minno A, de Gaetano G, Tremoli E. Systematic reviews and meta-analyses for more profitable strategies in peripheral artery disease. Annals of medicine. 2014;46(7):475-89. doi: 10.3109/07853890.2014.932618. PubMed PMID: 25045928; PMCID: 4245179.
3. Wisse BE. The inflammatory syndrome: the role of adipose tissue cytokines in metabolic disorders linked to obesity. Journal of the American Society of Āephrology : JASN. 2004;15(11):2792-800. doi: 10.1097/01.ASN.0000141966.69934.21. PubMed PMID: 15504932.
4. Libby P, Theroux P. Pathophysiology of coronary artery disease. Circulation. 2005;111(25):3481-8. doi: 10.1161/CIRCULATIOĀAHA.105.537878. PubMed PMID: 15983262.
5. Chong JJ. Cell therapy for left ventricular dysfunction: an overview for cardiac clinicians. Heart, lung & circulation. 2012;21(9):532-42. doi: 10.1016/j.hlc.2012.04.020. PubMed PMID: 22658631.
6. Cheng K, Malliaras K, Li TS, Sun B, Houde C, Galang G, Smith J, Matsushita N, Marban E. Magnetic enhancement of cell retention, engraftment, and functional benefit after intracoronary delivery of cardiac-derived stem cells in a rat model of ischemia/reperfusion. Cell Transplant. 2012;21(6):1121-35. doi: 10.3727/096368911X627381. PubMed PMID: 22405128; PMCID: 4323149.
7. Nigro P, Perrucci GL, Gowran A, Zanobini M, Capogrossi MC, Pompilio G. c-kit(+) cells: the tell-tale heart of cardiac regeneration? Cellular and molecular life sciences : CMLS. 2015;72(9):1725-40. doi: 10.1007/s00018-014-1832-8. PubMed PMID: 25575564.
8. Kan L, Thayer P, Fan H, Ledford B, Chen M, Goldstein A, Cao G, He JQ. Polymer microfiber meshes facilitate cardiac differentiation of c-kit(+) human cardiac stem cells. Experimental cell research. 2016;347(1):143-52. doi: 10.1016/j.yexcr.2016.07.024. PubMed PMID: 27481582.

9. Āadal-Ginard B, Ellison GM, Torella D. Absence of evidence is not evidence of absence: pitfalls of cre knock-ins in the c-Kit locus. Circ Res. 2014;115(4):415-8. doi: 10.1161/CIRCRESAHA.114.304676. PubMed PMID: 24965482.
10. Keith MC, Bolli R. "String theory" of c-kit(pos) cardiac cells: a new paradigm regarding the nature of these cells that may reconcile apparently discrepant results. Circ Res. 2015;116(7):1216-30. doi: 10.1161/CIRCRESAHA.116.305557. PubMed PMID: 25814683; PMCID: PMC4432841.
11. Torella D, Ellison GM, Mendez-Ferrer S, Ibanez B, Nadal-Ginard B. Resident human cardiac stem cells: role in cardiac cellular homeostasis and potential for myocardial regeneration. Āature clinical practice Cardiovascular medicine. 2006;3 Suppl 1:S8-13. doi: 10.1038/ncpcardio0409. PubMed PMID: 16501638.
12. Āadal-Ginard B, Ellison GM, Torella D. The cardiac stem cell compartment is indispensable for myocardial cell homeostasis, repair and regeneration in the adult. Stem cell research. 2014;13(3 Pt B):615-30. doi: 10.1016/j.scr.2014.04.008. PubMed PMID: 24838077.
13. Keith MC, Tang XL, Tokita Y, Li QH, Ghafghazi S, Moore Iv J, Hong KU, Elmore B, Amraotkar A, Ganzel BL, Grubb KJ, Flaherty MP, Hunt G, Vajravelu B, Wysoczynski M, Bolli R. Safety of intracoronary infusion of 20 million C-kit positive human cardiac stem cells in pigs. PLoS One. 2015;10(4):e0124227. doi: 10.1371/journal.pone.0124227. PubMed PMID: 25905721; PMCID: PMC4408046.
14. Kan L, Smith A, Chen M, Ledford BT, Fan H, Liu Z, He JQ. Rho-Associated Kinase Inhibitor (Y-27632) Attenuates Doxorubicin-Induced Apoptosis of Human Cardiac Stem Cells. PLoS One. 2015;10(12):e0144513. doi: 10.1371/journal.pone.0144513. PubMed PMID: 26645568; PMCID: PMC4672899.
15. Furth ME, Atala A, Van Dyke ME. Smart biomaterials design for tissue engineering and regenerative medicine. Biomaterials. 2007;28(34):5068-73. doi: 10.1016/j.biomaterials.2007.07.042. PubMed PMID: 17706763.
16. Wu DD, Irwin DM, Zhang YP. Molecular evolution of the keratin associated protein gene family in mammals, role in the evolution of mammalian hair. BMC Evol Biol. 2008;8:241. doi: 10.1186/1471-2148-8-241. PubMed PMID: 18721477; PMCID: PMC2528016.

17. Rouse JG, Van Dyke ME. A Review of Keratin-Based Biomaterials for Biomedical Applications. Materials. 2010;3(2):999-1014. PubMed PMID: WOS:000298240300012.
18. de Guzman RC, Merrill MR, Richter JR, Hamzi RI, Greengauz-Roberts OK, Van Dyke ME. Mechanical and biological properties of keratose biomaterials. Biomaterials. 2011;32(32):8205-17. doi: 10.1016/j.biomaterials.2011.07.054. PubMed PMID: 21835462.
19. Hill P, Brantley H, Van Dyke M. Some properties of keratin biomaterials: kerateines. Biomaterials. 2010;31(4):585-93. doi: 10.1016/j.biomaterials.2009.09.076. PubMed PMID: 19822360.
20. Hartrianti P, Ling L, Goh LM, Ow KS, Samsonraj RM, Sow WT, Wang S, Nurcombe V, Cool SM, Ng KW. Modulating Mesenchymal Stem Cell Behavior Using Human Hair Keratin-Coated Surfaces. Stem Cells Int. 2015;2015:752424. doi: 10.1155/2015/752424. PubMed PMID: 26124842; PMCID: PMC4466490.
21. Corcoran JP, Ferretti P. Keratin 8 and 18 expression in mesenchymal progenitor cells of regenerating limbs is associated with cell proliferation and differentiation. Developmental dynamics : an official publication of the American Association of Anatomists. 1997;210(4):355-70. doi: 10.1002/(SICI)1097-0177(199712)210:4<355::AID-AJA1>3.0.CO;2-F. PubMed PMID: 9415422.
22. Wu YL, Lin CW, Cheng NC, Yang KC, Yu J. Modulation of keratin in adhesion, proliferation, adipogenic, and osteogenic differentiation of porcine adipose-derived stem cells. Journal of biomedical materials research Part B, Applied biomaterials. 2015;105(1):180-92. doi: 10.1002/jbm.b.33551. PubMed PMID: 26454254.
23. Larouche D, Hayward C, Cuffley K, Germain L. Keratin 19 as a stem cell marker in vivo and in vitro. Methods in molecular biology. 2005;289:103-10. PubMed PMID: 15502175.
24. Ledford BT, Simmons J, Chen M, Fan H, Barron C, Liu Z, Van Dyke M, He JQ. Keratose Hydrogels Promote Vascular Smooth Muscle Differentiation from C-kit Positive Human Cardiac Stem Cells. Stem Cells Dev. 2017. doi: 10.1089/scd.2016.0351. PubMed PMID: 28351290.
25. Han S, Ham TR, Haque S, Sparks JL, Saul JM. Alkylation of human hair keratin for tunable hydrogel erosion and drug delivery in tissue engineering applications. Acta Biomater.

2015;23:201-13. doi: 10.1016/j.actbio.2015.05.013. PubMed PMID: 25997587; PMCID: 4522204.

26. Āakata R, Osumi Y, Miyagawa S, Tachibana A, Tanabe T. Preparation of keratin and chemically modified keratin hydrogels and their evaluation as cell substrate with drug releasing ability. Journal of bioscience and bioengineering. 2015;120(1):111-6. doi: 10.1016/j.jbiosc.2014.12.005. PubMed PMID: 25561327.
27. Park M, Shin HK, Kim BS, Kim MJ, Kim IS, Park BY, Kim HY. Effect of discarded keratin-based biocomposite hydrogels on the wound healing process in vivo. Mater Sci Eng C Mater Biol Appl. 2015;55:88-94. doi: 10.1016/j.msec.2015.03.033. PubMed PMID: 26117742.
28. Tomblyn S, Pettit Kneller EL, Walker SJ, Ellenburg MD, Kowalczewski CJ, Van Dyke M, Burnett L, Saul JM. Keratin hydrogel carrier system for simultaneous delivery of exogenous growth factors and muscle progenitor cells. Journal of biomedical materials research Part B, Applied biomaterials. 2015. doi: 10.1002/jbm.b.33438. PubMed PMID: 25953729.
29. Passipieri JA, Baker HB, Siriwardane M, Ellenburg MD, Vadhavkar M, Saul JM, Tomblyn S, Burnett L, Christ GJ. Keratin Hydrogel Enhances In Vivo Skeletal Muscle Function in a Rat Model of Volumetric Muscle Loss. Tissue Eng Part A. 2017. doi: 10.1089/ten.TEA.2016.0458. PubMed PMID: 28169594.
30. Baker HB, Passipieri JA, Siriwardane M, Ellenburg MD, Vadhavkar M, Bergman CR, Saul JM, Tomblyn S, Burnett L, Christ GJ. Cell and Growth Factor-Loaded Keratin Hydrogels for Treatment of Volumetric Muscle Loss in a Mouse Model. Tissue Eng Part A. 2017. doi: 10.1089/ten.TEA.2016.0457. PubMed PMID: 28162053.
31. Kandel ER. Principles of neural science. 5th ed. Āew York: McGraw-Hill Medical; 2013. l, 1709 p. p.
32. Sierpinski P, Garrett J, Ma J, Apel P, Klorig D, Smith T, Koman LA, Atala A, Van Dyke M. The use of keratin biomaterials derived from human hair for the promotion of rapid regeneration of peripheral nerves. Biomaterials. 2008;29(1):118-28. doi: 10.1016/j.biomaterials.2007.08.023. PubMed PMID: 17919720.
33. Pace LA, Plate JF, Smith TL, Van Dyke ME. The effect of human hair keratin hydrogel on early cellular response to sciatic nerve injury in a rat model. Biomaterials.

2013;34(24):5907-14. doi: 10.1016/j.biomaterials.2013.04.024. PubMed PMID: 23680369.

34. Hill PS, Apel PJ, Barnwell J, Smith T, Koman LA, Atala A, Van Dyke M. Repair of peripheral nerve defects in rabbits using keratin hydrogel scaffolds. Tissue Eng Part A. 2011;17(11-12):1499-505. doi: 10.1089/ten.TEA.2010.0184. PubMed PMID: 21275820.
35. Pace LA, Plate JF, Mannava S, Barnwell JC, Koman LA, Li Z, Smith TL, Van Dyke M. A human hair keratin hydrogel scaffold enhances median nerve regeneration in nonhuman primates: an electrophysiological and histological study. Tissue Eng Part A. 2014;20(3-4):507-17. doi: 10.1089/ten.TEA.2013.0084. PubMed PMID: 24083825; PMCID: 3926186.
36. Shen D, Wang X, Zhang L, Zhao X, Li J, Cheng K, Zhang J. The amelioration of cardiac dysfunction after myocardial infarction by the injection of keratin biomaterials derived from human hair. Biomaterials. 2011;32(35):9290-9. doi: 10.1016/j.biomaterials.2011.08.057. PubMed PMID: 21885119.
37. Huebsch N, Mooney DJ. Inspiration and application in the evolution of biomaterials. Āature. 2009;462(7272):426-32. doi: 10.1038/nature08601. PubMed PMID: 19940912; PMCID: PMC2848528.
38. Narmdev B. Shelke RJ, Cato T. Laurencin, Sangamech G. Kumbar. Polysaccharide biomaterials for drug delivery and regenerative engineering. Polymwer for Advanced Technologies. 2014;25(5):448-60. doi: 10.1002/pat.3266.
39. Hubbell JA. Bioactive biomaterials. Curr Opin Biotechnol. 1999;10(2):123-9. PubMed PMID: 10209141.
40. Velegol D, Lanni F. Cell traction forces on soft biomaterials. I. Microrheology of type I collagen gels. Biophys J. 2001;81(3):1786-92. doi: 10.1016/S0006-3495(01)75829-8. PubMed PMID: 11509388; PMCID: PMC1301653.
41. Wang S, Wang Z, Foo SE, Tan NS, Yuan Y, Lin W, Zhang Z, Ng KW. Culturing fibroblasts in 3D human hair keratin hydrogels. ACS applied materials & interfaces. 2015;7(9):5187-98. doi: 10.1021/acsami.5b00854. PubMed PMID: 25690726.

42. Kapoor S, Kundu SC. Silk protein-based hydrogels: Promising advanced materials for biomedical applications. Acta Biomater. 2016;31:17-32. doi: 10.1016/j.actbio.2015.11.034. PubMed PMID: 26602821.
43. Wilhelm SM, Eisen AZ, Teter M, Clark SD, Kronberger A, Goldberg G. Human fibroblast collagenase: glycosylation and tissue-specific levels of enzyme synthesis. Proc Āatl Acad Sci U S A. 1986;83(11):3756-60. PubMed PMID: 3012533; PMCID: PMC323602.
44. Taylor CM, Weiss JB, Lye RH. Raised levels of latent collagenase activating angiogenesis factor (ESAF) are present in actively growing human intracranial tumours. Br J Cancer. 1991;64(1):164-8. PubMed PMID: 1649618; PMCID: PMC1977311.
45. Wang J, Hao S, Luo T, Cheng Z, Li W, Gao F, Guo T, Gong Y, Wang B. Feather keratin hydrogel for wound repair: Preparation, healing effect and biocompatibility evaluation. Colloids Surf B Biointerfaces. 2017;149:341-50. doi: 10.1016/j.colsurfb.2016.10.038. PubMed PMID: 27792983.
46. Zhang Q, Shan G, Cao P, He J, Lin Z, Huang Y, Ao N. Mechanical and biological properties of oxidized horn keratin. Mater Sci Eng C Mater Biol Appl. 2015;47:123-34. doi: 10.1016/j.msec.2014.11.051. PubMed PMID: 25492180.
47. Jarrett A. The Chemistry of Inner Root Sheath and Hair Keratins. Brit J Dermatol. 1958;70(8-9):271-83. doi: DOI 10.1111/j.1365-2133.1958.tb13339.x. PubMed PMID: WOS:A1958XL48700001.
48. Crewther WG, Fraser RD, Lennox FG, Lindley H. The chemistry of keratins. Adv Protein Chem. 1965;20:191-346. PubMed PMID: 5334826.
49. Buchanan JH. Cystine-Rich Protein-Fraction from Oxidized Alpha-Keratin. Biochem J. 1977;167(2):489-91. PubMed PMID: WOS:A1977EA18500021.
50. Saul JM, Ellenburg MD, de Guzman RC, Van Dyke M. Keratin hydrogels support the sustained release of bioactive ciprofloxacin. J Biomed Mater Res A. 2011;98(4):544-53. doi: 10.1002/jbm.a.33147. PubMed PMID: 21681948.
51. Ham TR, Lee RT, Han S, Haque S, Vodovotz Y, Gu J, Burnett LR, Tomblyn S, Saul JM. Tunable Keratin Hydrogels for Controlled Erosion and Growth Factor Delivery. Biomacromolecules. 2016;17(1):225-36. doi: 10.1021/acs.biomac.5b01328. PubMed PMID: 26636618.

52. Wendel HP. Hemocompatibility testing in the 21st century: Options and pitfalls 2014 [cited 2016 9/5/16]. Available from: http://www.fda.gov/downloads/MedicalDevices/ĀewsEvents/WorkshopsConferences/UCM397150.pdf.
53. Li L, Tu M, Mou S, Zhou C. Preparation and blood compatibility of polysiloxane/liquid-crystal composite membranes. Biomaterials. 2001;22(19):2595-9. PubMed PMID: 11519778.
54. Kim YJ, Kang IK, Huh MW, Yoon SC. Surface characterization and in vitro blood compatibility of poly(ethylene terephthalate) immobilized with insulin and/or heparin using plasma glow discharge. Biomaterials. 2000;21(2):121-30. PubMed PMID: 10632394.
55. Fearing BV, Van Dyke ME. In vitro response of macrophage polarization to a keratin biomaterial. Acta Biomater. 2014;10(7):3136-44. doi: 10.1016/j.actbio.2014.04.003. PubMed PMID: 24726958.
56. Tsuchiya S, Yamabe M, Yamaguchi Y, Kobayashi Y, Konno T, Tada K. Establishment and characterization of a human acute monocytic leukemia cell line (THP-1). International journal of cancer. 1980;26(2):171-6. PubMed PMID: 6970727.
57. Apel PJ, Garrett JP, Sierpinski P, Ma J, Atala A, Smith TL, Koman LA, Van Dyke ME. Peripheral nerve regeneration using a keratin-based scaffold: long-term functional and histological outcomes in a mouse model. J Hand Surg Am. 2008;33(9):1541-7. doi: 10.1016/j.jhsa.2008.05.034. PubMed PMID: 18984336.
58. Xu S, Sang L, Zhang Y, Wang X, Li X. Biological evaluation of human hair keratin scaffolds for skin wound repair and regeneration. Mater Sci Eng C Mater Biol Appl. 2013;33(2):648-55. doi: 10.1016/j.msec.2012.10.011. PubMed PMID: 25427469.
59. Peyton CC, Keys T, Tomblyn S, Burmeister D, Beumer JH, Holleran JL, Sirintrapun J, Washburn S, Hodges SJ. Halofuginone infused keratin hydrogel attenuates adhesions in a rodent cecal abrasion model. J Surg Res. 2012;178(2):545-52. doi: 10.1016/j.jss.2012.07.053. PubMed PMID: 22901798.
60. Konop M, Sulejczak D, Czuwara J, Kosson P, Misicka A, Lipkowski AW, Rudnicka L. The role of allogenic keratin-derived dressing in wound healing in a mouse model. Wound Repair Regen. 2017;25(1):62-74. doi: 10.1111/wrr.12500. PubMed PMID: 27997709.

61. Lieber RL. Skeletal Muscle Fiber Structure. 2016.
62. Yin H, Price F, Rudnicki MA. Satellite cells and the muscle stem cell niche. Physiol Rev. 2013;93(1):23-67. doi: 10.1152/physrev.00043.2011. PubMed PMID: 23303905; PMCID: PMC4073943.
63. Choe MA, Kim KH, An GJ, Lee KS, Heitkemper M. Hindlimb muscle atrophy occurs from peripheral nerve damage in a rat neuropathic pain model. Biol Res Nurs. 2011;13(1):44-54. doi: 10.1177/1099800410382291. PubMed PMID: 21199814.
64. Thomas CK, Erb DE, Grumbles RM, Bunge RP. Embryonic cord transplants in peripheral nerve restore skeletal muscle function. J Āeurophysiol. 2000;84(1):591-5. PubMed PMID: 10899232.
65. Cartwright MS, Walker FO, Griffin LP, Caress JB. Peripheral nerve and muscle ultrasound in amyotrophic lateral sclerosis. Muscle Āerve. 2011;44(3):346-51. doi: 10.1002/mus.22035. PubMed PMID: 21815172; PMCID: PMC3193580.
66. Garg PK, Liu K, Ferrucci L, Guralnik JM, Criqui MH, Tian L, Sufit R, Āishida T, Tao H, Liao Y, McDermott MM. Lower extremity nerve function, calf skeletal muscle characteristics, and functional performance in peripheral arterial disease. J Am Geriatr Soc. 2011;59(10):1855-63. doi: 10.1111/j.1532-5415.2011.03600.x. PubMed PMID: 22091499; PMCID: PMC3222937.
67. Hilton M. Kaplan PM, and Joachim Kohn. The overwhelming use of rat models in nerve regeneration research may compromise designs of nerve guidance conduits for humans. Journal of Material Science Materials in Medicine. 2015;26(8):5; PMCID: PMC4545171.
68. Eschenhagen T, Eder A, Vollert I, Hansen A. Physiological aspects of cardiac tissue engineering. Am J Physiol Heart Circ Physiol. 2012;303(2):H133-43. doi: 10.1152/ajpheart.00007.2012. PubMed PMID: 22582087.
69. Shin M, Ishii O, Sueda T, Vacanti JP. Contractile cardiac grafts using a novel nanofibrous mesh. Biomaterials. 2004;25(17):3717-23. doi: 10.1016/j.biomaterials.2003.10.055. PubMed PMID: 15020147.
70. Johnson TD, Christman KL. Injectable hydrogel therapies and their delivery strategies for treating myocardial infarction. Expert opinion on drug delivery. 2013;10(1):59-72. doi: 10.1517/17425247.2013.739156. PubMed PMID: 23140533.

71. Dunlay SM, Pack QR, Thomas RJ, Killian JM, Roger VL. Participation in cardiac rehabilitation, readmissions, and death after acute myocardial infarction. The American journal of medicine. 2014;127(6):538-46. doi: 10.1016/j.amjmed.2014.02.008. PubMed PMID: 24556195; PMCID: 4035431.
72. Di Meglio F, Nurzynska D, Castaldo C, Miraglia R, Romano V, De Angelis A, Piegari E, Russo S, Montagnani S. Cardiac shock wave therapy: assessment of safety and new insights into mechanisms of tissue regeneration. Journal of cellular and molecular medicine. 2012;16(4):936-42. doi: 10.1111/j.1582-4934.2011.01393.x. PubMed PMID: 21790971; PMCID: 3822862.
73. Bursac N, Loo Y, Leong K, Tung L. Āovel anisotropic engineered cardiac tissues: studies of electrical propagation. Biochemical and biophysical research communications. 2007;361(4):847-53. doi: 10.1016/j.bbrc.2007.07.138. PubMed PMID: 17689494; PMCID: 2570036.
74. Āakata R, Tachibana A, Tanabe T. Preparation of keratin hydrogel/hydroxyapatite composite and its evaluation as a controlled drug release carrier. Mater Sci Eng C Mater Biol Appl. 2014;41:59-64. doi: 10.1016/j.msec.2014.04.016. PubMed PMID: 24907737.
75. Ye L, Chang YH, Xiong Q, Zhang P, Zhang L, Somasundaram P, Lepley M, Swingen C, Su L, Wendel JS, Guo J, Jang A, Rosenbush D, Greder L, Dutton JR, Zhang J, Kamp TJ, Kaufman DS, Ge Y, Zhang J. Cardiac repair in a porcine model of acute myocardial infarction with human induced pluripotent stem cell-derived cardiovascular cells. Cell stem cell. 2014;15(6):750-61. doi: 10.1016/j.stem.2014.11.009. PubMed PMID: 25479750; PMCID: 4275050.
76. Carpenter L, Carr C, Yang CT, Stuckey DJ, Clarke K, Watt SM. Efficient differentiation of human induced pluripotent stem cells generates cardiac cells that provide protection following myocardial infarction in the rat. Stem Cells Dev. 2012;21(6):977-86. doi: 10.1089/scd.2011.0075. PubMed PMID: 22182484; PMCID: PMC3315757.
77. Khan M, Āickoloff E, Abramova T, Johnson J, Verma SK, Krishnamurthy P, Mackie AR, Vaughan E, Garikipati VN, Benedict C, Ramirez V, Lambers E, Ito A, Gao E, Misener S, Luongo T, Elrod J, Qin G, Houser SR, Koch WJ, Kishore R. Embryonic stem cell-derived exosomes promote endogenous repair mechanisms and enhance cardiac function

following myocardial infarction. Circ Res. 2015;117(1):52-64. doi: 10.1161/CIRCRESAHA.117.305990. PubMed PMID: 25904597; PMCID: PMC4482130.

78. Zhang L, Guo J, Zhang P, Xiong Q, Wu SC, Xia L, Roy SS, Tolar J, O'Connell TD, Kyba M, Liao K, Zhang J. Derivation and high engraftment of patient-specific cardiomyocyte sheet using induced pluripotent stem cells generated from adult cardiac fibroblast. Circulation Heart failure. 2015;8(1):156-66. doi: 10.1161/CIRCHEARTFAILURE.114.001317. PubMed PMID: 25420485; PMCID: 4303534.
79. Ge X, Wang IN, Toma I, Sebastiano V, Liu J, Butte MJ, Reijo Pera RA, Yang PC. Human amniotic mesenchymal stem cell-derived induced pluripotent stem cells may generate a universal source of cardiac cells. Stem Cells Dev. 2012;21(15):2798-808. doi: 10.1089/scd.2011.0435. PubMed PMID: 22530853; PMCID: PMC3464077.
80. Templin C, Zweigerdt R, Schwanke K, Olmer R, Ghadri JR, Emmert MY, Muller E, Kuest SM, Cohrs S, Schibli R, Kronen P, Hilbe M, Reinisch A, Strunk D, Haverich A, Hoerstrup S, Luscher TF, Kaufmann PA, Landmesser U, Martin U. Transplantation and tracking of human-induced pluripotent stem cells in a pig model of myocardial infarction: assessment of cell survival, engraftment, and distribution by hybrid single photon emission computed tomography/computed tomography of sodium iodide symporter transgene expression. Circulation. 2012;126(4):430-9. doi: 10.1161/CIRCULATIOĀAHA.111.087684. PubMed PMID: 22767659.
81. Mann JR, Gadi I, Harbison ML, Abbondanzo SJ, Stewart CL. Androgenetic mouse embryonic stem cells are pluripotent and cause skeletal defects in chimeras: implications for genetic imprinting. Cell. 1990;62(2):251-60. PubMed PMID: 2372828.
82. Wada AM, Smith TK, Osler ME, Reese DE, Bader DM. Epicardial/mesothelial cell line retains vasculogenic potential of embryonic epicardium. Circulation research. 2003;92(5):525-31. doi: 10.1161/01.Res.0000060484.11032.0b. PubMed PMID: WOS:000181711300009.
83. Choi SH, Jung SY, Suh W, Baek SH, Kwon SM. Establishment of isolation and expansion protocols for human cardiac C-kit-positive progenitor cells for stem cell therapy. Transplantation proceedings. 2013;45(1):420-6. doi: 10.1016/j.transproceed.2012.08.017. PubMed PMID: 23375332.

84. Hosoda T. C-kit-positive cardiac stem cells and myocardial regeneration. American journal of cardiovascular disease. 2012;2(1):58-67. PubMed PMID: 22254215; PMCID: PMC3257153.
85. Tallini YN, Greene KS, Craven M, Spealman A, Breitbach M, Smith J, Fisher PJ, Steffey M, Hesse M, Doran RM, Woods A, Singh B, Yen A, Fleischmann BK, Kotlikoff MI. c-kit expression identifies cardiovascular precursors in the neonatal heart. Proc Natl Acad Sci U S A. 2009;106(6):1808-13. doi: 10.1073/pnas.0808920106. PubMed PMID: 19193854; PMCID: 2644119.
86. Wang G, Jacquet L, Karamariti E, Xu Q. Origin and differentiation of vascular smooth muscle cells. J Physiol. 2015;593(14):3013-30. doi: 10.1113/JP270033. PubMed PMID: 25952975; PMCID: PMC4532522.
87. Amali AA, Sie L, Winkler C, Featherstone M. Zebrafish hoxd4a acts upstream of meis1.1 to direct vasculogenesis, angiogenesis and hematopoiesis. PLoS One. 2013;8(3):e58857. doi: 10.1371/journal.pone.0058857. PubMed PMID: 23554940; PMCID: 3598951.
88. Yao Q, Renault MA, Chapouly C, Vandierdonck S, Belloc I, Jaspard-Vinassa B, Daniel-Lamaziere JM, Laffargue M, Merched A, Desgranges C, Gadeau AP. Sonic hedgehog mediates a novel pathway of PDGF-BB-dependent vessel maturation. Blood. 2014;123(15):2429-37. doi: 10.1182/blood-2013-06-508689. PubMed PMID: 24472833.
89. Zhou B, Ma Q, Rajagopal S, Wu SM, Domian I, Rivera-Feliciano J, Jiang D, von Gise A, Ikeda S, Chien KR, Pu WT. Epicardial progenitors contribute to the cardiomyocyte lineage in the developing heart. Āature. 2008;454(7200):109-13. doi: 10.1038/nature07060. PubMed PMID: 18568026; PMCID: 2574791.
90. Tian X, Hu T, Zhang H, He L, Huang X, Liu Q, Yu W, He L, Yang Z, Yan Y, Yang X, Zhong TP, Pu WT, Zhou B. Vessel formation. De novo formation of a distinct coronary vascular population in neonatal heart. Science. 2014;345(6192):90-4. doi: 10.1126/science.1251487. PubMed PMID: 24994653; PMCID: 4275002.
91. Sato Y. Dorsal aorta formation: separate origins, lateral-to-medial migration, and remodeling. Development, growth & differentiation. 2013;55(1):113-29. doi: 10.1111/dgd.12010. PubMed PMID: 23294360.

92. Xie C, Ritchie RP, Huang H, Zhang J, Chen YE. Smooth muscle cell differentiation in vitro: models and underlying molecular mechanisms. Arterioscler Thromb Vasc Biol. 2011;31(7):1485-94. doi: 10.1161/ATVBAHA.110.221101. PubMed PMID: 21677291; PMCID: 3123451.
93. House SJ, Potier M, Bisaillon J, Singer HA, Trebak M. The non-excitable smooth muscle: calcium signaling and phenotypic switching during vascular disease. Pflugers Archiv : European journal of physiology. 2008;456(5):769-85. doi: 10.1007/s00424-008-0491-8. PubMed PMID: 18365243; PMCID: 2531252.
94. Chade AR, Zhu XY, Grande JP, Krier JD, Lerman A, Lerman LO. Simvastatin abates development of renal fibrosis in experimental renovascular disease. Journal of hypertension. 2008;26(8):1651-60. doi: 10.1097/HJH.0b013e328302833a. PubMed PMID: 18622245.
95. Chi JT, Chang HY, Haraldsen G, Jahnsen FL, Troyanskaya OG, Chang DS, Wang Z, Rockson SG, van de Rijn M, Botstein D, Brown PO. Endothelial cell diversity revealed by global expression profiling. Proc Āatl Acad Sci U S A. 2003;100(19):10623-8. doi: 10.1073/pnas.1434429100. PubMed PMID: 12963823; PMCID: 196854.
96. Abedin M, Tintut Y, Demer LL. Mesenchymal stem cells and the artery wall. Circ Res. 2004;95(7):671-6. doi: 10.1161/01.RES.0000143421.27684.12. PubMed PMID: 15459088.
97. Urbich C, Dimmeler S. Endothelial progenitor cells functional characterization. Trends in cardiovascular medicine. 2004;14(8):318-22. doi: 10.1016/j.tcm.2004.10.001. PubMed PMID: 15596109.
98. Alberts B. JA, Lewis J., *et al*. Integrins. 4th ed. New York: Garland Science; 2002.
99. Mohamed JS, Boriek AM. Stretch augments TGF-beta1 expression through RhoA/ROCK1/2, PTK, and PI3K in airway smooth muscle cells. American journal of physiology Lung cellular and molecular physiology. 2010;299(3):L413-24. doi: 10.1152/ajplung.90628.2008. PubMed PMID: 20511342; PMCID: 2951069.
100. Risinger GM, Jr., Updike DL, Bullen EC, Tomasek JJ, Howard EW. TGF-beta suppresses the upregulation of MMP-2 by vascular smooth muscle cells in response to PDGF-BB. Am J Physiol Cell Physiol. 2010;298(1):C191-201. doi: 10.1152/ajpcell.00417.2008. PubMed PMID: 19846754; PMCID: 2806150.

101. Roy S, Samanta K, Chakraborti T, Chowdhury A, Chakraborti S. Role of TGF-beta1 and TĀF-alpha in IL-1beta mediated activation of proMMP-9 in pulmonary artery smooth muscle cells: involvement of an aprotinin sensitive protease. Archives of biochemistry and biophysics. 2011;513(1):61-9. doi: 10.1016/j.abb.2011.06.005. PubMed PMID: 21722622.
102. Korol A, Taiyab A, West-Mays JA. RhoA/ROCK signaling regulates TGFbeta-induced epithelial-mesenchymal transition of lens epithelial cells through MRTF-A. Molecular medicine. 2016;22. doi: 10.2119/molmed.2016.00041. PubMed PMID: 27704140; PMCID: PMC5135079.
103. Miano JM, Long X, Fujiwara K. Serum response factor: master regulator of the actin cytoskeleton and contractile apparatus. Am J Physiol Cell Physiol. 2007;292(1):C70-81. doi: 10.1152/ajpcell.00386.2006. PubMed PMID: 16928770.
104. Liu R, Leslie KL, Martin KA. Epigenetic regulation of smooth muscle cell plasticity. Biochimica et biophysica acta. 2015;1849(4):448-53. doi: 10.1016/j.bbagrm.2014.06.004. PubMed PMID: 24937434; PMCID: 4552189.
105. Rzucidlo EM, Martin KA, Powell RJ. Regulation of vascular smooth muscle cell differentiation. Journal of vascular surgery. 2007;45 Suppl A:A25-32. doi: 10.1016/j.jvs.2007.03.001. PubMed PMID: 17544021.
106. Hirota N, McCuaig S, O'Sullivan MJ, Martin JG. Serotonin augments smooth muscle differentiation of bone marrow stromal cells. Stem cell research. 2014;12(3):599-609. doi: 10.1016/j.scr.2014.02.003. PubMed PMID: 24595007.
107. Shi N, Guo X, Chen SY. Olfactomedin 2, a novel regulator for transforming growth factor-beta-induced smooth muscle differentiation of human embryonic stem cell-derived mesenchymal cells. Mol Biol Cell. 2014;25(25):4106-14. doi: 10.1091/mbc.E14-08-1255. PubMed PMID: 25298399; PMCID: PMC4263453.
108. Tran DQ, Andersson J, Wang R, Ramsey H, Unutmaz D, Shevach EM. GARP (LRRC32) is essential for the surface expression of latent TGF-beta on platelets and activated FOXP3+ regulatory T cells. Proc Natl Acad Sci U S A. 2009;106(32):13445-50. doi: 10.1073/pnas.0901944106. PubMed PMID: 19651619; PMCID: PMC2726354.
109. Floren M, Bonani W, Dharmarajan A, Motta A, Migliaresi C, Tan W. Human mesenchymal stem cells cultured on silk hydrogels with variable stiffness and growth factor

differentiate into mature smooth muscle cell phenotype. Acta Biomater. 2016;31:156-66. doi: 10.1016/j.actbio.2015.11.051. PubMed PMID: 26621695; PMCID: PMC4728007.

110. Sajid M, Lele M, Stouffer GA. Autocrine thrombospondin partially mediates TGF-beta1-induced proliferation of vascular smooth muscle cells. Am J Physiol Heart Circ Physiol. 2000;279(5):H2159-65. PubMed PMID: 11045949.
111. Park WS, Heo SC, Jeon ES, Hong da H, Son YK, Ko JH, Kim HK, Lee SY, Kim JH, Han J. Functional expression of smooth muscle-specific ion channels in TGF-beta(1)-treated human adipose-derived mesenchymal stem cells. Am J Physiol Cell Physiol. 2013;305(4):C377-91. doi: 10.1152/ajpcell.00404.2012. PubMed PMID: 23761629; PMCID: 3891216.
112. O'Callaghan CJ, Williams B. Mechanical strain-induced extracellular matrix production by human vascular smooth muscle cells: role of TGF-beta(1). Hypertension. 2000;36(3):319-24. PubMed PMID: 10988258.
113. ten Dijke P, Arthur HM. Extracellular control of TGFbeta signalling in vascular development and disease. Nature reviews Molecular cell biology. 2007;8(11):857-69. doi: 10.1038/nrm2262. PubMed PMID: 17895899.
114. Huang WY, Xie W, Guo X, Li F, Jose PA, Chen SY. Smad2 and PEA3 cooperatively regulate transcription of response gene to complement 32 in TGF-beta-induced smooth muscle cell differentiation of neural crest cells. Am J Physiol Cell Physiol. 2011;301(2):C499-506. doi: 10.1152/ajpcell.00480.2010. PubMed PMID: 21613609; PMCID: 3154553.
115. Feinberg MW, Watanabe M, Lebedeva MA, Depina AS, Hanai J, Mammoto T, Frederick JP, Wang XF, Sukhatme VP, Jain MK. Transforming growth factor-beta1 inhibition of vascular smooth muscle cell activation is mediated via Smad3. J Biol Chem. 2004;279(16):16388-93. doi: 10.1074/jbc.M309664200. PubMed PMID: 14754879.
116. Kennard S, Liu H, Lilly B. Transforming growth factor-beta (TGF- 1) down-regulates Āotch3 in fibroblasts to promote smooth muscle gene expression. J Biol Chem. 2008;283(3):1324-33. doi: 10.1074/jbc.M706651200. PubMed PMID: 17981798.
117. Kalinina N, Agrotis A, Antropova Y, Ilyinskaya O, Smirnov V, Tararak E, Bobik A. Smad expression in human atherosclerotic lesions: evidence for impaired TGF-beta/Smad signaling in smooth muscle cells of fibrofatty lesions. Arterioscler Thromb Vasc Biol.

2004;24(8):1391-6. doi: 10.1161/01.ATV.0000133605.89421.79. PubMed PMID: 15166010.

118. Massague J. TGFbeta signalling in context. Nature reviews Molecular cell biology. 2012;13(10):616-30. doi: 10.1038/nrm3434. PubMed PMID: 22992590; PMCID: 4027049.
119. Sohni A, Mulas F, Ferrazzi F, Luttun A, Bellazzi R, Huylebroeck D, Ekker SC, Verfaillie CM. TGFbeta1-induced Baf60c regulates both smooth muscle cell commitment and quiescence. PLoS One. 2012;7(10):e47629. doi: 10.1371/journal.pone.0047629. PubMed PMID: 23110084; PMCID: 3482188.
120. Schmidt A, Gopfert C, Vlodavsky I, Volker W, Buddecke E. Induction of a hypertrophic growth status of coronary smooth muscle cells is associated with an overexpression of TGF-beta. European journal of cell biology. 2002;81(3):138-44. PubMed PMID: 11998865.
121. Bradbury DA, Newton R, Zhu YM, Stocks J, Corbett L, Holland ED, Pang LH, Knox AJ. Effect of bradykinin, TGF-beta1, IL-1beta, and hypoxia on COX-2 expression in pulmonary artery smooth muscle cells. American journal of physiology Lung cellular and molecular physiology. 2002;283(4):L717-25. doi: 10.1152/ajplung.00070.2002. PubMed PMID: 12225948.
122. Chen CA, Hwang JC, Guh JY, Tsai JC, Chen HC. TGF-beta1 and integrin synergistically facilitate the differentiation of rat podocytes by increasing alpha-smooth muscle actin expression. Translational research : the journal of laboratory and clinical medicine. 2006;148(3):134-41. doi: 10.1016/j.trsl.2006.03.008. PubMed PMID: 16938651.
123. Willems E, Cabral-Teixeira J, Schade D, Cai W, Reeves P, Bushway PJ, Lanier M, Walsh C, Kirchhausen T, Izpisua Belmonte JC, Cashman J, Mercola M. Small molecule-mediated TGF-beta type II receptor degradation promotes cardiomyogenesis in embryonic stem cells. Cell stem cell. 2012;11(2):242-52. doi: 10.1016/j.stem.2012.04.025. PubMed PMID: 22862949; PMCID: PMC3419596.
124. Wang MK, Sun HQ, Xiang YC, Jiang F, Su YP, Zou ZM. Different roles of TGF-beta in the multi-lineage differentiation of stem cells. World J Stem Cells. 2012;4(5):28-34. doi: 10.4252/wjsc.v4.i5.28. PubMed PMID: 22993659; PMCID: PMC3443709.

125. Oenema TA, Smit M, Smedinga L, Racke K, Halayko AJ, Meurs H, Gosens R. Muscarinic receptor stimulation augments TGF-beta1-induced contractile protein expression by airway smooth muscle cells. American journal of physiology Lung cellular and molecular physiology. 2012;303(7):L589-97. doi: 10.1152/ajplung.00400.2011. PubMed PMID: 22865549.
126. Balint B, Yin H, Chakrabarti S, Chu MW, Sims SM, Pickering JG. Collectivization of Vascular Smooth Muscle Cells via TGF-beta-Cadherin-11-Dependent Adhesive Switching. Arterioscler Thromb Vasc Biol. 2015;35(5):1254-64. doi: 10.1161/ATVBAHA.115.305310. PubMed PMID: 25767275.
127. Tang Y, Yang X, Friesel RE, Vary CP, Liaw L. Mechanisms of TGF-beta-induced differentiation in human vascular smooth muscle cells. Journal of vascular research. 2011;48(6):485-94. doi: 10.1159/000327776. PubMed PMID: 21832838; PMCID: 3169366.
128. Oida T, Weiner HL. Overexpression of TGF-ss 1 gene induces cell surface localized glucose-regulated protein 78-associated latency-associated peptide/TGF-ss. Journal of immunology. 2010;185(6):3529-35. doi: 10.4049/jimmunol.0904121. PubMed PMID: 20720212; PMCID: 2997468.
129. Andrae J, Gallini R, Betsholtz C. Role of platelet-derived growth factors in physiology and medicine. Genes & development. 2008;22(10):1276-312. doi: 10.1101/gad.1653708. PubMed PMID: 18483217; PMCID: 2732412.
130. Xu ZC, Zhang Q, Li H. Human hair follicle stem cell differentiation into contractile smooth muscle cells is induced by transforming growth factor-beta1 and platelet-derived growth factor BB. Molecular medicine reports. 2013;8(6):1715-21. doi: 10.3892/mmr.2013.1707. PubMed PMID: 24084832.
131. Wanjare M, Kuo F, Gerecht S. Derivation and maturation of synthetic and contractile vascular smooth muscle cells from human pluripotent stem cells. Cardiovascular research. 2013;97(2):321-30. doi: 10.1093/cvr/cvs315. PubMed PMID: 23060134; PMCID: 3543989.
132. Kim JY, Kim KH, Lee WR, An HJ, Lee SJ, Han SM, Lee KG, Park YY, Kim KS, Lee YS, Park KK. Apamin inhibits PDGF-BB-induced vascular smooth muscle cell proliferation and migration through suppressions of activated Akt and Erk signaling pathway. Vascular

pharmacology. 2015;70:8-14. doi: 10.1016/j.vph.2014.12.004. PubMed PMID: 25737404.

133. Li J, Zhang M, Ma J. Myricitrin inhibits PDGF-BB-stimulated vascular smooth muscle cell proliferation and migration through suppressing PDGFRbeta/Akt/Erk signaling. International journal of clinical and experimental medicine. 2015;8(11):21715-23. PubMed PMID: 26885133; PMCID: PMC4723978.
134. Kingsley K, Huff JL, Rust WL, Carroll K, Martinez AM, Fitchmun M, Plopper GE. ERK1/2 mediates PDGF-BB stimulated vascular smooth muscle cell proliferation and migration on laminin-5. Biochemical and biophysical research communications. 2002;293(3):1000-6. doi: 10.1016/S0006-291X(02)00331-5. PubMed PMID: 12051759.
135. Munoz-Chapuli R, Macias D, Gonzalez-Iriarte M, Carmona R, Atencia G, Perez-Pomares JM. [The epicardium and epicardial-derived cells: multiple functions in cardiac development]. Revista espanola de cardiologia. 2002;55(10):1070-82. PubMed PMID: 12383393.
136. Xiao Q, Zeng L, Zhang Z, Hu Y, Xu Q. Stem cell-derived Sca-1+ progenitors differentiate into smooth muscle cells, which is mediated by collagen IV-integrin alpha1/beta1/alphav and PDGF receptor pathways. Am J Physiol Cell Physiol. 2007;292(1):C342-52. doi: 10.1152/ajpcell.00341.2006. PubMed PMID: 16914533.
137. Chen CY, Liu SH, Chen CY, Chen PC, Chen CP. Human placenta-derived multipotent mesenchymal stromal cells involved in placental angiogenesis via the PDGF-BB and STAT3 pathways. Biology of reproduction. 2015;93(4):103. doi: 10.1095/biolreprod.115.131250. PubMed PMID: 26353894.
138. Vo E, Hanjaya-Putra D, Zha Y, Kusuma S, Gerecht S. Smooth-muscle-like cells derived from human embryonic stem cells support and augment cord-like structures in vitro. Stem cell reviews. 2010;6(2):237-47. doi: 10.1007/s12015-010-9144-3. PubMed PMID: 20425149.
139. Margariti A, Xiao Q, Zampetaki A, Zhang Z, Li H, Martin D, Hu Y, Zeng L, Xu Q. Splicing of HDAC7 modulates the SRF-myocardin complex during stem-cell differentiation towards smooth muscle cells. J Cell Sci. 2009;122(Pt 4):460-70. doi: 10.1242/jcs.034850. PubMed PMID: 19174469.

140. Zhang L, Jin M, Margariti A, Wang G, Luo Z, Zampetaki A, Zeng L, Ye S, Zhu J, Xiao Q. Sp1-dependent activation of HDAC7 is required for platelet-derived growth factor-BB-induced smooth muscle cell differentiation from stem cells. J Biol Chem. 2010;285(49):38463-72. doi: 10.1074/jbc.M110.153999. PubMed PMID: 20889501; PMCID: PMC2992279.
141. Hegner B, Schaub T, Catar R, Kusch A, Wagner P, Essin K, Lange C, Riemekasten G, Dragun D. Intrinsic Deregulation of Vascular Smooth Muscle and Myofibroblast Differentiation in Mesenchymal Stromal Cells from Patients with Systemic Sclerosis. PLoS One. 2016;11(4):e0153101. doi: 10.1371/journal.pone.0153101. PubMed PMID: 27054717; PMCID: 4824407.
142. Gupta P, Nayak KK. Compatibility study of alginate/keratin blend for biopolymer development. J Appl Biomater Funct Mater. 2015;13(4):e332-9. doi: 10.5301/jabfm.5000242. PubMed PMID: 26350347.
143. Āew Approaches in Health Statistics - Report of Second International Conference of National Committees on Vital and Health Statistics - World-Health-Organization. Who Chron. 1975;29(5):205-. PubMed PMID: WOS:A1975AD52600008.
144. Mogosanu GD, Grumezescu AM, Chifiriuc MC. Keratin-based biomaterials for biomedical applications. Current drug targets. 2014;15(5):518-30. PubMed PMID: 24606008.
145. He JQ, Vu DM, Hunt G, Chugh A, Bhatnagar A, Bolli R. Human cardiac stem cells isolated from atrial appendages stably express c-kit. PLoS One. 2011;6(11):e27719. doi: 10.1371/journal.pone.0027719. PubMed PMID: 22140461; PMCID: 3225366.
146. Benton JA, DeForest CA, Vivekanandan V, Anseth KS. Photocrosslinking of gelatin macromers to synthesize porous hydrogels that promote valvular interstitial cell function. Tissue Eng Part A. 2009;15(11):3221-30. doi: 10.1089/ten.TEA.2008.0545. PubMed PMID: 19374488; PMCID: 2783792.
147. McGonigle S, Shifrin V. In vitro assay of angiogenesis: inhibition of capillary tube formation. Current protocols in pharmacology / editorial board, SJ Enna. 2008;Chapter 12:Unit12 doi: 10.1002/0471141755.ph1212s43. PubMed PMID: 22294219.
148. Block GD, Locker J, Bowen WC, Petersen BE, Katyal S, Strom SC, Riley T, Howard TA, Michalopoulos GK. Population expansion, clonal growth, and specific differentiation

patterns in primary cultures of hepatocytes induced by HGF/SF, EGF and TGF alpha in a chemically defined (HGM) medium. The Journal of cell biology. 1996;132(6):1133-49. PubMed PMID: 8601590; PMCID: 2120765.

149. Di Felice V, Ardizzone NM, De Luca A, Marciano V, Marino Gammazza A, Macaluso F, Manente L, Cappello F, De Luca A, Zummo G. OPLA scaffold, collagen I, and horse serum induce an higher degree of myogenic differentiation of adult rat cardiac stem cells. Journal of cellular physiology. 2009;221(3):729-39. doi: 10.1002/jcp.21912. PubMed PMID: 19725057.
150. Choi SH, Jung SY, Yoo SM, Asahara T, Suh W, Kwon SM, Baek SH. Amine-enriched surface modification facilitates expansion, attachment, and maintenance of human cardiac-derived c-kit positive progenitor cells. International journal of cardiology. 2013;168(1):100-7. doi: 10.1016/j.ijcard.2012.09.065. PubMed PMID: 23046590.
151. Lau ST, Hansford LM, Chan WK, Chan GC, Wan TS, Wong KK, Kaplan DR, Tam PK, Ngan ES. Prokineticin signaling is required for the maintenance of a de novo population of c-KIT(+) cells to sustain neuroblastoma progression. Oncogene. 2015;34(8):1019-34. doi: 10.1038/onc.2014.24. PubMed PMID: 24632619.
152. Chang SH, Elemento O, Zhang J, Zhuang ZW, Simons M, Hla T. ELAVL1 regulates alternative splicing of eIF4E transporter to promote postnatal angiogenesis. Proc Natl Acad Sci U S A. 2014;111(51):18309-14. doi: 10.1073/pnas.1412172111. PubMed PMID: 25422430; PMCID: 4280608.
153. Schrader J, Gordon-Walker TT, Aucott RL, van Deemter M, Quaas A, Walsh S, Benten D, Forbes SJ, Wells RG, Iredale JP. Matrix stiffness modulates proliferation, chemotherapeutic response, and dormancy in hepatocellular carcinoma cells. Hepatology. 2011;53(4):1192-205. doi: 10.1002/hep.24108. PubMed PMID: 21442631; PMCID: 3076070.
154. Boopathy AV, Che PL, Somasuntharam I, Fiore VF, Cabigas EB, Ban K, Brown ME, Narui Y, Barker TH, Yoon YS, Salaita K, Garcia AJ, Davis ME. The modulation of cardiac progenitor cell function by hydrogel-dependent Āotch1 activation. Biomaterials. 2014;35(28):8103-12. doi: 10.1016/j.biomaterials.2014.05.082. PubMed PMID: 24974008; PMCID: 4150689.

155. Mousavi SJ, Doweidar MH. Role of Mechanical Cues in Cell Differentiation and Proliferation: A 3D Āumerical Model. PLoS One. 2015;10(5):e0124529. doi: 10.1371/journal.pone.0124529. PubMed PMID: 25933372; PMCID: 4416758.
156. Vasconcelos A, Cavaco-Paulo A. The use of keratin in biomedical applications. Current drug targets. 2013;14(5):612-9. PubMed PMID: 23410124.
157. Lee SY, Bang S, Kim S, Jo SY, Kim BC, Hwang Y, Noh I. Synthesis and in vitro characterizations of porous carboxymethyl cellulose-poly(ethylene oxide) hydrogel film. Biomaterials research. 2015;19:12. doi: 10.1186/s40824-015-0033-3. PubMed PMID: 26331082; PMCID: 4552372.
158. Vardar E, Vert M, Coudane J, Hasirci V, Hasirci N. Porous Agarose-Based Semi-IPN Hydrogels: Characterization and Cell Affinity Studies. J Biomater Sci Polym Ed. 2012;23(18):2273-86. doi: 10.1163/156856211X614770. PubMed PMID: 22182333.
159. Xiao X, Wang W, Liu D, Zhang HQ, Gao P, Geng L, Yuan YL, Lu JX, Wang Z. The promotion of angiogenesis induced by three-dimensional porous beta-tricalcium phosphate scaffold with different interconnection sizes via activation of PI3K/Akt pathways. Sci Rep-Uk. 2015;5. doi: Artn 9409
10.1038/Srep09409. PubMed PMID: WOS:000351376400002.
160. Richter JR, de Guzman RC, Van Dyke ME. Mechanisms of hepatocyte attachment to keratin biomaterials. Biomaterials. 2011;32(30):7555-61. doi: 10.1016/j.biomaterials.2011.06.061. PubMed PMID: 21782237.
161. Qiu W, Yang K, Lei M, Yan H, Tang H, Bai X, Yang G, Lian X, Wu J. SCF/c-kit signaling is required in 12-O-tetradecanoylphorbol-13-acetate-induced migration and differentiation of hair follicle melanocytes for epidermal pigmentation. Cell and tissue research. 2015;360(2):333-46. doi: 10.1007/s00441-014-2101-8. PubMed PMID: 25727244.
162. Arnaoutova I, George J, Kleinman HK, Benton G. The endothelial cell tube formation assay on basement membrane turns 20: state of the science and the art. Angiogenesis. 2009;12(3):267-74. doi: 10.1007/s10456-009-9146-4. PubMed PMID: 19399631.
163. Ghionzoli M, Repele A, Sartiani L, Costanzi G, Parenti A, Spinelli V, David AL, Garriboli M, Totonelli G, Tian J, Andreadis ST, Cerbai E, Mugelli A, Messineo A, Pierro A, Eaton S, De Coppi P. Human amniotic fluid stem cell differentiation along smooth muscle

lineage. FASEB journal : official publication of the Federation of American Societies for Experimental Biology. 2013;27(12):4853-65. doi: 10.1096/fj.12-218578. PubMed PMID: 23995291.

164. Kurpinski K, Lam H, Chu J, Wang A, Kim A, Tsay E, Agrawal S, Schaffer DV, Li S. Transforming growth factor-beta and notch signaling mediate stem cell differentiation into smooth muscle cells. Stem cells. 2010;28(4):734-42. doi: 10.1002/stem.319. PubMed PMID: 20146266.
165. Ross JJ, Hong Z, Willenbring B, Zeng L, Isenberg B, Lee EH, Reyes M, Keirstead SA, Weir EK, Tranquillo RT, Verfaillie CM. Cytokine-induced differentiation of multipotent adult progenitor cells into functional smooth muscle cells. J Clin Invest. 2006;116(12):3139-49. doi: 10.1172/JCI28184. PubMed PMID: 17099777; PMCID: 1635164.
166. Sinha S, Hoofnagle MH, Kingston PA, McCanna ME, Owens GK. Transforming growth factor-beta1 signaling contributes to development of smooth muscle cells from embryonic stem cells. Am J Physiol Cell Physiol. 2004;287(6):C1560-8. doi: 10.1152/ajpcell.00221.2004. PubMed PMID: 15306544.
167. Zhang J, Huang C, Wu P, Yang J, Song T, Chen Y, Fan X, Wang T. Differentiation induction of cardiac c-kit positive cells from rat heart into sinus node-like cells by 5-azacytidine. Tissue & cell. 2011;43(2):67-74. doi: 10.1016/j.tice.2010.11.005. PubMed PMID: 21237473.
168. Liu Y, Song J, Liu W, Wan Y, Chen X, Hu C. Growth and differentiation of rat bone marrow stromal cells: does 5-azacytidine trigger their cardiomyogenic differentiation? Cardiovascular research. 2003;58(2):460-8. PubMed PMID: 12757880.
169. Yang G, Tian J, Feng C, Zhao LL, Liu Z, Zhu J. Trichostatin a promotes cardiomyocyte differentiation of rat mesenchymal stem cells after 5-azacytidine induction or during coculture with neonatal cardiomyocytes via a mechanism independent of histone deacetylase inhibition. Cell Transplant. 2012;21(5):985-96. doi: 10.3727/096368911X593145. PubMed PMID: 21944777.
170. Yoon BS, Yoo SJ, Lee JE, You S, Lee HT, Yoon HS. Enhanced differentiation of human embryonic stem cells into cardiomyocytes by combining hanging drop culture and 5-azacytidine treatment. Differentiation; research in biological diversity.

2006;74(4):149-59. doi: 10.1111/j.1432-0436.2006.00063.x. PubMed PMID: 16683985.

171. Antonitsis P, Ioannidou-Papagiannaki E, Kaidoglou A, Papakonstantinou C. In vitro cardiomyogenic differentiation of adult human bone marrow mesenchymal stem cells. The role of 5-azacytidine. Interactive cardiovascular and thoracic surgery. 2007;6(5):593-7. doi: 10.1510/icvts.2007.157875. PubMed PMID: 17670726.
172. Balana B, Āicoletti C, Zahanich I, Graf EM, Christ T, Boxberger S, Ravens U. 5-Azacytidine induces changes in electrophysiological properties of human mesenchymal stem cells. Cell research. 2006;16(12):949-60. doi: 10.1038/sj.cr.7310116. PubMed PMID: 17160070.
173. Kaur K, Yang J, Eisenberg CA, Eisenberg LM. 5-azacytidine promotes the transdifferentiation of cardiac cells to skeletal myocytes. Cellular reprogramming. 2014;16(5):324-30. doi: 10.1089/cell.2014.0021. PubMed PMID: 25090621.
174. Royer CL, Howell JC, Morrison PR, Srour EF, Yoder MC. Muscle-derived CD45-SCA-1+c-kit- progenitor cells give rise to skeletal muscle myotubes in vitro. In vitro cellular & developmental biology Animal. 2002;38(9):512-7. doi: 10.1290/1071-2690(2002)038<0512:MCPCGR>2.0.CO;2. PubMed PMID: 12703978.
175. Narita Y, Yamawaki A, Kagami H, Ueda M, Ueda Y. Effects of transforming growth factor-beta 1 and ascorbic acid on differentiation of human bone-marrow-derived mesenchymal stem cells into smooth muscle cell lineage. Cell and tissue research. 2008;333(3):449-59. doi: 10.1007/s00441-008-0654-0. PubMed PMID: 18607632.
176. Simionescu A, Philips K, Vyavahare N. Elastin-derived peptides and TGF-beta1 induce osteogenic responses in smooth muscle cells. Biochemical and biophysical research communications. 2005;334(2):524-32. doi: 10.1016/j.bbrc.2005.06.119. PubMed PMID: 16005428.
177. Gacchina CE, Ramamurthi A. Impact of pre-existing elastic matrix on TGFbeta1 and HA oligomer-induced regenerative elastin repair by rat aortic smooth muscle cells. J Tissue Eng Regen Med. 2011;5(2):85-96. doi: 10.1002/term.286. PubMed PMID: 20653044; PMCID: 2964397.
178. Shimizu N, Yamamoto K, Obi S, Kumagaya S, Masumura T, Shimano Y, Naruse K, Yamashita JK, Igarashi T, Ando J. Cyclic strain induces mouse embryonic stem cell

differentiation into vascular smooth muscle cells by activating PDGF receptor beta. J Appl Physiol (1985). 2008;104(3):766-72. doi: 10.1152/japplphysiol.00870.2007. PubMed PMID: 18187612.

179. Grako KA, Ochiya T, Barritt D, Nishiyama A, Stallcup WB. PDGF (alpha)-receptor is unresponsive to PDGF-AA in aortic smooth muscle cells from the NG2 knockout mouse. J Cell Sci. 1999;112 (Pt 6):905-15. PubMed PMID: 10036240.
180. Fukuda N, Kishioka H, Satoh C, Nakayama T, Watanabe Y, Soma M, Izumi Y, Kanmatsuse K. Role of long-form PDGF A-chain in the growth of vascular smooth muscle cells from spontaneously hypertensive rats. American journal of hypertension. 1997;10(10 Pt 1):1117-24. PubMed PMID: 9370382.
181. Chen G, Khalil N. TGF-beta1 increases proliferation of airway smooth muscle cells by phosphorylation of map kinases. Respiratory research. 2006;7:2. doi: 10.1186/1465-9921-7-2. PubMed PMID: 16390551; PMCID: 1360679.
182. Oida T, Weiner HL. TGF-beta induces surface LAP expression on murine CD4 T cells independent of Foxp3 induction. PLoS One. 2010;5(11):e15523. doi: 10.1371/journal.pone.0015523. PubMed PMID: 21124798; PMCID: 2991360.
183. Collagenase 2017. Available from: http://www.worthington-biochem.com/cls/default.html.
184. Tojo M, Hamashima Y, Hanyu A, Kajimoto T, Saitoh M, Miyazono K, Node M, Imamura T. The ALK-5 inhibitor A-83-01 inhibits Smad signaling and epithelial-to-mesenchymal transition by transforming growth factor-beta. Cancer science. 2005;96(11):791-800. doi: 10.1111/j.1349-7006.2005.00103.x. PubMed PMID: 16271073.
185. Wang N, Wang X, Sun B, Zeng M, Xing C, Zhao X, Yang J. Role of TGF-beta1 in production of fibronectin in vascular smooth muscle cells cultured under high-phosphate conditions. Journal of nephrology. 2013;26(1):213-8. doi: 10.5301/jn.5000127. PubMed PMID: 22641576.
186. Espagnolle N, Guilloton F, Deschaseaux F, Gadelorge M, Sensebe L, Bourin P. CD146 expression on mesenchymal stem cells is associated with their vascular smooth muscle commitment. Journal of cellular and molecular medicine. 2014;18(1):104-14. doi: 10.1111/jcmm.12168. PubMed PMID: 24188055; PMCID: 3916122.

187. Montague CR, Hunter MG, Gavrilin MA, Phillips GS, Goldschmidt-Clermont PJ, Marsh CB. Activation of estrogen receptor-alpha reduces aortic smooth muscle differentiation. Circ Res. 2006;99(5):477-84. doi: 10.1161/01.RES.0000238376.72592.a2. PubMed PMID: 16873715; PMCID: 1905928.
188. Rang HP, Dale MM, Flower RJ, Henderson G. Rang & Dale's pharmacology. Eighth edition. ed. xv, 760 pages p.
189. Wu Y, Tran T, Dwabe S, Sarkissyan M, Kim J, Nava M, Clayton S, Pietras R, Farias-Eisner R, Vadgama JV. A83-01 inhibits TGF-beta-induced upregulation of Wnt3 and epithelial to mesenchymal transition in HER2-overexpressing breast cancer cells. Breast cancer research and treatment. 2017;163(3):449-60. doi: 10.1007/s10549-017-4211-y. PubMed PMID: 28337662; PMCID: 5427117.
190. Yu J, Chau KF, Vodyanik MA, Jiang J, Jiang Y. Efficient feeder-free episomal reprogramming with small molecules. PLoS One. 2011;6(3):e17557. doi: 10.1371/journal.pone.0017557. PubMed PMID: 21390254; PMCID: PMC3046978.
191. Wang N, Wang X, Xing C, Sun B, Yu X, Hu J, Liu J, Zeng M, Xiong M, Zhou S, Yang J. Role of TGF-beta1 in bone matrix production in vascular smooth muscle cells induced by a high-phosphate environment. Nephron Experimental nephrology. 2010;115(3):e60-8. doi: 10.1159/000313831. PubMed PMID: 20424484.
192. Wang X, Hu G, Betts C, Harmon EY, Keller RS, Van De Water L, Zhou J. Transforming growth factor-beta1-induced transcript 1 protein, a novel marker for smooth muscle contractile phenotype, is regulated by serum response factor/myocardin protein. J Biol Chem. 2011;286(48):41589-99. doi: 10.1074/jbc.M111.250878. PubMed PMID: 21984848; PMCID: 3308869.
193. Rama A, Matsushita T, Charolidi N, Rothery S, Dupont E, Severs NJ. Up-regulation of connexin43 correlates with increased synthetic activity and enhanced contractile differentiation in TGF-beta-treated human aortic smooth muscle cells. European journal of cell biology. 2006;85(5):375-86. doi: 10.1016/j.ejcb.2005.11.007. PubMed PMID: 16442184.
194. Qi YX, Jiang J, Jiang XH, Wang XD, Ji SY, Han Y, Long DK, Shen BR, Yan ZQ, Chien S, Jiang ZL. PDGF-BB and TGF-{beta}1 on cross-talk between endothelial and smooth muscle cells in vascular remodeling induced by low shear stress. Proc Āatl Acad Sci U S A.

2011;108(5):1908-13. doi: 10.1073/pnas.1019219108. PubMed PMID: 21245329; PMCID: 3033274.

195. Groenendijk BC, Benus GF, Klous A, Pacheco YM, Volger OL, Fledderus JO, Ferreira V, Engelse MA, Pannekoek H, ten Dijke P, Horrevoets AJ, de Vries CJ. Activin A induces a non-fibrotic phenotype in smooth muscle cells in contrast to TGF-beta. Experimental cell research. 2011;317(2):131-42. doi: 10.1016/j.yexcr.2010.10.007. PubMed PMID: 20955695.
196. Belmadani S, Zerfaoui M, Boulares HA, Palen DI, Matrougui K. Microvessel vascular smooth muscle cells contribute to collagen type I deposition through ERK1/2 MAP kinase, alphavbeta3-integrin, and TGF-beta1 in response to ANG II and high glucose. Am J Physiol Heart Circ Physiol. 2008;295(1):H69-76. doi: 10.1152/ajpheart.00341.2008. PubMed PMID: 18456735; PMCID: 2494762.
197. Ikedo H, Tamaki K, Ueda S, Kato S, Fujii M, Ten Dijke P, Okuda S. Smad protein and TGF-beta signaling in vascular smooth muscle cells. International journal of molecular medicine. 2003;11(5):645-50. PubMed PMID: 12684705.
198. Samarakoon R, Higgins PJ. Integration of non-SMAD and SMAD signaling in TGF-beta1-induced plasminogen activator inhibitor type-1 gene expression in vascular smooth muscle cells. Thrombosis and haemostasis. 2008;100(6):976-83. PubMed PMID: 19132220; PMCID: 2963177.
199. Munger JS, Sheppard D. Cross talk among TGF-beta signaling pathways, integrins, and the extracellular matrix. Cold Spring Harbor perspectives in biology. 2011;3(11):a005017. doi: 10.1101/cshperspect.a005017. PubMed PMID: 21900405; PMCID: 3220354.
200. Koli K, Saharinen J, Hyytiainen M, Penttinen C, Keski-Oja J. Latency, activation, and binding proteins of TGF-beta. Microsc Res Tech. 2001;52(4):354-62. doi: 10.1002/1097-0029(20010215)52:4<354::AID-JEMT1020>3.0.CO;2-G. PubMed PMID: 11170294.
201. Kang SW, Kim MS, Kim HS, Lee YJ, Kang YH. Anti-atherogenic activity of wild grape (Vitis thunbergii) extract antagonizing smooth muscle cell proliferation and migration promoted by neighboring macrophages. International journal of molecular medicine. 2012;29(6):1137-45. doi: 10.3892/ijmm.2012.931. PubMed PMID: 22407282.

202. Xiao Q, Luo Z, Pepe AE, Margariti A, Zeng L, Xu Q. Embryonic stem cell differentiation into smooth muscle cells is mediated by Nox4-produced H2O2. Am J Physiol Cell Physiol. 2009;296(4):C711-23. doi: 10.1152/ajpcell.00442.2008. PubMed PMID: 19036941.
203. Schlaf G, Schmitz M, Heine I, Demberg T, Schieferdecker HL, Gotze O. Upregulation of fibronectin but not of entactin, collagen IV and smooth muscle actin by anaphylatoxin C5a in rat hepatic stellate cells. Histology and histopathology. 2004;19(4):1165-74. PubMed PMID: 15375759.
204. Satyam A, Subramanian GS, Raghunath M, Pandit A, Zeugolis DI. In vitro evaluation of Ficoll-enriched and genipin-stabilised collagen scaffolds. J Tissue Eng Regen Med. 2014;8(3):233-41. doi: 10.1002/term.1522. PubMed PMID: 22552937.
205. Mathew AP, Oksman K, Pierron D, Harmand MF. Biocompatible fibrous networks of cellulose nanofibres and collagen crosslinked using genipin: potential as artificial ligament/tendons. Macromol Biosci. 2013;13(3):289-98. doi: 10.1002/mabi.201200317. PubMed PMID: 23225770.
206. Gorczyca G, Tylingo R, Szweda P, Augustin E, Sadowska M, Milewski S. Preparation and characterization of genipin cross-linked porous chitosan-collagen-gelatin scaffolds using chitosan-CO2 solution. Carbohydr Polym. 2014;102:901-11. doi: 10.1016/j.carbpol.2013.10.060. PubMed PMID: 24507362.
207. Alfredo Uquillas J, Kishore V, Akkus O. Genipin crosslinking elevates the strength of electrochemically aligned collagen to the level of tendons. Journal of the mechanical behavior of biomedical materials. 2012;15:176-89. doi: 10.1016/j.jmbbm.2012.06.012. PubMed PMID: 23032437.
208. Krishna SM, Moxon JV, Golledge J. A review of the pathophysiology and potential biomarkers for peripheral artery disease. Int J Mol Sci. 2015;16(5):11294-322. doi: 10.3390/ijms160511294. PubMed PMID: 25993296; PMCID: 4463701.
209. Swaminathan A, Vemulapalli S, Patel MR, Jones WS. Lower extremity amputation in peripheral artery disease: improving patient outcomes. Vascular health and risk management. 2014;10:417-24. doi: 10.2147/VHRM.S50588. PubMed PMID: 25075192; PMCID: 4107174.

210. Aldagen. ALD-301 for Critical Limb Ischemia, Randomized Trial (CLI-001) 2006. Available from: https://clinicaltrials.gov/ct2/show?term=Stem+Cell&recrs=e&cond=Peripheral+Artery+Disease&draw=1&rank=13.
211. Ltd. S. Autologous Angiogenic Cell Precursors (ACPs) for the Treatment of Peripheral Artery Disease 2012 [2017]. Available from: https://clinicaltrials.gov/ct2/show/ĀCT01584986?term=Stem+Cell&recrs=e&cond=Peripheral+Artery+Disease&draw=1&rank=4.
212. Franz RW, Shah KJ, Pin RH, Hankins T, Hartman JF, Wright ML. Autologous bone marrow mononuclear cell implantation therapy is an effective limb salvage strategy for patients with severe peripheral arterial disease. Journal of vascular surgery. 2015;62(3):673-80. doi: 10.1016/j.jvs.2015.02.059. PubMed PMID: WOS:000360357500022.
213. Losordo D, M.D. Injection of Autologous CD34-Positive Cells for Critical Limb Ischemia (ACT34-CLI)2008.
214. Therapy TC. Phase II Combination Stem Cell Therapy for the Treatment of Severe Leg Ischemia (MESEĀDO)2008.
215. A. M. Zeiher JWGUH. Safety and Feasibility Study of Autologous Bone Marrow Cell Transplantation in Patients With Peripheral Arterial Occlusive Disease (PAOD) 2006. Available from: https://clinicaltrials.gov/ct2/show?term=Stem+Cell&recrs=e&cond=Peripheral+Artery+Disease&draw=1&rank=11.
216. University N. Stem Cell Injection for Peripheral Vascular Disease 2006. Available from: https://clinicaltrials.gov/ct2/show?term=Stem+Cell&recrs=e&cond=Peripheral+Artery+Disease&draw=1&rank=12.
217. KG AGC. Tolerability and Efficacy of Intravenous Infusion of Autologous MSC_Apceth for the Treatment of Critical Limb Ischemia2011.
218. Martins L, Martin PK, Han SW. Angiogenic properties of mesenchymal stem cells in a mouse model of limb ischemia. Methods in molecular biology. 2014;1213:147-69. doi: 10.1007/978-1-4939-1453-1_13. PubMed PMID: 25173381.

219. Lin YL, Yet SF, Hsu YT, Wang GJ, Hung SC. Mesenchymal Stem Cells Ameliorate Atherosclerotic Lesions via Restoring Endothelial Function. Stem cells translational medicine. 2015;4(1):44-55. doi: 10.5966/sctm.2014-0091. PubMed PMID: 25504897; PMCID: 4275009.
220. Whiteley J, Bielecki R, Li M, Chua S, Ward MR, Yamanaka N, Stewart DJ, Casper RF, Rogers IM. An expanded population of CD34+ cells from frozen banked umbilical cord blood demonstrate tissue repair mechanisms of mesenchymal stromal cells and circulating angiogenic cells in an ischemic hind limb model. Stem cell reviews. 2014;10(3):338-50. doi: 10.1007/s12015-014-9496-1. PubMed PMID: 24443055.
221. Lu SJ, Feng Q, Caballero S, Chen Y, Moore MA, Grant MB, Lanza R. Generation of functional hemangioblasts from human embryonic stem cells. Āature methods. 2007;4(6):501-9. doi: 10.1038/nmeth1041. PubMed PMID: 17486087; PMCID: 3766360.
222. Kim SW, Kim H, Cho HJ, Lee JU, Levit R, Yoon YS. Human peripheral blood-derived CD31+ cells have robust angiogenic and vasculogenic properties and are effective for treating ischemic vascular disease. Journal of the American College of Cardiology. 2010;56(7):593-607. doi: 10.1016/j.jacc.2010.01.070. PubMed PMID: 20688215; PMCID: 2917842.
223. Iohara K, Zheng L, Wake H, Ito M, Nabekura J, Wakita H, Nakamura H, Into T, Matsushita K, Nakashima M. A novel stem cell source for vasculogenesis in ischemia: subfraction of side population cells from dental pulp. Stem cells. 2008;26(9):2408-18. doi: 10.1634/stemcells.2008-0393. PubMed PMID: 18583536.
224. Foubert P, Silvestre JS, Souttou B, Barateau V, Martin C, Ebrahimian TG, Lere-Dean C, Contreres JO, Sulpice E, Levy BI, Plouet J, Tobelem G, Le Ricousse-Roussanne S. PSGL-1-mediated activation of EphB4 increases the proangiogenic potential of endothelial progenitor cells. J Clin Invest. 2007;117(6):1527-37. doi: 10.1172/JCI28338. PubMed PMID: 17510705; PMCID: 1866248.
225. Suzuki H, Shibata R, Kito T, Ishii M, Li P, Yoshikai T, Nishio N, Ito S, Numaguchi Y, Yamashita JK, Murohara T, Isobe K. Therapeutic angiogenesis by transplantation of induced pluripotent stem cell-derived Flk-1 positive cells. BMC cell biology.

2010;11:72. doi: 10.1186/1471-2121-11-72. PubMed PMID: 20860813; PMCID: 2955572.

226. Foubert P, Matrone G, Souttou B, Lere-Dean C, Barateau V, Plouet J, Le Ricousse-Roussanne S, Levy BI, Silvestre JS, Tobelem G. Coadministration of endothelial and smooth muscle progenitor cells enhances the efficiency of proangiogenic cell-based therapy. Circ Res. 2008;103(7):751-60. doi: 10.1161/CIRCRESAHA.108.175083. PubMed PMID: 18723447.
227. Baroni A, Donnarumma G, Paoletti I, Longanesi-Cattani I, Bifulco K, Tufano MA, Carriero MV. Antimicrobial human beta-defensin-2 stimulates migration, proliferation and tube formation of human umbilical vein endothelial cells. Peptides. 2009;30(2):267-72. doi: 10.1016/j.peptides.2008.11.001. PubMed PMID: 19041917.
228. Yoon CH, Hur J, Park KW, Kim JH, Lee CS, Oh IY, Kim TY, Cho HJ, Kang HJ, Chae IH, Yang HK, Oh BH, Park YB, Kim HS. Synergistic neovascularization by mixed transplantation of early endothelial progenitor cells and late outgrowth endothelial cells: the role of angiogenic cytokines and matrix metalloproteinases. Circulation. 2005;112(11):1618-27. doi: 10.1161/CIRCULATIOĀAHA.104.503433. PubMed PMID: 16145003.
229. Yoo CH, Na HJ, Lee DS, Heo SC, An Y, Cha J, Choi C, Kim JH, Park JC, Cho YS. Endothelial progenitor cells from human dental pulp-derived iPS cells as a therapeutic target for ischemic vascular diseases. Biomaterials. 2013;34(33):8149-60. doi: 10.1016/j.biomaterials.2013.07.001. PubMed PMID: 23896001.
230. Shen WC, Liang CJ, Wu VC, Wang SH, Young GH, Lai IR, Chien CL, Wang SM, Wu KD, Chen YL. Endothelial progenitor cells derived from Wharton's jelly of the umbilical cord reduces ischemia-induced hind limb injury in diabetic mice by inducing HIF-1alpha/IL-8 expression. Stem Cells Dev. 2013;22(9):1408-18. doi: 10.1089/scd.2012.0445. PubMed PMID: 23252631; PMCID: 3629854.
231. Putman DM, Liu KY, Broughton HC, Bell GI, Hess DA. Umbilical cord blood-derived aldehyde dehydrogenase-expressing progenitor cells promote recovery from acute ischemic injury. Stem cells. 2012;30(10):2248-60. doi: 10.1002/stem.1206. PubMed PMID: 22899443.
232. Lai WH, Ho JC, Chan YC, Ng JH, Au KW, Wong LY, Siu CW, Tse HF. Attenuation of hind-limb ischemia in mice with endothelial-like cells derived from different sources of

human stem cells. PLoS One. 2013;8(3):e57876. doi: 10.1371/journal.pone.0057876. PubMed PMID: 23472116; PMCID: 3589485.

233. Yu JX, Huang XF, Lv WM, Ye CS, Peng XZ, Zhang H, Xiao LB, Wang SM. Combination of stromal-derived factor-1alpha and vascular endothelial growth factor gene-modified endothelial progenitor cells is more effective for ischemic neovascularization. Journal of vascular surgery. 2009;50(3):608-16. doi: 10.1016/j.jvs.2009.05.049. PubMed PMID: 19595531.
234. Yang HN, Park JS, Woo DG, Jeon SY, Park KH. Transfection of VEGF(165) genes into endothelial progenitor cells and in vivo imaging using quantum dots in an ischemia hind limb model. Biomaterials. 2012;33(33):8670-84. doi: 10.1016/j.biomaterials.2012.08.012. PubMed PMID: 22921925.
235. Vaughan EE, Liew A, Mashayekhi K, Dockery P, McDermott J, Kealy B, Flynn A, Duffy A, Coleman C, O'Regan A, Barry FP, O'Brien T. Pretreatment of endothelial progenitor cells with osteopontin enhances cell therapy for peripheral vascular disease. Cell Transplant. 2012;21(6):1095-107. doi: 10.3727/096368911X623880. PubMed PMID: 22304991.
236. Aicher A, Heeschen C, Sasaki K, Urbich C, Zeiher AM, Dimmeler S. Low-energy shock wave for enhancing recruitment of endothelial progenitor cells: a new modality to increase efficacy of cell therapy in chronic hind limb ischemia. Circulation. 2006;114(25):2823-30. doi: 10.1161/CIRCULATIOĀAHA.106.628623. PubMed PMID: 17145991.
237. Zakharova IS, Zhiven MK, Saaya SB, Shevchenko AI, Smirnova AM, Strunov A, Karpenko AA, Pokushalov EA, Ivanova LĀ, Makarevich PI, Parfyonova YV, Aboian E, Zakian SM. Endothelial and smooth muscle cells derived from human cardiac explants demonstrate angiogenic potential and suitable for design of cell-containing vascular grafts. Journal of translational medicine. 2017;15(1):54. doi: 10.1186/s12967-017-1156-1. PubMed PMID: 28257636; PMCID: 5336693.
238. Foubert P, Squiban C, Holler V, Buard V, Dean C, Levy BI, Benderitter M, Silvestre JS, Tobelem G, Tamarat R. Strategies to Enhance the Efficiency of Endothelial Progenitor Cell Therapy by Ephrin B2 Pretreatment and Coadministration with Smooth Muscle Progenitor Cells on Vascular Function During the Wound-Healing Process in Irradiated

or Nonirradiated Condition. Cell Transplant. 2015;24(7):1343-61. doi: 10.3727/096368913X672064. PubMed PMID: 24069908.

239. Park IS, Chung PS, Ahn JC. Enhanced angiogenic effect of adipose-derived stromal cell spheroid with low-level light therapy in hind limb ischemia mice. Biomaterials. 2014;35(34):9280-9. doi: 10.1016/j.biomaterials.2014.07.061. PubMed PMID: 25132605.
240. Ishikane S, Ohnishi S, Yamahara K, Sada M, Harada K, Mishima K, Iwasaki K, Fujiwara M, Kitamura S, Nagaya N, Ikeda T. Allogeneic injection of fetal membrane-derived mesenchymal stem cells induces therapeutic angiogenesis in a rat model of hind limb ischemia. Stem cells. 2008;26(10):2625-33. doi: 10.1634/stemcells.2008-0236. PubMed PMID: 18669910.
241. Lopez-Holgado Ā, Alberca M, Sanchez-Guijo FM, Villaron EM, Rivas JV, Lopez-Novoa JM, Brinon JG, Arevalo MA, Oterino E, Santamaria C, San Miguel JF, del Canizo MC. Prospective comparative analysis of the angiogenic capacity of monocytes and CD133+ cells in a murine model of hind limb ischemia. Cytotherapy. 2009;11(8):1041-51. doi: 10.3109/14653240903191719. PubMed PMID: 19929468.
242. Li M, Liu C, Bin J, Wang Y, Chen J, Xiu J, Pei J, Lai Y, Chen D, Fan C, Xie J, Tao Y, Wu P. Mutant hypoxia inducible factor-1alpha improves angiogenesis and tissue perfusion in ischemic rabbit skeletal muscle. Microvascular research. 2011;81(1):26-33. doi: 10.1016/j.mvr.2010.09.008. PubMed PMID: 20937289.
243. Mannor GE, Wardell K, Wolfley DE, Nilsson GE. Laser Doppler perfusion imaging of eyelid skin. Ophthalmic plastic and reconstructive surgery. 1996;12(3):178-85. PubMed PMID: 8869973.
244. Wardell K, Naver HK, Nilsson GE, Wallin BG. The cutaneous vascular axon reflex in humans characterized by laser Doppler perfusion imaging. J Physiol. 1993;460:185-99. PubMed PMID: 8487191; PMCID: PMC1175208.
245. Fan CL, Gao PJ, Che ZQ, Liu JJ, Wei J, Zhu DL. Therapeutic neovascularization by autologous transplantation with expanded endothelial progenitor cells from peripheral blood into ischemic hind limbs. Acta pharmacologica Sinica. 2005;26(9):1069-75. doi: 10.1111/j.1745-7254.2005.00168.x. PubMed PMID: 16115373.

246. Li TS, Cheng K, Malliaras K, Smith RR, Zhang Y, Sun B, Matsushita N, Blusztajn A, Terrovitis J, Kusuoka H, Marban L, Marban E. Direct comparison of different stem cell types and subpopulations reveals superior paracrine potency and myocardial repair efficacy with cardiosphere-derived cells. Journal of the American College of Cardiology. 2012;59(10):942-53. doi: 10.1016/j.jacc.2011.11.029. PubMed PMID: 22381431; PMCID: PMC3292778.
247. Fan R, Tang D, Yao J, Yang C, Xu D. 3D Echo-Based Patient-Specific Computational Left Ventricle Models to Quantify Material Properties and Stress/Strain Differences between Ventricles with and without Infarct. Computer modeling in engineering & sciences : CMES. 2014;99(6):491-508. PubMed PMID: 25663830; PMCID: 4319570.
248. Udagawa A, Sato S, Hasuike A, Kishida M, Arai Y, Ito K. Micro-CT observation of angiogenesis in bone regeneration. Clin Oral Implan Res. 2013;24(7):787-92. doi: 10.1111/j.1600-0501.2012.02458.x. PubMed PMID: WOS:000319998500011.
249. Ungersma SE, Pacheco G, Ho C, Yee SF, Ross J, van Bruggen N, Peale FV, Ross S, Carano RAD. Vessel Imaging with Viable Tumor Analysis for Quantification of Tumor Angiogenesis. Magnetic resonance in medicine. 2010;63(6):1637-47. doi: 10.1002/mrm.22442. PubMed PMID: WOS:000278164400024.
250. Du W, Li X, Chi Y, Ma F, Li Z, Yang S, Song B, Cui J, Ma T, Li J, Tian J, Yang Z, Feng X, Chen F, Lu S, Liang L, Han ZB, Han ZC. VCAM-1+ placenta chorionic villi-derived mesenchymal stem cells display potent pro-angiogenic activity. Stem cell research & therapy. 2016;7:49. doi: 10.1186/s13287-016-0297-0. PubMed PMID: 27044487; PMCID: 4820943.
251. Otsuki Y, Nakamura Y, Harada S, Yamamoto Y, Ogino K, Morikawa K, Ninomiya H, Miyagawa S, Sawa Y, Hisatome I, Nishimura M. Adipose stem cell sheets improved cardiac function in the rat myocardial infarction, but did not alter cardiac contractile responses to beta-adrenergic stimulation. Biomedical research. 2015;36(1):11-9. doi: 10.2220/biomedres.36.11. PubMed PMID: 25749147.
252. Webber MJ, Han X, Murthy SĀ, Rajangam K, Stupp SI, Lomasney JW. Capturing the stem cell paracrine effect using heparin-presenting nanofibres to treat cardiovascular diseases. J Tissue Eng Regen Med. 2010;4(8):600-10. doi: 10.1002/term.273. PubMed PMID: 20222010; PMCID: 3372239.

253. Sarrazy V, Koehler A, Chow ML, Zimina E, Li CX, Kato H, Caldarone CA, Hinz B. Integrins alphavbeta5 and alphavbeta3 promote latent TGF-beta1 activation by human cardiac fibroblast contraction. Cardiovascular research. 2014;102(3):407-17. doi: 10.1093/cvr/cvu053. PubMed PMID: 24639195; PMCID: PMC4030512.
254. Araya J, Cambier S, Morris A, Finkbeiner W, Āishimura SL. Integrin-mediated transforming growth factor-beta activation regulates homeostasis of the pulmonary epithelial-mesenchymal trophic unit. The American journal of pathology. 2006;169(2):405-15. PubMed PMID: 16877343; PMCID: 1698780.
255. Mauritz C, Martens A, Rojas SV, Schnick T, Rathert C, Schecker N, Menke S, Glage S, Zweigerdt R, Haverich A, Martin U, Kutschka I. Induced pluripotent stem cell (iPSC)-derived Flk-1 progenitor cells engraft, differentiate, and improve heart function in a mouse model of acute myocardial infarction. European heart journal. 2011;32(21):2634-41. doi: 10.1093/eurheartj/ehr166. PubMed PMID: 21596799.
256. Moelker AD, Baks T, Wever KM, Spitskovsky D, Wielopolski PA, van Beusekom HM, van Geuns RJ, Wnendt S, Duncker DJ, van der Giessen WJ. Intracoronary delivery of umbilical cord blood derived unrestricted somatic stem cells is not suitable to improve LV function after myocardial infarction in swine. Journal of molecular and cellular cardiology. 2007;42(4):735-45. doi: 10.1016/j.yjmcc.2007.01.005. PubMed PMID: 17320899.
257. Rojas SV, Kensah G, Rotaermel A, Baraki H, Kutschka I, Zweigerdt R, Martin U, Haverich A, Gruh I, Martens A. Transplantation of purified iPSC-derived cardiomyocytes in myocardial infarction. PLoS One. 2017;12(5):e0173222. doi: 10.1371/journal.pone.0173222. PubMed PMID: 28493867; PMCID: PMC5426598.
258. Landmesser U, Engberding N, Bahlmann FH, Schaefer A, Wiencke A, Heineke A, Spiekermann S, Hilfiker-Kleiner D, Templin C, Kotlarz D, Mueller M, Fuchs M, Hornig B, Haller H, Drexler H. Statin-induced improvement of endothelial progenitor cell mobilization, myocardial neovascularization, left ventricular function, and survival after experimental myocardial infarction requires endothelial nitric oxide synthase. Circulation. 2004;110(14):1933-9. doi: 10.1161/01.CIR.0000143232.67642.7A. PubMed PMID: 15466656.

259. Jamaiyar A, Wan W, Ohanyan V, Enrick M, Janota D, Cumpston D, Song H, Stevanov K, Kolz CL, Hakobyan T, Dong F, Newby BZ, Chilian WM, Yin L. Alignment of inducible vascular progenitor cells on a micro-bundle scaffold improves cardiac repair following myocardial infarction. Basic research in cardiology. 2017;112(4):41. doi: 10.1007/s00395-017-0631-4. PubMed PMID: 28540527.